UC Riverside
UC Riverside Electronic Theses and Dissertations

Title

The Effects of Direct and Indirect Ethanol Exposure on Brain and Behavioral Development in Mice

Permalink

Author

Bottom, Riley Thomas

Publication Date

2021

Peer reviewed|Thesis/dissertation

UNIVERSITY OF CALIFORNIA
RIVERSIDE

The Effects of Direct and Indirect Ethanol Exposure on Brain and Behavioral
Development in Mice

A Dissertation submitted in partial satisfaction
of the requirements for the degree of

Doctor of Philosophy

in

Neuroscience

by

Riley Thomas Bottom

June 2021

Dissertation Committee:
        Dr. Kelly Huffman, Chairperson
        Dr. Khaleel Razak
        Dr. Martin Riccomagno

The Dissertation of Riley Thomas Bottom is approved:

_____

_____

_____
Committee Chairperson

University of California, Riverside

Acknowledgements

First, I would like to thank my advisor, Dr. Kelly Huffman, for her unwavering support of myself from both a scientific and personal perspective. Kelly's guidance has pushed me to become the researcher I am today, and her creativity and drive have instilled unique characteristics in me that will indubitably help me in my future endeavors. I am grateful to consider Kelly a friend of mine and her personality and openness have forever made a substantial impact on my life.

I would also like to thank my guidance committee members, Dr. Khaleel Razak and Dr. Martin Riccomagno. Their expertise and knowledge as top-notch scientists pushed my development in exceedingly positive ways and their support helped me actualize the goals I once considered impossible in my early years.

Thank you to all Huffman Lab members, past and present, for all of your help. Whether it was troubleshooting protocols or just shooting the breeze, I could always rely on my lab mates for support and nurture, and I will be forever grateful for this. I would also like to thank my friends, at both UCR and otherwise, who provided moral support and allowed me to ease the stress of the graduate years.

I would like to thank my parents, Gary and Sylvia Bottom, for supporting my dreams, as capricious as they were, throughout my life. Your pride in me and your flexibility made this dream possible. Thank you to all my family members,

iv

particularly my sister Allison Bottom, as well as my many uncles, aunts, cousins, and grandparents for all of your love and backing.

Lastly, I would like to thank my wonderful fiancé Vivian Nguyen. Thank you for your enduring support through all the ups and downs and demands that come with an academic career. I know it is not easy, but with you by my side I fear nothing in the future.

I would like to dedicate this dissertation to the memory of my beloved grandmother Dalia Valenzuela Solis. You realized my potential at an age where I was too young to see it myself and although you are not here today, I know you are beaming with pride from the afterlife.

ABSTRACT OF THE DISSERTATION

The Effects of Direct and Indirect Ethanol Exposure on Brain and Behavioral
Development in Mice

by

Riley Thomas Bottom

Doctor of Philosophy, Graduate Program in Neuroscience
University of California, Riverside, June 2021
Dr. Kelly Huffman, Chairperson

Prenatal ethanol exposure (PrEE) is a leading cause of preventable birth defects

and neurobehavioral disorders; PrEE can lead to Fetal Alcohol Spectrum

Disorders (FASD). Clinical profiles of patients with FASD indicate damage to the

central nervous system (CNS), including the neocortex, may underlie the varied,

cognitive deficits associated with FASD. Recent preclinical evidence has

suggested that PrEE may induce epigenetic dysregulation in offspring, producing

adverse heritable, transgenerational behavioral effects, however the

neurobiological underpinnings remain unclear. Preventive or therapeutic

treatments for FASD have not yet been discovered and need to reflect the

neurobiological damage inflicted by PrEE as well as the abstinence-resistant

population. Additionally, although much research has focused on maternal PrEE,

much less is known about the impact of paternal ethanol exposure (PatEE) and

how development of the neocortex may be disrupted by preconception alcohol use by fathers.

The research presented within this dissertation attempts to fill these gaps in knowledge using three, distinct research designs and multi-level neurobiological and behavioral approaches. First, in Chapter 1, we assessed the full extent of behavioral disruptions that are passed several generations following PrEE and attempted to find novel mechanistic links within the CNS using a transgenerational mouse model of FASD. We found multi-modality behavioral abnormalities that extend several generations and novel CNS anomalies in directly exposed offspring. Second, in Chapter 2, we investigated how co-administration of choline could prevent PrEE-induced neurobehavioral deficits. We found choline has a robust protective effect on several parameters of neocortical development and behaviors that are normally disrupted by PrEE in a mouse model. Lastly, in Chapter 3, we described the impact of preconception ethanol exposure on early postnatal development of the neocortex in an novel PatEE mouse model. We found that PatEE induced several alterations within the developing CNS including altered cortical gene expression as well as patterns of early sensory area connectivity. Overall, the results gleaned from these studies provide key descriptive, mechanistic, and therapeutic information on the still unclear etiology of FASD, as well as novel information on how paternal alcohol use may impact future offspring. Conclusions drawn from this dissertation have clear implications for the substantial impact of alcohol on human health.

Table of Contents

Chapter 1: Prenatal ethanol exposure induces adverse, transgenerational effects within adolescent behaviors in a murine model of FASD

Chapter 2: Rescue of ethanol-induced FASD-like phenotypes via prenatal co-administration of choline

Chapter 3: The impact of paternal alcohol consumption on early postnatal development of the neocortex

List of Tables

List of Figures

Chapter 3: The impact of paternal alcohol consumption on early postnatal development of the neocortex

Abbreviations:

Prenatal Ethanol Exposure (PrEE)

Fetal Alcohol Spectrum Disorders (FASD)

Central Nervous System (CNS)

Paternal Ethanol Exposure (PatEE)

Ethanol (EtOH)

Intraneocortical Connections (INCs)

Retinoid Z Receptor Beta (RZRβ)

Inhibitor of DNA Binding 2 (Id2)

Postnatal day (P)

Gestational day (GD)

First Filial Generation (F1)

Second Filial Generation (F2)

Third Filial Generation (F3)

Paraformaldehyde (PFA)

4′,6-diamidino-2-phenylindole (DAPI)

1,1' -Dioctadecyl-3,3,3',3' -tetramethylindocarbocynanine Perchlorate (DiI)

(4-(4-(Dihexadecylamino)styryl)-N-Methylpyridinium Iodide (DiA)

In Situ Hybridization (ISH)

Golgi-Cox Stain (GCS)

Phosphate-Buffered Saline (PBS)

Primary Somatosensory Cortex (S1)

Primary Visual Cortex (V1)

Choline Ethanol (CE)

Choline Water (CW)

Con (Control)

S-Adenosyl Methionine (SAM)

MicroRNA (miRNA)

Blood Ethanol Concentration (BEC)

Plasma osmolality (POSM)

Dye Placement Location (DPL)

Region of Interest (ROI)

5-Methylcytosine (5-mC)

One Carbon Metabolism (OCM)

Elevated Plus Maze (EPM)

Forced Swim Test (FST)

General Introduction

Development of the central nervous system (CNS) is a highly dynamic process which relies on a series of precise, sequential events including cell proliferation, migration, and the precise establishment of synaptic connectivity. Genetic mutations, as well as a plethora of prenatal environmental insults, have been shown to disrupt these events, ultimately leading to long-lasting changes in brain and behavioral function.

Alcohol, or ethanol (EtOH), is a toxic substance with psychoactive properties which is highly prevalent in many cultures globally (World Health Organization). Prenatal ethanol exposure, or PrEE, occurs from the maternal consumption of EtOH during gestation and represents a leading cause of non-genetic neurodevelopmental disorders (Denny et al., 2017). Fetal alcohol spectrum disorders (FASD) is an umbrella term describing the wide range of clinically diagnosed conditions that result from PrEE. Despite evidence indicating the negative impact of PrEE on developing offspring, 19.6% of pregnant women within the US report first trimester alcohol use (England et al., 2020). Recent reports have estimated that the prevalence of FASD in the US is as high as 5% (May et al., 2018) and the economic burden of FASD is approximately $5.5 billion dollars a year (Lupton et al., 2004), establishing PrEE as a formidable issue within our alcohol-centric society.

FASD and the Neocortex.

The broad extent of behavioral/cognitive disabilities associated with FASD have been described within the clinical population and include deficits in several modalities such as general intelligence, executive functions, sensorimotor processing, as well increased incidence of mental disorders such as depression and anxiety (Mattson et al., 2011). Due to the nature of these deficits, it has been postulated that the neocortex, a complex structure essential for higher-order behaviors, may represent a focal point of the harmful effects of PrEE. Clinical studies with patients of FASD have largely confirmed these notions, describing structural (Zhou et al., 2011; 2018) and functional deficits (Kodali et al., 2017) within the neocortex.

In order to assess the neurological underpinnings of the adverse effects of PrEE on the neocortex, animal models of FASD have been utilized and have proven to be largely faithful representations of the human conditions (Sulik et al., 1981). A wide range of negative consequences on neocortical development due to PrEE have been reported including increased apoptosis (Komada et al., 2017), altered migration/layer formation (Cuzon et al., 2008; Delatour et al., 2019), and physiological deficits (Delatour et al., 2020). Additionally, PrEE has been shown to induce widespread dysregulation of gene expression within rodent cortex (Hashimoto-Torii et al., 2011; Mohammad et al., 2020), which may underlie some of the described phenotypes.

A key feature of the neocortex is its complex organization. The neocortex is comprised of functionally and anatomically distinct areas which rely on development of precise interconnectivity to produce complex behaviors. Intraneocortical connections (INCs) or ipsilateral cortico-cortical connections represent an early defining characteristic of these distinct areas (Kaas, 1995). Genetic regulation, including expression of genes such as *RZRβ*, *Id2*, *Cad8*, and *Nr2f1* (COUP-TFI) have been implicated in this process termed arealization (Rubenstein et al, 1999; Huffman et al., 2004; Armentano et al., 2007). Key studies from the Huffman laboratory have indicated that severe disruptions of these processes are present within newborn mice exposed to prenatal ethanol, including altered cortical expression of *RZRβ*, *Id2*, and *Cad8,* and dramatic disorganization of sensory area INCs, including aberrant projections (El Shawa et al., 2013). These same mice display behavioral deficits at postnatal day (P) 20 that mirror those seen in the clinical FASD population, including altered sensorimotor integration and increased anxiety-like behavior. Overall, these novel results suggested that altered organization of early cortical connectivity (likely due to dysregulation of important gene expression patterns) may underlie the behavioral deficits seen in patients with FASD.

Underlying epigenetic mechanisms and transgenerational effects of FASD.

Epigenetic regulation, including DNA methylation, histone modifications, and non-coding RNAs, is the process by which gene expression is controlled in a

manner that does not rely on changes to the genetic sequence. This process is highly important for development of the CNS and the diversification of all cell types (Bacon and Brinton, 2021). A current hypothesis within the field of FASD suggest that epigenetic dysregulation induced by PrEE may be a major driving feature of the described brain alterations and subsequent behavioral deficits (Lussier et al., 2017). Supporting this idea, diverse features of epigenetic regulation have been described to be perturbed by PrEE within the developing neocortex, including altered histone modifications and DNA methylation (Subbana et al., 2014; Öztürk et al., 2017).

Recently, mounting evidence has supported the idea of epigenetic inheritance of phenotypic variations that extends several generations following adverse environmental exposures (Nilsson et al., 2018). Thus, a highly-relevant question to human health is: if PrEE causes epigenetic dysregulation within the developing CNS which may underlie the behavioral deficits, are these phenotypes able to be passed transgenerationally? Evidence from our lab and others have suggested that this phenomenon does occur in rodent models of FASD (Govorko et al., 2012; Abbott et al., 2018; Gangisetty et al., 2020).

In particular, within our model, disorganized INC patterns and altered gene expression are present up to the 3rd flial (F3) generation in P0 mice, as well as distinct behavioral phenotypes at P20. Additionally, we found altered epigenetic regulation that persisted several generations including reduced global DNA methylation and gene-specific promoter methylation (Abbott et al., 2018). This

suggests that this process may be driven epigenetically. Despite these exciting and novel results, it remains to be understood how these early life changes in cortical development ultimately produce the behavioral deficits seen in adolescence, as well as the true extent of the behaviors affected.

Therapeutic and preventive measures of FASD.

Due to the prevalence of FASD as well as the high incidence of consumption of EtOH amongst pregnant women, it is of paramount importance to develop effective therapeutic and/or preventive measures to reduce the effects of PrEE on developing offspring. Several studies have demonstrated reliable results within FASD animal models (Vaglenova et al., 2007; Wellman et al., 2015; Cantacorps et al., 2020), but often relatively low degrees of translation to the clinical population (Davis et al., 2011). Choline, a vitamin-like essential nutrient important for proper brain development and function (Zeisel, 2006), has shown very high promise amongst the many proposed. Importantly, choline use in humans has shown the remarkable ability to improve FASD behavioral outcomes when given to pregnant women who suffered from alcoholism (Jacobson et al., 2018), as well as directly to children with FASD (Wozniak et al., 2020), suggesting it may have robust preventive and therapeutic abilities against EtOH's harmful effects.

Use of animal models have supported these positive results, suggesting that many neurological deficits, including altered hypothalamic gene expression

(Bekdash et al., 2013) and behavioral deficits, such as impaired working memory (Thomas et al., 2010), are prevented by concurrent choline supplementation at the time of EtOH insult. However, it is unclear if concurrent choline supplementation also provides any protective effects against the PrEE-induced cortical phenotypes described in our model, as well as against a multitude of clinically-relevant, cortically-involved behaviors. Additionally, the precise molecular mechanisms underlying the choline's amelioration of FASD phenotypes in humans and animal models remains unclear. Due to the epigenetic dysregulation present due to PrEE (Lussier et al., 2017) and choline's involvement in epigenetic regulation as methyl-group donor (Jiang et al., 2014), an attractive hypothesis is that choline may be mediating these effects epigenetically. Currently, these hypotheses have yet to be tested within the capacity of neocortical development.

Preconceptual ethanol exposure: paternal considerations.

Although a multitude of preclinical and clinical research have cemented the harmful consequences of PrEE on affected offspring, much less is known about the contribution of paternal ethanol exposure (PatEE). Despite not being able to directly affect developing offspring via direct transmission such as in maternal, prenatal exposures, paternal exposures have been gaining traction as potential mediators of inherited phenotypic variation via germ cells (Braun and Champagne, 2014; Rutkowska et al., 2020). Interestingly, clinical data have

shown a negative effect of heavy paternal drinking on offspring outcomes (Zhou et al., 2021). Very recently, animal models of PatEE have suggested that the paternal preconception environment is also an important aspect for proper development of offspring and exposure to EtOH may negatively affect behavioral outputs (Abel, 1991; Kim et al., 2014; Hollander et al., 2019), which may be mediated through epigenetic dysregulation of sperm, the male germ cells (Rompala et al., 2018). These described behavioral effects, including hyperactivity and depressive-like behavior, mirror those seen in traditional FASD, suggesting there may be a shared lineage of disruption amongst PatEE and PrEE.

Despite this substantial evidence, it remains unclear what the CNS-based underpinnings of these phenomena are. Very sparse studies have examined this topic but have found various adverse effects in PatEE offspring CNS including altered gene expression within the brain (Finegersh and Homanics, 2014; Przybycien-Szymanska, et al., 2014). In order to fully assess the impact of PatEE within the developing brain, it is crucial to investigate how development of the neocortex may be disrupted within PatEE models. Specifically, does PatEE produce similar disruptions in neocortical development and arealization that are consistently reported within our FASD model (El Shawa et al., 2013; Abbott et al., 2018)?

Summary and conclusions.

Previous research by our group and others have indicated the severe consequences of PrEE on offspring brain and behavior, which may be mediated, at least in part, through damage to the developing neocortex. Despite this, many key topics remain to be fully elucidated. Specifically, transgenerational effects of PrEE have been shown and are missing key mediating information between the described behavioral disruptions and CNS structure and function. Use of choline as a preventive measure has gained support from preclinical and clinical models however its ability in preventing PrEE-induced neocortical dysfunction as well as crucial mechanistic information are lacking. Additionally, the spectrum of effects PatEE has on offspring neocortical development are unknown. Therefore, the research within this dissertation aimed to address these broad issues within the following 3 chapters.

In Chapter 1, we investigate several behavioral and CNS-based aspects within mice at adolescent age in a transgenerational model of FASD. In Chapter 2, we examine the ability of concurrent choline supplementation to rescue the phenotypic deficits seen within neocortical development and behavior within a FASD mouse model. Lastly, in Chapter 3, we shift focus in order to describe the impact PatEE has on several aspects of early postnatal development of the neocortex. Results from this dissertation serve to uncover several unknown aspects of FASD, including novel transgenerational effects and preventive/therapeutic preclinical validation, as well as to outline the burden of

preconception paternal exposures on developing offspring, all issues of upmost

importance for human health.

REFERENCES

Abbott CW, Rohac DJ, Bottom RT, Patadia S, Huffman KJ (2018) Prenatal Ethanol Exposure and Neocortical Development: A Transgenerational Model of FASD. Cereb Cortex 28:2908–2921.

Bekdash RA, Zhang C, Sarkar DK (2013) Gestational choline supplementation normalized fetal alcohol-induced alterations in histone modifications, DNA methylation, and proopiomelanocortin (POMC) gene expression in ??-endorphin-producing POMC neurons of the hypothalamus. Alcohol Clin Exp Res 37:1133–1142.

Cuzon VC, Yeh PWL, Yanagawa Y, Obata K, Yeh HH (2008) Ethanol Consumption during Early Pregnancy Alters the Disposition of Tangentially Migrating GABAergic Interneurons in the Fetal Cortex. J Neurosci 28:1854–1864.

Delatour LC, Yeh PWL, Yeh HH (2020) Prenatal Exposure to Ethanol Alters Synaptic Activity in Layer V/VI Pyramidal Neurons of the Somatosensory Cortex. Cereb Cortex 30:1735–1751.

Delatour LC, Yeh PW, Yeh HH (2019) Ethanol Exposure *In Utero* Disrupts Radial Migration and Pyramidal Cell Development in the Somatosensory Cortex. Cereb Cortex 29:2125–2139.

Denny L, Coles S, Blitz R (2017) Fetal Alcohol Syndrome and Fetal Alcohol Spectrum Disorders, American Family Physician.

England LJ, Bennett C, Denny CH, Honein MA, Gilboa SM, Kim SY, Guy GP, Tran EL, Rose CE, Bohm MK, Boyle CA (2020) Alcohol Use and Co-Use of Other Substances Among Pregnant Females Aged 12–44 Years — United States, 2015–2018. MMWR Morb Mortal Wkly Rep 69:1009–1014.

Finegersh A, Homanics GE (2014) Paternal Alcohol Exposure Reduces Alcohol Drinking and Increases Behavioral Sensitivity to Alcohol Selectively in Male Offspring. PLoS One 9:e99078.

Gangisetty O, Palagani A, Sarkar DK (2020) Transgenerational inheritance of fetal alcohol exposure adverse effects on immune gene interferon-γ. Clin Epigenetics 12:70.

Govorko D, Bekdash RA, Zhang C, Sarkar DK (2012) Male Germline Transmits Fetal Alcohol Adverse Effect on Hypothalamic Proopiomelanocortin Gene Across Generations. Biol Psychiatry 72:378–388.

Hashimoto-Torii K, Kawasawa YI, Kuhn A, Rakic P (2011) Combined transcriptome analysis of fetal human and mouse cerebral cortex exposed to alcohol. Proc Natl Acad Sci U S A 108:4212–7.

Hollander J, McNivens M, Pautassi RM, Nizhnikov ME (2019) Offspring of male rats exposed to binge alcohol exhibit heightened ethanol intake at infancy and alterations in T-maze performance. Alcohol 76:65–71.

Huffman KJ, Garel S, Rubenstein JLR (2004) Fgf8 Regulates the Development of Intra-Neocortical Projections. J Neurosci 24:8917–8923.

Jacobson SW, Carter RC, Molteno CD, Stanton ME, Herbert JS, Lindinger NM, Lewis CE, Dodge NC, Hoyme HE, Zeisel SH, Meintjes EM, Duggan CP, Jacobson JL (2018) Efficacy of Maternal Choline Supplementation During Pregnancy in Mitigating Adverse Effects of Prenatal Alcohol Exposure on Growth and Cognitive Function: A Randomized, Double-Blind, Placebo-Controlled Clinical Trial. Alcohol Clin Exp Res 42:1327–1341.

Kaas JH (1995) The Segregation of Function in the Nervous System: Why Do Sensory Systems Have So Many Subdivisions? Contrib Sens Physiol 7:201–240.

Kim P, Choi CS, Park JH, Joo SH, Kim SY, Ko HM, Kim KC, Jeon SJ, Park SH, Han S-H, Ryu JH, Cheong JH, Han JY, Ko KN, Shin CY (2014) Chronic exposure to ethanol of male mice before mating produces attention deficit hyperactivity disorder-like phenotype along with epigenetic dysregulation of dopamine transporter expression in mouse offspring. J Neurosci Res 92:658–670.

Kodali VN, Jacobson JL, Lindinger NM, Dodge NC, Molteno CD, Meintjes EM, Jacobson SW (2017) Differential Recruitment of Brain Regions During Response Inhibition in Children Prenatally Exposed to Alcohol. Alcohol Clin Exp Res 41:334–344.

Komada M, Hara N, Kawachi S, Kawachi K, Kagawa N, Nagao T, Ikeda Y (2017) Mechanisms underlying neuro-inflammation and neurodevelopmental toxicity in the mouse neocortex following prenatal exposure to ethanol. Sci Rep 7:4934.

Lupton C, Burd L, Harwood R (2004) Cost of fetal alcohol spectrum disorders. Am J Med Genet 127C:42–50.

Lussier AA, Weinberg J, Kobor MS (2017) Epigenetics studies of fetal alcohol spectrum disorder: Where are we now? Epigenomics 9:291–311.

Mattson SN, Crocker N, Nguyen TT (2011) Fetal alcohol spectrum disorders: Neuropsychological and behavioral features. Neuropsychol Rev 21:81–101.

May PA, Chambers CD, Kalberg WO, Zellner J, Feldman H, Buckley D, Kopald D, Hasken JM, Xu R, Honerkamp-Smith G, Taras H, Manning MA, Robinson LK, Adam MP, Abdul-Rahman O, Vaux K, Jewett T, Elliott AJ, Kable JA, Akshoomoff N, Daniel F, Arroyo JA, Hereld D, Riley EP, Charness ME, Coles CD, Warren KR, Jones KL, Hoyme HE (2018) Prevalence of fetal alcohol spectrum disorders in 4 US communities. JAMA - J Am Med Assoc 319:474–482.

Mohammad S, Page SJ, Wang L, Ishii S, Li P, Sasaki T, Basha A, Salzberg A, Quezado Z, Imamura F, Nishi H, Isaka K, Corbin JG, Liu JS, Kawasawa YI, Torii M, Hashimoto-Torii K (2020) Kcnn2 blockade reverses learning deficits in a mouse model of fetal alcohol spectrum disorders. Nat Neurosci 23:533–543.

Nilsson EE, Sadler-Riggleman I, Skinner MK (2018) Environmentally induced epigenetic transgenerational inheritance of disease. Environ Epigenetics 4.

Przybycien-Szymanska MM, Rao YS, Prins SA, Pak TR (2014) Parental Binge Alcohol Abuse Alters F1 Generation Hypothalamic Gene Expression in the Absence of Direct Fetal Alcohol Exposure. PLoS One 9:e89320.

Rompala GR, Mounier A, Wolfe CM, Lin Q, Lefterov I, Homanics GE (2018) Heavy Chronic Intermittent Ethanol Exposure Alters Small Noncoding RNAs in Mouse Sperm and Epididymosomes. Front Genet 9:32.

Rubenstein JLR, Anderson S, Shi L, Miyashita-Lin E, Bulfone A, Hevner R (1999) Genetic Control of Cortical Regionalization and Connectivity. Cereb Cortex 9:524–532.

Subbanna S, Nagre NN, Shivakumar M, Umapathy NS, Psychoyos D, Basavarajappa BS (2014) Ethanol induced acetylation of histone at G9a exon1 and G9a-mediated histone H3 dimethylation leads to neurodegeneration in neonatal mice. Neuroscience 258:422–32.

Sulik KK, Johnston MC, Webb MA (1981) Fetal alcohol syndrome: embryogenesis in a mouse model. Science 214:936–938.

Thomas JD, Idrus NM, Monk BR, Dominguez HD (2010) Prenatal choline supplementation mitigates behavioral alterations associated with prenatal alcohol exposure in rats. Birth Defects Res Part A Clin Mol Teratol 88:827–837.

World Health Organization (2009) Harmful use of alcohol. NMH Fact Sheet. Available at: https://www.who.int/health-topics/alcohol#tab=tab_1 Accessed May 7, 2021.

Zeisel SH (2006) Choline: Critical Role During Fetal Development and Dietary Requirements in Adults. Annu Rev Nutr 26:229–250.

Zhou D, Lebel C, Lepage C, Rasmussen C, Evans A, Wyper K, Pei J, Andrew G, Massey A, Massey D, Beaulieu C (2011) Developmental cortical thinning in fetal alcohol spectrum disorders. Neuroimage 58:16–25.

Zhou D, Rasmussen C, Pei J, Andrew G, Reynolds JN, Beaulieu C (2018) Preserved cortical asymmetry despite thinner cortex in children and adolescents with prenatal alcohol exposure and associated conditions. Hum Brain Mapp 39:72–88.

Zhou Q, Song L, Chen J (2021) Association of preconception paternal alcohol consumption with increased fetal birth defect risk. JAMA Pediatr doi:10.1001/jamapediatrics.2021.0291.

Chapter 1: Prenatal ethanol exposure induces adverse, transgenerational effects within adolescent behaviors in a murine model of FASD

ABSTRACT

Fetal alcohol spectrum disorders (FASD) represent a leading cause of non-genetic neuropathologies. Recent preclinical evidence suggests that prenatal ethanol exposure (PrEE), like other environmental exposures, may have a significant, transgenerational impact on the offspring of directly exposed individuals, including altered neocortical development at birth and behavior in adolescents. How these adverse behavioral outcomes are manifested within the brain at the time of behavioral disruption remains unknown. A transgenerational mouse model of FASD was used to generate up to a third filial generation of offspring to study. Using a multi-modal battery of behavioral assays, we assessed motor coordination/function, sensorimotor processing, risk-taking behavior, and depressive-like behavior in postnatal day (P) 20 mice. Additionally, sensory cortical area connectivity using dye tracing, cortical gene expression using *in situ* hybridization, and spine density analysis of spiny stellate cells in the somatosensory cortex using Golgi-Cox staining were examined in mice at P20. We found that PrEE induces behavioral abnormalities including abnormal sensorimotor processing, increased risk-taking behavior, and increased depressive-like behaviors that extend to the F3 generation at P20. Assessment of both somatosensory and visual cortical connectivity, as well as cortical *RZRβ*

expression, yielded no significant differences amongst any experimental generations. In contrast, only directly-exposed F1 mice displayed altered cortical expression of *Id2* and decreased spine density amongst layer IV spiny stellate cells within somatosensory cortex. Our results suggest that robust, clinically-relevant behavioral abnormalities are passed transgenerationally to the offspring of mice directly exposed to ethanol. Additionally, our lack of transgenerational findings within the brain illuminates the critical need for future studies to discover the link between neurological function and heritable behavioral change. Overall, our study suggests that multi-generational effects of PrEE may have a substantial impact on human health.

INTRODUCTION

Fetal alcohol spectrum disorders, or FASD, is an umbrella term describing a group of clinically-diagnosed conditions that result from maternal consumption of alcohol, or ethanol, during pregnancy. In the United States alone, 19.6% of pregnant women report first-trimester alcohol use (England et al., 2020) and that the prevalence of FASD may be as high as 5% in children (May et al., 2018). The adverse neurobehavioral effects of prenatal ethanol exposure (PrEE) present in patients with FASD are highly diverse and represent a leading cause of preventable intellectual disability worldwide (Lange et al., 2017). However, the neuropathology underlying these deficits remains to are not well understood.

Much of what has been discovered about the underlying effects of PrEE on the developing central nervous system (CNS) has been through the use of animal models of FASD. Within the CNS, several preclinical studies have shown multi-faceted aberrations in the development of the neocortex (Cuzon et al., 2008; El Shawa et al., 2013; Komada et al., 2017; Delatour et al., 2019; 2020; Mohammad et al., 2020), the brain region responsible for many higher-order behaviors in mammals. Clinical studies in humans with FASD also report adverse outcomes in neocortex structure and function (Kodali et al., 2017; Hendrickson et al., 2018). Considering the cortical-associated behavioral disabilities in FASD, these data collectively support the notion that the neocortex may represent a focal point of ethanol's teratogenic effects. Nevertheless, the full range of PrEE-related neocortical developmental events, how they are related to neurological and behavioral impairments in later life, and the underlying mechanisms are still unclear.

Precise epigenetic regulation, or the control of gene expression not related to changes in DNA sequence, is crucial for the complex development of the neocortex (Adam and Harwell, 2020; Lewis et al., 2021). Notably, PrEE induces widespread epigenetic dysregulation with the developing rodent cortex (Subbana et al., 2014; Öztürk et al., 2017), forming an attractive hypothesis for the underlying mechanism driving FASD-associated adverse outcomes as one that may be epigenetically-driven.

Another relevant question that is particularly important to human health, is does PrEE have the ability to produce heritable, transgenerational effects in offspring that are not directly exposed to ethanol? Substantial recent evidence has suggested that varied environmental exposures may produce transgenerational inheritance of disease phenotypes that are epigenetically driven (Nilsson et al., 2018). Indeed, several recent reports have suggested that phenotypic variation induced by PrEE can extend several generations (Govorko et al., 2012; Gangisetty et al., 2020), likely via epigenetic modifications (Chastain and Sarkar, 2017).

Still, it is not fully understood how these findings apply to neocortical development and how they may ultimately produce detrimental behavioral outcomes. Recently, our lab found distinct phenotypes within cortical development, including altered gene expression and cortical connectivity in newborn mice and behavioral abnormalities that mirror those in patients with FASD in adolescent mice; these phenotypes extended to the F3 generation following a single generation (F1) prenatal ethanol exposure (Abbott et al., 2018). However, exactly how cortical dysfunction may underlie the robust behavioral disruptions seen in later life, as well as if other clinically-relevant behaviors are affected, also remains unclear.

Here, we confirm and extend these findings by assessing several, multi-modal behavioral phenotypes, as well as several facets of typical cortical characteristics in P20 mice using our established transgenerational mouse model

of FASD. Specifically, we found robust behavioral disruption that extended multiple generations due to PrEE, including sensorimotor processing, risk-taking behavior, as well as depressive-like behavior. After assessing P20 gross CNS morphology, sensory cortical connectivity, relevant gene expression, and cortical neuron spine density, we found that only the directly-exposed F1 generation display deficits in these measures, including reduced spine density in somatosensory spiny stellate cells and altered *Id2* expression. Overall, our results suggest that substantial behavioral abnormalities are passed transgenerationally following PrEE and that the particular neurological changes driving these phenomena remain to be discovered. Outcomes from this study support the notion that the negative effects of PrEE are impactful beyond even the directly exposed offspring and may require further consideration within humans.

MATERIALS AND METHODS

Transgenerational FASD mouse model.

All studies were conducted under a research protocol approved by the Institutional Animal Care and Use Committee at the University of California, Riverside. All control and experimental mice used in this study were of CD1 background, originally purchased from Charles River Laboratories International, Inc. (Wilmington, Massachusetts, USA) were housed under normal illumination conditions (12-hour light/dark cycle). For this study, we utilized a

transgenerational FASD model previously established by our laboratory to generate control, F1, F2, and F3 subjects (Fig. 1.1). Full details on this transgenerational model are described elsewhere (Abbott et al., 2018). The male germline was used to produce subsequent generations following a single generation ethanol exposure. Briefly, 8-10 week old mice were paired for mating. Upon confirmation of vaginal plug, F0 dams were exposed to 25% ethanol in water (experimental) or water (control) *ad libitum* throughout gestation. EtOH-exposed dams gave birth to directly-exposed F1 mice. Subsets of first filial 8-10 week old generation (F1) males were bred with alcohol-naïve females to produce a subsequent F2 generation, where this process was repeated to produce a final F3 generation. The assurance of proper maternal nutrition in our transgenerational FASD mouse model including measures of weight gain, food and liquid intake, blood ethanol content, and blood osmolality has been previously documented (Abbott et al., 2018). Upon birth (P0), pups from ethanol-treated dams (F1, F2, and F3) and control dams were cross-fostered with alcohol-naïve dams. Once mice reached P20, subsets of litters were subjected to behavioral testing, or were sacrificed and used for brain-based examination. For each experimental generation, control animals were included during testing. Pups included for analysis were limited to 1 per litter for brain-based analysis and 2 per litter for behavioral analysis to limit litter effects. All experimental replicates per group (*n*) are reported in Table 1.1.

Brain tissue preparation and measures.

Following behavioral testing, PrEE F1, F2, F3 and control animals were given a lethal dose of sodium pentobarbital (100 mg/kg) and were transcardially perfused with 4% paraformaldehyde (PFA) in 0.1M phosphate buffer (pH 7.4). Brains were then extracted from the skull, post-fixed in PFA for 24-hours and hemisected. A separate subset of brains from each group was reserved for dendritic spine density analyses and were stored in 4% PFA for no longer than two months.

P20 pup and brain measures.

At P20, prior to behavioral testing, body weight measurements took place in order to assess general development in F1, F2, F3 and control mice. Standard weight measurements (in grams) took place using a standard Fisher Scientific scale. After perfusion and dissection of P20 brain tissue, brain weights in all groups were also performed using a standard scale. Following weighing, dorsal views of whole brains were acquired using a digital high-resolution Zeiss Axio camera attached to a Zeiss Stereo Discovery V12 stereomicroscope using Axiovision software (Version 4.7). In all groups, cortical lengths were obtained from dorsal view images using an electronic micrometer in ImageJ (NIH).

Anatomical tracing techniques and analyses.

Ipsilateral patterns of intraneocortical connections in control and PrEE F1, F2, and F3 P20 mice were examined by placing single DiI and DiA crystals in somatosensory and visual cortices. Dye crystal placement reliability across

experimental and control cases was promoted by using a dye placement grid in order to position crystals in a morphologically defined area. Following dye placement, brains were re-immersed in 4% PFA and stored in room temperature for 8-12 weeks to allow for transport of the tracer. F1, F2, F3 and control tissue was then embedded in 5% low melting point agarose and sectioned in the coronal plane at 100µm using a Vibratome. Sections were then counterstained with crystallized 4',6-diamidine-2-phenylindole dihydrochloride (DAPI; Roche, Nutley, NJ, USA), mounted onto glass slides, coverslipped using Vectashield mounting medium for fluorescence (Vector Laboratories, Inc., Burlingame, CA, USA) and photographed with a digital high-resolution Zeiss Axio camera using Axiovision software (Version 4.7). Anatomical tracing sections were analyzed using a Zeiss Axio Imager Upright Microscope equipped with fluorescence at 40x magnification. All fluorescent sections were digitally imaged three times for analysis of dye tracing experiments using three filters: blue for DAPI counterstain, red for DiI, and green for DiA labeling. Captured images were then combined in a high-resolution format for analysis. To analyze the effects of transgenerational PrEE on INCs at P20, sections from experimental and control brains were matched using anatomical landmarks. In depth tracing methodology has been previously described elsewhere (El Shawa et al., 2013; Abbott et al., 2018).

Gene expression assays and analysis.

Standard non-radioactive free-floating *in situ* RNA hybridization methods (Dye et al., 2011a; 2011b; El Shawa et al., 2013) were used to visualize patterns of $RZR\beta$ and *Id2* expression in F1, F2, F3, and control neocortical tissue. Briefly, post-fixed hemispheres were embedded in gelatin-albumin and sectioned at 100µm in the coronal plane using a Vibratome. Following hybridization to probes for $RZR\beta$ and *Id2* (gifts from John Rubenstein, UCSF), all sections were mounted in glycerol onto glass slides, cover slipped and photographed with a digital high-resolution Zeiss Axio camera using Axiovision software (Version 4.7). Both experimental and control sections were analyzed using a bright field on a Zeiss Stereo Discovery V12 stereomicroscope. Gene expression data, from ISH techniques, were used as qualitative measures for positional expression in F1, F2, F3, and control neocortex. To do this, sections were viewed side-by-side so that expression levels in exact or near-exact anatomical levels could be qualitatively compared. Trained researchers, who were blind to condition, carefully examined tissue for phenotypic differences. Following qualitative analyses, ImageJ software was used to statistically analyze *Id2* transcript positional levels between experimental groups. In order to quantify a visually-identified medial shift in layer II/III *Id2* expression in caudal cortex (at the level of visual cortex) of experimental brains, the distance from the midline to the furthest lateral point of robust layer II/III *Id2* expression was measured in brains from all groups using an electronic micrometer in ImageJ.

Spine density measurements.

To assess the impact of transgenerational FASD on dendritic spine development within the neocortex, a modified Golgi-Cox stain (GCS) protocol was used. Directly derived from two recent papers (Bayram-Weston et al., 2016; Zaquot and Kaindl, 2016), this particular modified GCS protocol was chosen for its ability to stain dendritic spines in extended post-fixed brain tissues (up to 2 months in 4% PFA). First, GCS stain was generated using two distinct solutions whose compositions are as follows: *Solution A.* 100 ml of 5% potassium dichromate solution (Sigma-Aldrich, no. P5271, USA) stirred into warm deionized water, with 100 ml 5% mercuric chloride (Sigma-Aldrich, no. M136, India) stirred into hot deionized water. *Solution B.* 200 ml of dH_2O and 80 ml of 5% potassium chromate (Sigma-Aldrich, no. 216615, USA) stirred into cold deionized water. Solution A was then slowly poured into solution B with constantly stirring. Following correct mixing, a red yellow precipitate was formed.

Following GCS generation, hemisected brains from all 4 groups were placed into small, clean glass bottles that contained 15-20 mL of GCS. After 1 day, GCS was replaced with a fresh solution. Brains remained submerged in GCS in the dark for 14 days. After 14 days, brains were briefly blotted and washed with PBS to remove excess GCS, then placed in 15-20 mL of 30% sucrose/0.1 M phosphate-buffered saline (PBS) in foil-covered container in 4°C until brains sank to the bottom (~3 days). As a note, 30% sucrose/PBS solution was also removed and replenished after 1 day of submersion. Following

23

confirmation of sinking, hemisects were embedded in 5% agarose and sliced via Vibratome at 150μm in the coronal plane. Sections collected in 30% sucrose/PBS were then mounted onto gelatin-coated "subbed" slides and were left to dry in racks in the dark for 2-3 days.

After drying, slides were developed by placing them into standard histological staining racks and submerging them through a series of solutions as follows: 1.) Distilled water twice for 5 min each 2.) 20% ammonia solution for 10 min 3.) Distilled water twice for 5 min each 4.) 70, 95, and 100% ethanol for 5 min each and 5.) Xylene for 40 min. Immediately after removal from Xylenes, slides were cover slipped with Permount (Fisher Scientific, #SP15-500). Special care was taken to coverslip immediately due to rapid drying of sections following removal from Xylenes. Cover slipped slides were kept in a horizontal slide box in the dark for 2 days prior to imaging.

Immediately before imaging, primary somatosensory cortex (S1) was located in Golgi-Cox stained sections using anatomical landmarks. All cells within these sections were imaged using brightfield microscopy at 630X magnification using a Leica DFC 450C camera attached to a Leica Dmi8 microscope using Leica Application Suite software (version 4.6.0). Within S1, spiny stellate cells (confirmed via morphological characteristics) within layer IV were chosen to be imaged using random sampling. For S1 spiny stellate cell spine density measurements, a combination of primary and secondary branch dendrites were analyzed.

Following imaging, spine densities (spines/μm) for individual cells were calculated by manually counting all spines on a particular dendrite with a known dendritic length (as measured by an electronic micrometer in ImageJ). All manual spine counting was accomplished by a trained researcher blind to experimental condition.

Behavioral methods and analyses.

For all behavioral testing, mice were acclimated to the dimly-lit behavior room for at least 1 hour prior to testing. All behavioral apparatuses were thoroughly disinfected and cleaned between subjects.

Accelerated rotarod**:** The Accelerated rotarod is a behavioral assay that is used to measure motor coordination, balance and learning ability in mice (Pritchett and Mulder, 2003). The Rotarod apparatus is composed of a rotating rod separated into 5 lanes by 4 plastic dividers. On the day of testing, mice were brought into the behavioral testing room in their home-cage and acclimated for 1 hour prior to testing. Post-acclimation, control and PrEE F1, F2, and F3 mice were tested on the rod apparatus, which accelerates from 4-40 rpm over a 5-minute trial period. Latency to fall from the rotating bar was recorded for each animal during 4 consecutive 5-minute trials, with each test trial being separated by a 30-minute interval.

Adhesive removal test: The adhesive removal test is a method previously used in mice to assess sensorimotor deficits in mice. The animal's somatosensory and

motor function is evaluated by measuring the time needed to sense and remove adhesive tape strips from the snout (Fleming et al., 2013). The test mouse was scruffed by the experimenter, followed by the placement of an adhesive label onto the snout with the use of small forceps and released. Latency to remove the label with the forepaws was recorded. In the case where the mouse did not remove the sticker within 90 seconds, the trial was ended, and the experimenter removed the sticker manually. All mice received 3 trials, with each trial separated by a 10-minute interval.

Forced swim test: The forced swim test is a common test used for evaluation of behavioral and neurobiological manipulations, particularly depressive-like states (Petit-Demouliere et al., 2005). The forced swim apparatus consisted of an acrylic glass cylinder, approximately 30 cm in height and 13 cm in diameter. Two-thirds of the cylinder was filled with room temperature water, with a video camera placed directly adjacent to the apparatus. All mice were assessed for a total of 6 minutes, however the first 2 minutes of activity is considered an adaptive period, therefore only the last 4 minutes of the testing session were scored. All mice were scored by trained-experimenters blind to condition for the total time spent immobile within the singular trial.

Elevated plus maze: The elevated plus maze test is a useful method typically employed to assess anxiety-related behaviors in rodents (Pellow et al., 1985). However, in young ages, CD-1 mice are known to defy these notions as they typically interact with the lower anxiety-associated open-arm regions at much

higher proportions, thought to reflect risk-taking behavior (Macrí et al., 2002). The plywood elevated plus maze apparatus was elevated 50 cm above the floor and consisted of four arms, 54 cm wide and 30 cm long aligned perpendicularly. Two arms were enclosed by 15 cm high-walls and the other two arms were exposed. The maze was placed in the center of the behavioral testing room with a video camera located directly above it. Post-habituation, each animal was placed in the center of the elevated plus maze facing an open arm and left on the maze for a 5-minute testing period. Time spent in the open arm, closed arm and center, as well as number of arm entries were scored from the video recordings.

Statistical Analyses.

All statistical analyses took place using GraphPad Prism 8 software (La Jolla, CA, USA). For all group comparisons, ordinary 1-way ANOVA followed by Tukey's multiple comparisons post-hoc tests were used, with the exception of the Adhesive Removal and Accelerated Rotarod behavioral analyses. For these measurements, repeated-measures 2-way ANOVAs (factors: trial and treatment) with Tukey's post-hoc tests were used. For all statistical tests, a *P*-value of >0.05 was used to establish significance. Full *P* value summaries of all pairwise comparisons are contained within Table 1.2. All data is presented as mean ± SEM.

RESULTS

Ethanol-induced transgenerational effects on complex animal behaviors.

Initially, F1, F2, and F3 mice were assessed for ethanol-induced behavioral effects in several distinct modalities at P20, a prepubescent age. First, motor function/coordination and learning were examined via the Accelerated Rotarod, where all mice were given 4 trials spaced 30 minutes apart within a single day of testing (Fig. 1.2A). A 2-way repeated-measures ANOVA revealed significant effects of trial [$F_{2.768,88.57}$= 24.39, P < 0.0001], treatment [$F_{3,32}$= 9.146, P = 0.0002], and a significant trial x treatment interaction [$F_{9,96}$= 2.108, P = 0.0453] in the Rotarod test. Post hoc tests revealed a significant decrease within trial 1 of F1 mice compared to controls (control: 228.3 ± 18.29 s, F1: 108.9 ± 7.228 s, ***P = 0.0005) and a significant decrease for both F1 and F2 mice compared to controls in trial 2 (control: 263.2 ± 27.47 s, F1: 106.6 ± 5.925 s, **P = 0.0018; F2: 145.4 ± 22.82 s, *P = 0.0218). However, F1 and F2 mice are not statistically significant from controls in trials 3 and 4, and F3 mice show no differences amongst all 4 trials, suggesting the motor coordination dysfunction that extends transgenerationally is recovered by the third filial generation and does not produce short-term motor learning impairments.

Next, sensorimotor processing and fine motor skills were examined via the Adhesive Removal task (Fig. 1.2B), where mice were given 3 trials, spaced 10 minutes apart within a single testing day. 2-way repeated-measures ANOVA showed a significant effect on trial [$F_{1.895,75.78}$= 6.476 , P = 0.0030] and treatment

[$F_{3,40}$= 7.722, P = 0.0003] within this test. Post hoc analyses displayed a

significant increase in time spent removing the adhesive in F1, F2 and F3 mice

compared to controls in Trial 1 (control: 21.97 ± 3.125 s, F1: 50.81 ± 4.307 s, *P

=0.0469; F2: 46.68 ± 3.434 s, *P = 0.0488; F3: 48.56 ± 3.327 s, *P = 0.0465),

and a significant increase in F2 mice compared to controls in Trial 2 (control:

34.22 ± 3.466 s, F2: 47.94 ± 3.137 s, * P = 0.0379), suggesting PrEE-induced

perturbed sensorimotor processing and fine motor skill is passed

transgenerationally.

Anxiety-like and risk-taking behavior was also assessed in all 3

experimental groups at P20 via the elevated plus maze (Fig. 1.2C). 1-way

ANOVA revealed a significant effect of treatment on time spent in the open arms

of the maze [$F_{3,28}$= 4.517, P = 0.0105], and post hoc tests revealed all 3

experimental groups showed a significant increase in time spent in the open

arms compared to controls (control: 23.88 ± 5.633 s, F1: 60.13 ± 9.480 s, *P

=0.0179; F2: 63.63 ± 10.80 s, *P = 0.0310; F3: 57.13 ± 7.296 s, *P = 0.0371),

suggesting that the normally elevated levels of risk-taking behavior in adolescent

CD-1 mice on this task (Macrí et al., 2002) are even greater in mice

transgenerationally-exposed PrEE mice.

Lastly, depressive-like behavior was evaluated via the Forced Swim Test

(Fig. 1.2D), and a significant effect of treatment was found on the time spent

immobile within this test [$F_{3,28}$= 4.647, P = 0.0093]. Post hoc tests revealed a

significant increase in time spent immobile in all 3 experimental generations

compared to controls (control: 39.24 ± 4.449 s, F1: 73.40 ± 6.598 s, *P =0.0270 ;

F2: 70.90 ± 7.616 s, *P = 0.0135 ; F3: 70.04 ± 10.49, *P = 0.0474), suggesting

increased depressive-like behavior due to PrEE that extends to the 3rd filial

generation. In summary, multi-modality behavioral testing revealed critical

impairments in several complex behaviors in adolescent mice that are passed

transgenerationally following single generation PrEE.

Effects of transgenerational ethanol exposure on body and brain development.

To first assess the impact of transgenerational PrEE on body and brain

development, body weights, brain weights, and cortical lengths were measured in

P20 mice across F1, F2 and F3 generations (Fig. 1.3). 1-way ANOVA analysis

showed a significant effect of treatment on P20 body weight [$F_{3,39}$= 12.67, *P* <

0.0001], and post hoc tests revealed a significant reduction in F1 body weight

compared to controls (Fig. 1.3A; control: 10.97 ± 0.6452 g, F1: 7.953 ± 0.3754 g,

***P = 0.0009). A significant effect of treatment was also present in both brain

weight [$F_{3,24}$= 5.565, *P* = 0.0045] and cortical length [$F_{3,20}$= 6.808, *P* = 0.0024]

measurements at P20 (Fig. 1.3B, 1.3C). Similar to P20 body weights, post hoc

tests revealed only a reduction in the F1 generation for both brain weight (Fig.

3B; control: 0.4004 ± 0.0107 g, F1: 0.3780 ± 0.0186 g, **P = 0.0084) and cortical

length (Fig. 1.3C; control: 7.619 ± 0.1385 g, F1: 6.875 ± 0.1125 g, **P = 0.0045)

compared to control animals. Overall, these results suggest that in prepubescent

mice, only the directly-exposed F1 generation display any significant effects of

PrEE on overt body and brain development, where the cortex is particularly susceptible to PrEE's effects.

Assessment of cortical connectivity of sensory areas.

Precise connectivity of cortical areas is required for the expression of complex behaviors and transgenerational ethanol-induced disorganization of sensory area intraneocortical connections (INCs) are present in newborn mice (Abbott et al., 2018). Here, we examined whether these early-life alterations persist in P20 mice, using lipophilic dye tracing (Fig. 4). Single hemispheres from all 3 experimental generations and control mice were assessed for cortical connectivity via green DiA crystal placements into somatosensory cortex (Fig. 1.4B1-4) and red DiI crystal placements into visual cortex (Fig. 1.4D1-4) and patterns of INCs were analyzed within a rostral to caudal series of coronal sections. Overall, no distinct differences were found amongst any of the 3 experimental generations compared to controls. Typical patterns of adolescent connectivity were found for somatosensory cortex, including labeled cells within somatosensory subareas and motor cortex in all mice. Visual cortex analysis yielded similar results, with all groups displaying typical connectivity patterns including labelled cells within cingulate, retrosplenial and visual areas. In summary, no discernible changes in sensory cortex connectivity patterns were present in P20 mice due to transgenerational PrEE, suggesting that the drastic

disorganization seen in newborn mice (Abbott et al., 2018) is recovered by this age.

Cortical gene expression: RZRβ and Id2.

Spatially and temporally-defined gene expression patterns guide key developmental events within the early postnatal cortex, including axonal targeting, outgrowth and synaptogenesis, which sculpt mature neural circuits. Newborn mice exposed to PrEE display altered expression patterns of key genes for cortical layer and area specification which are also passed transgenerationally, including *RZRβ* and *Id2* (Abbott et al., 2018). Here, we examined expression patterns of these two genes within P20 cortical using *in situ* hybridization in all 3 experimental generations and controls. Representative F1, F2, F3 and control cases are presented in rostral to caudal order of coronal sections for *RZRβ* (Fig. 1.5) and *Id2* (Fig. 1.6). For *RZRβ*, typical cortical expression patterns were found in all groups including strong layer-specific expression largely localized to layer IV, as well as area-specific patterns including robust somatosensory whisker barrel field expression, suggesting PrEE-induced transgenerational changes in *RZRβ* expression are recovered by adolescence in mice.

Expression patterns of *Id2* are highly dynamic across both cortical areas and layers (Rubenstein et al., 1999). Anatomically-matched section analysis revealed largely similar patterns of Id2 at P20 amongst the F1, F2, F3, and

control mice, particularly within rostral and medial sections (Fig. 1.6). Notably in caudal cortical sections, control mice typically displayed a strong, superficial layer expression band that wraps around the medial cortical wall and encapsulates primary visual, secondary visual, and retrosplenial cortices, as previously reported (Dye et al., 2011b). However, in F1 mice, the lateral limit of this expression band is shifted medially and does not extend to the position seen in control mice (Fig. 1.6A4, B4, arrows). However, in F2 and F3 cases (Fig. 1.6C4, D4) this lateral limit is phenotypically similar to controls, suggesting this phenomenon may not be transgenerationally passed.

To confirm this qualitative assessment of ID2 expression, we utilized a simple measurement from the midline of all cases to measure the lateral limit of this superficial expression band (Fig. 1.7). 1-way ANOVA of this measurements revealed a significant effect of treatment on the distance from the midline [$F_{3,13}$= 3.916, P = 0.0341], and post hoc tests revealed that this effect was largely driven by F1 mice, as only the F1 generation was shown to have a significant decrease in this measure compared to controls (control: 1.037 ± 0.0453 mm, F1: 0.7605 ± 0.0652 mm, *P = 0.0217). Overall, altered expression of *Id2* was found in P20 F1 mice, similar to deficits seen at P0 (Abbott et al., 2018), however F2 and F3 generations do not display such *Id2* expression differences suggesting that these PrEE-induced changes persist at P20 only in directly-exposed mouse offspring.

Spine density analyses within primary somatosensory cortex.

Spine density within cortical areas is associated with sensory processing (Pyronneau et al., 2017) and has also been correlated to alterations in behavioral outputs (Fox et al., 2020) To further uncover potential mechanisms underlying the strong behavioral dysfunction seen in mice exposed to prenatal ethanol transgenerationally, we investigated neuronal spine density within primary somatosensory cortex (S1). Specifically, spine densities were quantified in spiny stellate cells residing in layer IV of S1 following modified Golgi-Cox staining in F1, F2, F3 and control mice (Fig. 1.8)

Following quantification, 1-way ANOVA showed a significant effect of treatment on S1 spiny stellate cell spine density [$F_{3,54}$= 10.19, P < 0.0001]. Post hoc tests revealed a significant decrease in spine density in F1 compared to controls (control: 1.245 ± 0.0483 spines/µm, F1: 0.9872 ± 0.0356 spines/µm, **P = 0.0016). However, no differences were present between F2 or F3 mice compared to controls, suggesting that PrEE-induced reductions in S1 spine density are not passed transgenerationally.

DISCUSSION

In this study, we demonstrate robust behavioral disruptions in adolescent mice exposed to prenatal ethanol transgenerationally. F1, F2, and F3 mice display sensory processing deficits, increased risk-taking behavior, as well as increased depressive-like behavior. However, following a multi-level analysis of several key

neocortical components including sensory area connectivity, gene expression, and spine density analysis, we found no evidence of heritable, transgenerational phenotypes due to PrEE at P20 within the measures assessed. In contrast, F1 mice display decreased brain/body weights, altered *Id2* expression, and reduced spine density in S1 neurons, providing further insight into the underlying etiology of direct PrEE. Our findings highlight the need for an expanded, in-depth analysis of CNS aspects which may be driving the highly-stable behavioral phenotypes associated with transgenerational PrEE.

Transgenerational impact of PrEE on adolescent behavior.

Humans with FASD display sensory processing deficits (Jirkowic et al., 2020), increased risk-taking behavior and poor impulse control (Streissguth et al., 2004; Furtado et al., 2016), as well increased incidence of depression (O'Connor et al., 2002). Here, we found rodent behavioral correlates that mirror these FASD phenotypes are present within directly exposed offspring and also extend to F2 and F3 generations. These results support the notion that PrEE may have a much more lasting effect than previously thought, including the possibility of behavioral phenotypic penetrance to the offspring of FASD patients. Although yet to be explored within a clinical population, our findings confirm and extend our previous report, where transgenerational inheritance of anxiety-like behaviors and sensorimotor dysfunction was described in several generations of PrEE offspring (Abbott et al., 2018). Our research also adds to the growing collective of

transgenerational behavioral effects in rodent models of environmental

exposures including opiod and (Vassoler and Byrnes, 2021), cocaine exposure

(Le et al., 2017), as well as early postnatal stress (van Steenwyck et al., 2018).

Interestingly, despite the presence of several transgenerational behavioral

phenotypes due to PrEE, F1 mice display increased severity in some of these

phenotypes (i.e. within Accelerated Rotarod and Adhesive Removal tests).

Overall, these results suggest that environmental exposures, including PrEE,

may carry significant risk of abnormal behaviors for several generations of

offspring.

Lack of evidence for PrEE-induced transgenerational brain phenotypes in

adolescence.

Despite robust behavioral deficits that extend several generations, our multi-level

attempts were unsuccessful in finding any significant transgenerational changes

within the neocortex, suggesting that the neurological source(s) underlying the

altered behaviors have yet to be found. Previous reports have suggested that

PrEE-induced disrupted patterns of sensory cortex INCs in newborn mice may

underlie the described behavioral disruptions in adolescence (El Shawa et al.,

2013; Bottom et al., 2020), that were also present transgenerationally (Abbott et

al., 2018). However, using our methodology, we found no clear transgenerational

evidence for grossly disrupted sensory cortical area connectivity patterns due to

PrEE, even within the F1 generation, at P20, suggesting this effect may be

recovered by this age. However, as lipophilic dye tracing is not cell or direction-specific (Perrin and Stoeckli, 2000), it remains unclear if any cell-type specific or synapse-specific characteristics within these or a combination of other circuits are altered at P20, and how they may ultimately contribute to the transgenerationally-stable behavioral phenotypes. Additionally, functional deficits, which are not able to be probed by dye tracing and have been previously described within rodent cortex due to PrEE (Granato et al., 2012; Delatour et al., 2020). These deficits may also contribute to the behavioral phenotypes seen in F2 and F3 mice, as proper functional connectivity is essential for complex behaviors.

Regardless of the lack of transgenerational findings within this study, we report several novel phenotypes within the directly exposed F1 brains that may be instrumental for the presence of FASD-like behaviors. These findings include reduced brain weight and cortical length, altered cortical *Id2* expression, as well as reduced spine density within spiny stellate cells in layer IV of S1. The reported brain size reductions, especially within the neocortex, are associated with several diseases that display cognitive deficits (Hu et al., 2014), likely influencing the behavioral phenotypes of F1 mice.

Id2, or inhibitor of DNA binding 2, is a transcription factor important for several aspects of CNS development, including axonal outgrowth (Konishi et al., 2004, Huang et al., 2019) and proper positioning of subcerebral-projection neurons within the neocortex (Maruoka et al., 2011). Our results suggest that

these processes, or others, may be disrupted as a result of the consistent, shifted expression patterns of *Id2* in caudal cortex in F1 mice and may contribute to the altered behaviors seen in the same mice.

Finally, spiny stellate cells are a major excitatory neuron class within cortical layer IV which are essential to sensory signal processing (Schubert et al., 2003), and show reduced spine density within the somatosensory cortex of F1 mice, as reported here. As proper maintenance of spine density is essential for precise sensory processing (Sweet et al., 2008; Pyronneau et al., 2017), the reduced spine density in F1 mice seen here may directly underlie the somatosensory processing deficits within F1 mice also described within the Adhesive Removal test. Spine density has recently been correlated with behavioral outputs (Fox et al., 2020), providing further evidence for this potential underlying feature. Collectively, the differences seen in brain weight/size, *Id2* expression and stellate cell spine density may account for, at least in part, to the increased PrEE-induced severity of behavioral disruption in F1 mice discussed above.

Potential mechanisms underlying transgenerational inheritance.
It is equally important to find the driving mechanisms that may underlie the now unknown circuit/brain changes and the described behavioral disruptions within transgenerational PrEE offspring. Recent reports within animal models of PrEE have suggested transgenerational epigenetic inheritance may play a key role in

inducing adverse phenotypes in offspring (Govroko et al., 2012; Abbott et al.,
2018; Gangisetty et al., 2020). However, this proposed mechanism is still a topic
of debate (Horsthemke, 2018), largely due to the vast majority of the mammalian
epigenome undergoing resetting in very early development (Xia and Xie., 2020).
Despite this, evidence has suggested some epigenetic marks are resistant to
resetting and may act as candidates for epigenetic inheritance (Tang et al.,
2015). Recently, sperm RNA, histone modification, and DNA methylation has
been directly implicated in epigenetic inheritance of adverse phenotypes (Gapp
et al., 2014; Raad et al., 2021; Beck et al., 2021), providing credence to this
burgeoning mechanistic view on the impact environmental exposures have on
future generations of offspring. Whether these phenomena are contributing to the
transgenerational effects of PrEE has yet to be explored and should remain a key
point of interest in future studies.

Conclusions.

Here, we provide direct evidence for PrEE-induced transgenerational disruption
of clinically-relevant behavioral phenotypes in a mouse model of FASD, including
altered sensory processing, risk-taking behavior, and depressive-like behavior.
Although no mechanistic evidence was found for neurological impairments in
transgenerationally-exposed mice, we describe several novel phenotypes in
directly exposed F1 mice. These phenotypes included altered cortical *Id2*
expression and reduced spine density of spiny stellate cells within S1. Future

directions should include in-depth investigations into the CNS-based phenotypes which may be driving transgenerational behavioral deficits due to PrEE, including further circuit-based analyses, physiological/functional analyses, as well as analyses of genes important for circuit maturation and maintenance. Further studies should also aim to directly correlate the potential epigenetic mechanisms and the transgenerational inheritance of these detrimental phenotypes. Results from this study support the idea that environmental exposures, like PrEE, can produce drastic effects in future generations of offspring, a still-emerging concept highly important to human health.

REFERENCES

Adam MA, Harwell CC (2020) Epigenetic regulation of cortical neurogenesis; orchestrating fate switches at the right time and place. Curr Opin Neurobiol. 63:146-153.

Bayram-Weston Z, Olsen E, Harrison DJ, Dunnett SB, Brooks SP (2016) Optimising Golgi-Cox staining for use with perfusion-fixed brain tissue validated in the zQ175 mouse model of Huntington's disease. J Neurosci Methods 265:81–88.

Beck D, Ben Maamar M, Skinner MK (2021) Integration of sperm ncRNA-directed DNA methylation and DNA methylation-directed histone retention in epigenetic transgenerational inheritance. Epigenetics and Chromatin 14:1–14.

Chastain LG, Sarkar DK (2017) Alcohol effects on the epigenome in the germline: Role in the inheritance of alcohol-related pathology. Alcohol. 60:53-66.

Cuzon VC, Yeh PWL, Yanagawa Y, Obata K, Yeh HH (2008) Ethanol Consumption during Early Pregnancy Alters the Disposition of Tangentially Migrating GABAergic Interneurons in the Fetal Cortex. J Neurosci 28:1854–1864.

Delatour LC, Yeh PWL, Yeh HH (2020) Prenatal Exposure to Ethanol Alters Synaptic Activity in Layer V/VI Pyramidal Neurons of the Somatosensory Cortex. Cereb Cortex 30:1735–1751.

Delatour LC, Yeh PW, Yeh HH (2019) Ethanol Exposure *In Utero* Disrupts Radial Migration and Pyramidal Cell Development in the Somatosensory Cortex. Cereb Cortex 29:2125–2139.

Dye CA, El Shawa H, Huffman KJ (2011) A lifespan analysis of intraneocortical connections and gene expression in the mouse I. Cereb Cortex 21:1311–1330.

Dye CA, El Shawa H, Huffman KJ (2011) A lifespan analysis of intraneocortical connections and gene expression in the mouse II. Cereb Cortex 21:1331–1350.

El Shawa H, Abbott CW, Huffman KJ (2013) Prenatal Ethanol Exposure Disrupts Intraneocortical Circuitry, Cortical Gene Expression, and Behavior in a Mouse Model of FASD. J Neurosci 33:18893–18905.

England LJ, Bennett C, Denny CH, Honein MA, Gilboa SM, Kim SY, Guy GP, Tran EL, Rose CE, Bohm MK, Boyle CA (2020) Alcohol Use and Co-Use of Other Substances Among Pregnant Females Aged 12–44 Years — United States, 2015–2018. MMWR Morb Mortal Wkly Rep 69:1009–1014.

Fleming SM, Ekhator OR, Ghisays V (2013) Assessment of sensorimotor function in mouse models of Parkinson's disease. J Vis Exp 76:50303.

Furtado EF, Roriz ST de S (2016) Inattention and impulsivity associated with prenatal alcohol exposure in a prospective cohort study with 11-years-old Brazilian children. Eur Child Adolesc Psychiatry 25:1327–1335.

Gangisetty O, Palagani A, Sarkar DK (2020) Transgenerational inheritance of fetal alcohol exposure adverse effects on immune gene interferon-γ. Clin Epigenetics 12:70.

Gapp K, Jawaid A, Sarkies P, Bohacek J, Pelczar P, Prados J, Farinelli L, Miska E, Mansuy IM (2014) Implication of sperm RNAs in transgenerational inheritance of the effects of early trauma in mice. Nat Neurosci 17:667–669.

Govorko D, Bekdash RA, Zhang C, Sarkar DK (2012) Male Germline Transmits Fetal Alcohol Adverse Effect on Hypothalamic Proopiomelanocortin Gene Across Generations. Biol Psychiatry 72:378–388.

Granato A, Palmer LM, de Giorgio A, Tavian D, Larkum ME (2012) Early exposure to alcohol Leads to Permanent Impairment of dendritic Excitability in Neocortical pyramidal neurons. J Neurosci 32:1377–1382.

Hendrickson TJ, Mueller BA, Sowell ER, Mattson SN, Coles CD, Kable JA, Jones KL, Boys CJ, Lee S, Lim KO, Riley EP, Wozniak JR (2018) Two-year cortical trajectories are abnormal in children and adolescents with prenatal alcohol exposure. Dev Cogn Neurosci 30:123–133.

Horsthemke B (2018) A critical view on transgenerational epigenetic inheritance in humans. Nat Commun 9:2973.

Hu WF, Chahrour MH, Walsh CA (2014) The diverse genetic landscape of neurodevelopmental disorders. Annu Rev Genomics Hum Genet 15:195–213.

Huang Z, Liu J, Jin J, Chen Q, Shields LBE, Zhang YP, Shields CB, Zhou L, Zhou B, Yu P (2019) Inhibitor of DNA binding 2 promotes axonal growth through upregulation of Neurogenin2. Exp Neurol 320:112966.

Jirikowic TL, Thorne JC, McLaughlin SA, Waddington T, Lee AKC, Astley Hemingway SJ (2020) Prevalence and patterns of sensory processing behaviors in a large clinical sample of children with prenatal alcohol exposure. Res Dev Disabil 100:103617.

Kodali VN, Jacobson JL, Lindinger NM, Dodge NC, Molteno CD, Meintjes EM, Jacobson SW (2017) Differential Recruitment of Brain Regions During Response Inhibition in Children Prenatally Exposed to Alcohol. Alcohol Clin Exp Res 41:334–344.

Komada M, Hara N, Kawachi S, Kawachi K, Kagawa N, Nagao T, Ikeda Y (2017) Mechanisms underlying neuro-inflammation and neurodevelopmental toxicity in the mouse neocortex following prenatal exposure to ethanol. Sci Rep 7:4934.

Konishi Y, Stegmüller J, Matsuda T, Bonni S, Bonni A (2004) Cdh1-APC Controls Axonal Growth and Patterning in the Mammalian Brain. Science (80-) 303:1026–1030.

Lange S, Probst C, Gmel G, Rehm J, Burd L, Popova S (2017) Global prevalence of fetal alcohol spectrum disorder among children and youth: A systematic review and meta-analysis. JAMA Pediatr 171:948–956.

Le Q, Yan B, Yu X, Li Y, Song H, Zhu H, Hou W, Ma Di, Wu F, Zhou Y, Ma L (2017) Drug-seeking motivation level in male rats determines offspring susceptibility or resistance to cocaine-seeking behaviour. Nat Commun 8:1–13.

Lewis EMA, Kaushik K, Sandoval LA, Antony I, Dietmann S, Kroll KL (2021) Epigenetic regulation during human cortical development: seq-ing answers from the brain to the organoid. Neurochem Int 105039.

Maruoka H, Kubota K, Kurokawa R, Tsuruno S, Hosoya T (2011) Periodic organization of a major subtype of pyramidal neurons in neocortical layer V. J Neurosci 31:18522–18542.

May PA, Chambers CD, Kalberg WO, Zellner J, Feldman H, Buckley D, Kopald D, Hasken JM, Xu R, Honerkamp-Smith G, Taras H, Manning MA, Robinson LK, Adam MP, Abdul-Rahman O, Vaux K, Jewett T, Elliott AJ, Kable JA, Akshoomoff N, Daniel F, Arroyo JA, Hereld D, Riley EP, Charness ME, Coles CD, Warren KR, Jones KL, Hoyme HE (2018) Prevalence of fetal alcohol spectrum disorders in 4 US communities. JAMA - J Am Med Assoc 319:474–482.

Mohammad S, Page SJ, Wang L, Ishii S, Li P, Sasaki T, Basha A, Salzberg A, Quezado Z, Imamura F, Nishi H, Isaka K, Corbin JG, Liu JS, Kawasawa YI, Torii M, Hashimoto-Torii K (2020) Kcnn2 blockade reverses learning deficits in a mouse model of fetal alcohol spectrum disorders. Nat Neurosci 23:533–543.

Nilsson EE, Sadler-Riggleman I, Skinner MK (2018) Environmentally induced epigenetic transgenerational inheritance of disease. Environ Epigenetics 4(2): 1-13.

O'Connor MJ, Shah B, Whaley S, Cronin P, Gunderson B, Graham J (2002) Psychiatric Illness in a Clinical Sample of Children with Prenatal Alcohol Exposure. Am J Drug Alcohol Abuse 28:743–754.

Öztürk NC, Resendiz M, Öztürk H, Zhou FC (2017) DNA Methylation program in normal and alcohol-induced thinning cortex. Alcohol 60:135–147.

Pellow S, Chopin P, File SE, Briley M (1985) Validation of open : closed arm entries in an elevated plus-maze as a measure of anxiety in the rat. J Neurosci Methods 14:149–167.

Perrin FE, Stoeckli ET (2000) Use of lipophilic dyes in studies of axonal pathfinding in vivo. Microsc Res Tech 48:25–31.

Petit-Demouliere B, Chenu F, Bourin M (2005) Forced swimming test in mice: A review of antidepressant activity. Psychopharmacology (Berl) 177(3):245-255.

Pritchett K, Mulder GB (2003) The Rotarod. Contemp Top Lab Anim Sci 42(6):49.

Pyronneau A, He Q, Hwang JY, Porch M, Contractor A, Zukin RS (2017) Aberrant Rac1-cofilin signaling mediates defects in dendritic spines, synaptic function, and sensory perception in fragile X syndrome. Sci Signal 10.

Raad G, Serra F, Martin L, Derieppe MA, Gilleron J, Costa VL, Pisani DF, Amri EZ, Trabucchi M, Grandjean V (2021) Paternal multigenerational exposure to an obesogenic diet drives epigenetic predisposition to metabolic diseases in mice. Elife 10:e61736.

Rubenstein JLR, Anderson S, Shi L, Miyashita-Lin E, Bulfone A, Hevner R (1999) Genetic Control of Cortical Regionalization and Connectivity. Cereb Cortex 9:524–532.

Schubert D, Kötter R, Zilles K, Luhmann HJ, Staiger JF (2003) Cell type-specific circuits of cortical layer IV spiny neurons. J Neurosci 23:2961–2970.

Sweet RA, Henteleff RA, Zhang W, Sampson AR, Lewis DA (2009) Reduced dendritic spine density in auditory cortex of subjects with schizophrenia. Neuropsychopharmacology 34:374–389.

Tang WWC, Dietmann S, Irie N, Leitch HG, Floros VI, Bradshaw CR, Hackett JA, Chinnery PF, Surani MA (2015) A unique gene regulatory network resets the human germline epigenome for development. Cell 161:1453–1467.

Vassoler FM, Byrnes EM (2021) Transgenerational effects on anxiety-like behavior following adolescent morphine exposure in female rats. Behav Brain Res 406:113239.

Xia W, Xie W (2020) Rebooting the Epigenomes during Mammalian Early Embryogenesis. Stem Cell Reports 15(6):1158-1175.

Zaqout S, Kaindl AM (2016) Golgi-cox staining step by step. Front Neuroanat 10:38.

Chapter 2: Rescue of ethanol-induced FASD-like phenotypes via prenatal co-administration of choline

ABSTRACT

Maternal consumption of alcohol during pregnancy can generate a multitude of deficits in the offspring. Fetal Alcohol Spectrum Disorders, or FASD, describe a palette of potentially life-long phenotypes that result from exposure to ethanol during human gestation. There is no cure for FASD and cognitive-behavioral therapies typically have low success rates, especially in severe cases. The neocortex, responsible for complex cognitive and behavioral function, is altered by prenatal ethanol exposure (PrEE). Supplementation with choline, an essential nutrient, during the prenatal ethanol insult has been associated with a reduction of negative outcomes associated with PrEE. However, choline's ability to prevent deficits within the developing neocortex, as well as the underlying mechanisms, remain unclear. Here, we exposed pregnant mice to 25% ethanol in addition to a 642 mg/L choline chloride supplement throughout gestation to determine the impact of choline supplementation on neocortical and behavioral development in ethanol-exposed offspring. We found that concurrent choline supplementation prevented gross developmental abnormalities associated with PrEE including reduced body weight, brain weight, and cortical length as well as partially ameliorated PrEE-induced abnormalities in intraneocortical circuitry. Additionally, choline supplementation prevented altered expression of *RZRβ* and

Id2, two genes implicated in postmitotic patterning of neocortex, and global DNA hypomethylation within developing neocortex. Lastly, choline supplementation prevented sensorimotor behavioral dysfunction and partially ameliorated increased anxiety-like behavior observed in PrEE mice, as assessed by the Suok and Ledge tests. Our results suggest that choline supplementation may represent a potent preventative measure for the adverse outcomes associated with PrEE.

INTRODUCTION

Fetal Alcohol Spectrum Disorders, or FASD, refer to a wide range of life-long physical, neurological, and behavioral deficits that result from prenatal ethanol, or alcohol exposure. The more commonly known designation, Fetal Alcohol Syndrome, or FAS, represents the most severe cases on the spectrum. Prenatal ethanol exposure, or PrEE, is the leading cause of *preventable* intellectual disability in the Western world, and the prevalence of FASD has been recently estimated to be as high as 5% in the United States (US) (May et al., 2018), carrying an estimated financial burden of approximately $23,000 per year per diagnosed individual (Greenmyer et al., 2018). Alarmingly, the absence of diagnosis or misidentification of FASD has been reported to occur frequently (Chasnoff et al., 2015). Thus, the prevalence of FASD and the corresponding economic load are likely to be greatly underestimated. Despite a plethora of preclinical and clinical research studies, as well as government health agency

47

recommendations identifying the dangers of PrEE to the developing baby, 11.5% of all pregnant women in the US admit to drinking alcohol during pregnancy and some estimates for older women are greater than 18% (Denny et al., 2019). Thus, it is critical to look at preventative and therapeutic approaches beyond abstinence to address this serious health issue.

One such approach that has been studied is the use of choline. Choline, a vitamin-like essential nutrient (IOM, 1998) important for proper brain development, is essential for cell membrane formation, synthesis of the neurotransmitter acetylcholine, and is a source of the methyl groups needed to form the primary methyl donor S-adenosylmethionine (SAM) (reviewed in Zeisel, 2006). Additionally, alcohol consumption reduces brain choline levels (Biller et al., 2009) and the availability of related metabolites in liver (Barak et al., 1987), functionally increasing demand for choline.

Preclinical research has explored the ability of choline to prevent or ameliorate systemic PrEE-induced alterations in brain and behavior using rodent models for nearly twenty years (Thomas et al., 2000). Specifically, promising results from these studies have shown that prenatal or early postnatal choline supplementation can prevent altered behavior due to PrEE such as hyperactivity (Thomas et al., 2004b; 2007), spatial learning and memory deficits (Ryan et al., 2008; Thomas et al., 2010; Waddell and Mooney, 2017), and fear conditioning (Wagner and Hunt, 2006). In addition, choline supplementation has been shown to prevent or reduce PrEE-induced abnormalities within the brain such as altered

DNA methylation in the hippocampus and prefrontal cortex (Otero et al., 2012),

atypical gene expression and epigenetic regulation in the hypothalamus

(Bekdash et al., 2013), as well as hippocampal microRNA (miRNA) expression

variance (Balaraman et al., 2017). Supporting results have been also

demonstrated in human cohorts, which exhibited reduced behavioral deficits

following choline supplementation in patients afflicted with FASD (Wozniak, et al.,

2015; Jacobson et al., 2018). Thus, the use of choline may have potent

therapeutic promise in humans with FASD.

Despite the number of studies supporting choline's use as a preventative

measure for FASD-like phenotypes, one gap in the existing literature which has

yet to be fully investigated is the impact of choline on neocortical development in

the context of PrEE. The neocortex is responsible for processing several

modalities of sensory information, coordinating motor output, and mediating

higher order cognitive function. The highly ordered and complex circuitry that is

characteristic of this structure has been postulated as a focal point of ethanol's

impact due to the observed phenotypes in patients with FASD. Indeed, a mass of

both preclinical (Ikonomidou et al., 2000; Cuzon et al., 2008; Hashimoto-Torii et

al., 2011; Delatour et al., 2018) and clinical evidence (Infante et al., 2015; Kodali

et al, 2017; Zhou et al., 2018) have confirmed the adverse influence of PrEE on

the development of the neocortex.

Additionally, our laboratory has published a series of studies

demonstrating the consistent, simultaneous disruption of neocortical connectivity

and expression of genes thought to govern the development of these connections (such as *RZRβ* and *Id2*) in newborn mice. These phenotypes may underlie PrEE's ability to alter several aspects of behavior in pre-pubescent mice, such as sensorimotor integration, coordination, and anxiety-like behaviors (El Shawa et al., 2013; Abbott et al., 2016; Abbott et al., 2018). Taken together, these results indicate the need for a thorough examination of choline's ability to prevent both abnormal neocortical development and subsequent behavioral deficiencies induced by PrEE, which has yet to be evaluated in any previous study.

In this study, we employed the same FASD murine model to assess the ability of concurrent choline supplementation to fully or partially ameliorate atypical neocortical and behavioral development following PrEE. Specifically, we examined gross physical and morphological development, patterns of neuronal connectivity, gene expression, and epigenetic regulation within the cortex at postnatal day (P)0 following PrEE with or without choline supplementation. We then examined adolescent behavior using a battery of assays at P20. We hypothesized that choline, when given at the time of the PrEE insult, would partially or fully prevent aberrant development of cortex at P0 and subsequent altered behavior at P20, and that the underlying mechanisms would be epigenetically-mediated. Results from this study will provide both key neocortical and mechanistic information on this potential human preventative treatment, as well as on the general underlying mechanisms of FASD.

MATERIALS AND METHODS

Mouse colony.

All breeding and experimental studies were conducted in accordance with protocol guidelines approved by the Institutional Animal Care and Use Committee at the University of California, Riverside. CD-1 background mice were originally purchased from Charles River Laboratories and the breeding colony was maintained at UCR. Mice were housed in an environmentally controlled vivarium and were kept on a 12-hour light/dark cycle. Standard lab chow and water were provided *ad libitum* (except in gestational liquid treatment period).

FASD Mouse model, choline supplementation, and dam measures.
2 to 3-month-old mice were paired overnight for breeding. Upon confirmation of vaginal plug, the gestational day was recorded as 0.5. Immediately after, dams were randomly assigned to one of four treatment groups for the entirety of gestation: group 1-Water (Control), group 2-25% EtOH in water (EtOH), group 3-25% EtOH in water with 642 mg/L choline chloride (Sigma; St. Louis, MO, USA) (CE), and group 4-642 mg/L choline chloride in water (CW). Overall timeline for experiments seen in Figure 2.1. For all groups, 8 litters were treated for offspring generation. These treatments were available *ad libitum* to dams and were the only source of liquid provided. Choline dosage was based on a previous report which found choline supplementation ameliorated PrEE effects in the rodent brain (Bekdash et al., 2013). Daily liquid and food intakes of all dams were

measured daily at 0900h using a standard scale and graduated drinking bottle. Separate subsets of dams were sacrificed at either GD9 and 19 for blood ethanol content (BEC) and plasma osmolality (POSM) measurements during gestation (n=10, all groups). BEC was assayed in duplicate using whole blood samples. Briefly, whole blood samples were processed to obtain 5 μL of serum which was then mixed with 1 mL of alcohol reagent (Pointe Scientific; Canton, MI, USA) and assayed immediately using a Nanodrop 2000 spectrophotometer at 340 nm wavelength. POSM was assayed using whole blood samples taken from dams at GD 19. Blood samples were added to ice-cold tubes and centrifuged at 4°C/1100 g for 10 min, obtaining a clear supernatant. Blood plasma osmolality was then measured using a Vapro 5520 vapor pressure osmometer (Wescor; Logan, UT, USA).

Pup measurement and selection criteria.

For consistent staging of pups, the day of birth was designated as P0. Total litter sizes (# of pups) were recorded on P0. For experimental analyses in brain, 1 ± 1 pups were selected pseudo-randomly from each litter. Pups were then weighed via Fisher Scientific scale and sacrificed at P0 via 1 of 2 methods dependent on experimental endpoint (details below). Only pups used at P0 endpoints were weighed at P0 to avoid excess disturbance of both pups and dams to ensure successful viability. Pseudo-randomly chosen subsets of P0 brains from each group were weighed and digitally-imaged for cortical length measurements

accomplished via digital micrometer (ImageJ, NIH; Bethesda, MD). Although

subsequent behavioral analyses were sex-specific, no P0 endpoints were

conducted in a sex-specific manner, due to the difficulty of accurately sexing P0

pups non-genetically. Absence of distinguishing sexual characteristics at P0,

relative inaccuracy of using conventional methods, such as anogenital distance

(Wolterink-Donselaar et al., 2009), as well as the inability to use newly validated

methods (Deeney et al., 2016) due to use of an albino mouse strain prevented

P0 sex-separated analysis. For behavioral analysis, subsets of each litter in all

groups were cross-fostered to alcohol-naïve mothers until P20 when behavioral

testing of 3 ± 1 pups per litter took place. All rearing and housing conditions were

consistent among cross-fostered groups and all litters were pseudo-randomly

culled to 6 pups prior to cross fostering to prevent any off-target effects of varied

rearing experience. Experimental use of pups had strict upper limits of 2 pups/per

litter/per P0 endpoint and 4 pups/per litter/per P20 endpoint to reduce the

potential confounder of litter effects. A larger per-litter subset was used as the

upper limit for P20 behavioral analyses due to the inclusion of both male and

female offspring in near-equal ratios, as well as to control for the potential of non-

participants in behavioral tests. For global methylation and gene expression

assays, only a single pup per litter was included in analysis to prevent

confounding litter effects.

Dye tracing and ISH tissue preparation.

P0 pups used in dye tracing and *in situ* hybridization (ISH) studies were sacrificed via hypothermia, and transcardially perfused with 4% paraformaldehyde (PFA) in 0.1M phosphate buffer, pH 7.4. Brains were quickly removed, weighed, and dorsal whole brain photos taken via a Zeiss Axio HRm (Carl Zeiss; Oberkochen, Germany) camera attached to a dissecting microscope. Cortical length was measured using NIH ImageJ's measure function by drawing a diagonal line from the most anterior pole of the cortex to the furthest posterior pole. Following post-fixation in 4% PFA, brains were hemisected, and hemispheres were designated for either dye tracing or ISH assays to ensure even sampling of each litter for each assay. Previous studies from our laboratory (El Shawa et al., 2013; Abbott et al., 2018) have examined the potential asymmetric impact of PrEE on the early postnatal brain and have found no significant lateralization effects. Thus, random sampling of both right and left hemispheres was used in all P0 brain-based experiments to produce a homogenous population of data.

Global methylation tissue preparation

A separate subset from litters of each group were sacrificed for global methylation assays at P0 as follows. Pups were briefly placed on ice until a deep plane of anesthesia was reached via hypothermia which was confirmed via toe pinch. Once this was achieved, pups were sacrificed via decapitation and the

brain was quickly removed from the skull and underlying membranes. The brain was then hemisected and the whole neocortex was dissected from all subcortical structures. Once isolated, whole hemisected neocortical samples were measured using a grid system and partitioned into even rostral and caudal samples. Whole rostral and caudal divided portions of neocortex from each animal were then placed into Buffer RLT (Qiagen; Venlo, Netherlands) for further processing and DNA extraction via Qiagen AllPrep DNA/RNA extraction kit.

Anatomical tracing.

To determine the development of ipsilateral, intraneocortical connections (INCs) in P0 mice 1,1-Dioctadecyl-3,3,3,3-tetramethylindocarbocyanine (DiI; Invitrogen; Carlsbad, CA, USA) dye crystals were placed in putative primary visual cortex (VCx), as described previously (El Shawa et al. 2013). A coordinate grid was used for reliability of dye placement locations (DPLs) across cases. Following placement of crystals, hemispheres were placed in 4% PFA in the dark at room temperature for 4-6 weeks to allow for dye transport. Upon confirmation of retrograde thalamic nuclei labeling, brains were embedded in 5% low melt agarose, and sectioned at 100µm via vibratome in 1X phosphate buffered saline (PBS). Sections were then counterstained with 4′, 6-diamidino-2-phenylindole dihydrochloride (DAPI; Roche; Basel, Switzerland), mounted onto glass slides, and coverslipped using FluoroMount (Sigma; St. Louis, MO, USA).

Dye tracing analyses.

A Zeiss Axio Upright Imager microscope equipped with a Zeiss Axio high resolution (HRm) camera and two filters was used to visualize and capture images of dye labelled sections via PC running Axiovision software. The two filters used are detailed in the following: red for DiI and blue for DAPI counterstain labeling (Excitation wavelengths-red: Cyanine 3,550 nm; blue: DAPI, 359 nm. Emission wavelengths-red: Cyanine 3, 570 nm; blue: DAPI, 461 nm). Images from both filters per section were merged for subsequent analysis. Matched sections from all groups' brains using DAPI counter-stained landmarks were used to compare the development and trajectory of INCs among treatment and control groups. Retrogradely-labeled cell bodies were plotted and aligned using subcortical and blood vessel anatomy as guidelines to generate 2D reconstructions of "flattened" neocortex, illustrating the position of INCs labelled from DPLs. Section data was further quantified by projection zone and cell counting analyses. Projection zone analysis was accomplished by using combined 2D reconstruction and individual section data, measuring the furthest rostral and caudal cell labeling originating from a distinct cortical DPL. This parameter was measured in relationship to the center of the DPL and quantified as a percentage of total cortical length to control for possible neocortical reduction in experimental groups. DPL spreads were also measured in all cases to ensure consistent dye crystal size and uptake and are presented as percentage of total cortical length. This measurement technique controls for inherent cortical differences between brains and allows for statistical analysis of

INC development between the 4 groups. Frontal cortex cell counts took place in an electronically placed region of interest (ROI) (ImageJ) in anatomically matched sections across cases, as confirmed via the Paxinos developing mouse atlas (Paxinos et al., 2007), and retrogradely-labeled cells were counted by a trained researcher blind to condition. ROIs remained static in size and location for all cases and groups.

In Situ Hybridization (ISH) and transcript density analyses.

Standard protocols for free-floating non-radioactive ISH were used to visualize neocortical *Id2* and *RZRβ* gene expression of P0 brains, as previously described in detail elsewhere (Dye, et al., 2011a). Briefly, hemispheres were first embedded in gelatin-albumin, and sectioned at 100μm via vibratome. After hybridization to digoxigenin-labeled probes for *Id2* and *RZRβ* (gifts from John Rubenstein, UCSF), sections were developed in NBT/BCIP (Roche; Basel, Switzerland), mounted in a 50% glycerol solution onto glass slides, coverslipped, and imaged using a Zeiss Axio HRm camera attached to a dissecting microscope. Relative levels of *Id2* and *RZRβ* were measured via semi-quantitative mRNA transcript density analyses (Dye et al., 2012; El Shawa et al., 2013). Briefly, raw ISH data images among all groups were strictly matched anatomically and confirmed via atlas and subcortical landmarks, converted to binary via ImageJ and matched to a set threshold. ROIs were chosen based on qualitative observations of potential phenotypic variation due to condition. ROIs

were electronically placed onto matching locations within sections and the level of pixel density within ROIs was measured as a proxy for transcript signal density. Transcript densities are reported as area fraction of total ROIs. ROIs remained static in location for all cases and groups for each gene analyzed, however, due to the consistent reduction in brain size in EtOH-exposed pups, ROIs for the EtOH group were also reduced to control for this difference. Briefly, section area was calculated for all cases to produce an average percent reduction in section size from controls, which was determined to be 12%. Thus, ROIs in EtOH cases were reduced in area by 12% to account for overall brain size differences. Because no other groups displayed a brain size reduction, ROI size remained static within those analyses.

DNA extraction and global DNA methylation assay.

Following homogenization, genomic DNA was isolated from rapidly dissected rostral and caudal cortical samples at P0 via the Qiagen AllPrep DNA/RNA Mini kit. Extracted DNA was then assessed for quality and quantity via NanoDrop 2000 spectrophotometer (ThermoScientific; Waltham, MA, USA). 5-methylcytosine (5-mC) levels were then measured in DNA isolated from rostral and caudal cortical samples using the MethylFlash Global DNA Methylation (5-mC) ELISA easy kit (Epigentek; Brooklyn, NY, USA). Briefly, 200 ng of DNA was bound to plates treated to have high affinity for DNA. Methylated fractions of DNA (i.e. 5-mC) in samples were then assessed using detection antibodies and

absorbance was measured at 450 nm on a Victor 2 plate reader. The level of 5-mC in cortical tissue samples was quantified from absorbance measurements according to manufacturer's instructions and is reported as % of 5-mC relative to the total genomic DNA content.

Behavioral analyses.

Prior to all behavioral testing, P20 mice from all 4 experimental groups were acclimated to the dimly-lit experiment room. All behavioral scoring was conducted by trained researchers blind to condition. Each mouse tested underwent a single trial of the Suok test, followed by a single trial in the Ledge test after a period of rest. The Suok test was used to simultaneously assess potential anxiety-like behaviors and motor function, as previously described (Kalueff et al., 2008). In the Suok test, mice traverse an elevated cylindrical bar (2 m length, 3 cm diameter, 20 cm off ground) for a single 5-minute trial and are scored for several parameters. Anxiety-like behavioral parameters measured in the Suok assay include latency to leave the center of the bar (start position), directed exploration events, and rearing/grooming events. Potential sensorimotor integration and motor coordination are also assessed in the Suok test via number of missteps and falls from the rod. Additionally, the Ledge test was used to measure the animal's ability to integrate sensory inputs and motor outputs, as previously described (Wang et al., 2002). Here, mice were scored for their ability to maintain balance on a vertically-stabilized Plexiglass sheet, which was 50 cm

long, 30 cm tall, and 0.7 cm in width for a maximum score of 60 seconds (s). If the mouse was able to successfully traverse the length of ledge and returned to the starting position, a maximum score of 60 s was assigned. The ledge test is used to directly measure coordination in mice (Guyenet et al., 2010). As such, if a mouse displays adequate coordination to successfully traverse the very thin (0.7 cm) ledge twice, it can be considered to display no significant coordination impairments, and thus is awarded a maximum score (60 seconds). This established scoring methodology was used as previously published for the Ledge test (Schaefer et al., 2000; Wang et al., 2002; El Shawa et al., 2013). Following each trial in both Suok and Ledge tests, the behavioral apparatuses were thoroughly cleaned to remove any olfactory cues.

Statistical analyses.

All statistical analyses took place using GraphPad Prism 6 software (La Jolla, CA, USA). All data was initially analyzed for Gaussian distribution using the Shapiro-Wilk normality test. For between group comparisons that displayed normal distributions, two-way analysis of variance (ANOVA; factors: ethanol and choline) followed by Tukey's multiple comparisons test was used. For the 9 measures (Dam BEC, P0 body weight, frontal cortex labeled cell counts, ledge test scores, and latency to leave center, directed exploration events, rearing/grooming events, and falls on the Suok test) that did not display normal distributions, the Kruskal-Wallis test followed by Dunn's multiple comparison test

was used. For all behavioral measures at P20, individual animals from each group were separated by sex and additionally analyzed using tests described above. For all measures, statistical significance was set as $p < 0.05$. Data are presented as mean ± SEM. All group means and SEMs for quantified data are presented in supplemental materials (Table 2.1).

RESULTS

Dam measures.

In order to assess possible nutritional confounds in dams, we measured gestational food intake, liquid intake, blood ethanol content (BEC), plasma osmolality (POSM), weight gain, and litter size (Fig. 2.2). There was a significant effect of ethanol on gestational food intake [$F_{1,28} = 5.488$; $p = 0.027$], however post hoc tests revealed no significant differences between any groups (Fig. 2.2A). No significant effects or interaction were present in dam liquid intake measurements (Fig. 2.2B). A significant effect due to treatment was found in BEC levels at GD 9 and 19 [$H = 61.22$; $p < 0.0001$]. As expected, BEC levels (Fig. 2.2C) were only present in EtOH (106.5 ± 1.693 mg/dL, $n= 10$) and CE (106.9 ± 1.040 mg/dL, $n= 10$) dams at GD 9, and rose to 136.9 ± 2.794 mg/dL (EtOH, $n= 10$) and 136.3 ± 2.894 mg/dL (CE, $n= 10$) at GD 19. Post hoc comparisons revealed no significant differences between EtOH and CE dams BEC levels at either time point (GD 9: $p > 0.999$; GD 19: $p > 0.999$), suggesting similar levels of ethanol intoxication. Additionally, no statistically significant

differences were present between GD 9 and GD 19 BEC measures within EtOH ($p = 0.303$) or CE dams ($p = 0.667$). Dam POSM, which serves as a measure of hydration, displayed no significant main effects and post hoc tests revealed no significant differences among groups (Fig. 2.2D) at GD 19. No main effects were found for gestational weight gain, however a significant ethanol X choline interaction was present [$F_{1,28} = 6.375$; $p = 0.018$] and post hoc tests revealed that EtOH dams displayed a reduction in weight gain (Fig. 2.2E) compared to controls (*$p = 0.022$). Furthermore, a significant main effect of ethanol [$F_{1, 28} = 4.233$, $p= 0.049$] and an ethanol X choline interaction [$F_{1, 28} = 5.635$, $p= 0.025$] was found for litter size. Post hoc analysis revealed that EtOH dams also displayed a concomitant reduction in litter size (Fig. 2.2F) compared to both control (*$p = 0.020$) and CE dams (*$p = 0.043$), suggesting choline can prevent adverse pregnancy outcomes due to PrEE. As an additional control, we investigated potential group differences in gestational length and found no significant changes due to treatment [$F_{3, 28} = 2.333$, $p = 0.096$; Control: 19.88 ± 0.227 d, CW: 20.25 ± 0.164 d, EtOH: 20.50 ± 0.189 d, CE: 20.50 ± 0.189 d].

Physical development of pups.
Body weights and brain weights were measured in offspring at P0 to assess physical development (Fig. 2.3). A significant effect of treatment on P0 body weight was detected [$H = 19.49$, $p= 0.0002$], with post hoc analyses revealed a reduction in EtOH pups compared to control (**$p = 0.024$), CW (***$p = 0.029$),

and CE pups (**p = (Fig. 2.3A). In addition, 2-way ANOVA revealed significant main effects of ethanol [$F_{1, 51}$ = 8.281, p= 0.005] and choline [$F_{1, 51}$ = 6.954, p= 0.011] on P0 brain weight, as well as an ethanol X choline interaction [$F_{1, 51}$ = 8.281, p= 0.005]. Post hoc analyses showed that EtOH pups have reduced brain weights at P0 (Fig. 2.3B) compared to control (***p = 0.0002), CW (**p = 0.001), and CE pups (**p = 0.003). No main effects or interactions were present for brain/body weight ratios (Fig. 2.3C), which were not significantly altered among groups, likely reflecting the association of *both* reduced brain and body weights at P0 in EtOH pups.

Cortical length was measured at P0 (Fig. 2.4) in order to analyze gross neocortical developmental abnormalities associated with PrEE and the ability of choline to prevent such deficits. Black arrows in Fig. 2.4A-D indicate the cortical length measurements as assessed electronically in ImageJ. A significant main effect of ethanol [$F_{1, 36}$ = 12.07, p= 0.001] and an ethanol X choline interaction [$F_{1, 36}$ = 4.433, p= 0.042] was found for P0 cortical length, and post hoc analyses revealed that EtOH cortical lengths were significantly reduced (Fig. 2.4E) compared to control (**p = 0.002), CW (**p = 0.004), and CE brains (*p = 0.049) at P0. Overall, these results suggest concurrent choline supplementation can prevent adverse PrEE-induced physical and gross brain developmental deficits in very early life.

Development of ipsilateral INCs.

Intraneocortical connections (INCs) are a defining characteristic of distinct

cortical areas and are crucial for integration of sensory inputs and coordinating

outputs of the neocortex (Kaas, 1982). Previously, our lab has shown PrEE

significantly disrupts INC development of putative sensory areas in offspring at

P0, specifically resulting in a severely disorganized pattern of neocortical

connectivity (El Shawa et al., 2013; Abbott et al, 2018). Here, we analyze INC

patterns of putative visual cortex (VCx) using lipophilic dye tracing in order to

assess the ability of choline supplementation to mitigate abnormal neocortical

connectivity due to PrEE.

Analysis of ipsilateral INCs at P0 confirmed the ability of PrEE to perturb

development of patterns of neocortical connections (Fig. 2.5). EtOH brains

displayed abnormal patterns of labeled cells stemming from putative primary

visual cortex DPLs (*V, Fig. 2.5D1-4). Specifically, EtOH brains contained

labeled cells that extended into cortical areas within very far rostral sections

(arrows, Fig. 2.5A3, B3) not present in either control (Fig. 2.5A1, B1) nor CW

brains (Fig. 2.5A2, B2) at P0. In contrast, CE brains did not contain labeled cells

in very rostral sections that were present in the EtOH group at P0 (compare Fig.

2.5A3 to A4). However, CE brains still displayed an extended pattern of INCs

from VCx injections (arrow, Fig. 2.5B4) which were not present in either control

group (Fig. 2.5B1-2), suggesting concurrent choline administration can only

partially ameliorate PrEE-induced disruption of sensory cortical area INC

patterns. Importantly, the altered patterns of INCs were present without gross alteration of thalamocortical afferent connectivity, as labeled cells were present within the dorsal lateral geniculate nucleus in all groups (arrows, Fig. 2.5D1-4).

These overall patterns of INCs are more easily visualized via flattened lateral view reconstructions of the cortex in Fig. 2.5F1-4. Whereas control (Fig. 2.5F1) and CW (Fig. 2.5F2) brains displayed a tight pattern of labeled cells that reside in caudal cortical areas, EtOH (Fig. 2.5F3) and CE (Fig. 2.5F4) both show patterns of INCs extending into rostral sections not present at any age in control animals, (Dye et al., 2011a; 2011b), suggesting an abnormally defined border of putative visual cortex. However, the partial reduction of this extended pattern by choline was apparent when EtOH and CE brains were compared, where labeled cells did not extend as far rostrally in the CE group.

Analysis of DPL spread (to assess size of injections) revealed no significant main effects or an interaction (Fig. 2.6A), suggesting size of dye injections is consistent, and does not confound the observed results. In contrast, significant effects of ethanol [$F_{1, 18}$ = 173.8, $p < 0.0001$] and choline [$F_{1, 18}$ = 7.991, $p = 0.011$], as well as an ethanol X choline interaction [$F_{1, 18}$ = 9.367, $p = 0.007$] was observed for VCx projection zones. Post hoc analyses revealed that both EtOH and CE brains have significantly increased projection zones compared to control (EtOH: ****$p < 0.0001$; CE: ****$p < 0.0001$) and CW groups (EtOH: ****$p < 0.0001$; CE: ****$p < 0.0001$) (Fig. 2.6B). However, post hoc analysis also revealed a significant reduction in projection zone in CE brains compared to the

EtOH group (**p = 0.002), suggesting choline has the ability to partially prevent

abnormal INC patterns due to PrEE. This partial reduction by choline is further

demonstrated by the count of retrogradely-labeled cell bodies within the region of

interest (ROI) at the anatomical level illustrated in Fig. 2.6C. The static ROI

spans the putative prelimbic (PrL), cingulate (Cg), secondary motor (M2), and

primary motor (M1) cortical areas. Cell counts within this ROI (Fig. 2.6D) yielded

no results for any treatment group except for the EtOH treated animals, which

contained 25.33 ± 3.43 cells at this anatomical level [H= 20.33, p < 0.0001]. Post

hoc analyses expectedly revealed significant increases in EtOH brains compared

to control (**p = 0.002), CW (**p = 0.002), and CE brains (**p = 0.001). Overall,

results from these dye tracing experiments suggest that concurrent choline

supplementation can partially prevent the disruption of INC pattern development

of an early sensory cortical area that results due to PrEE.

Cortical gene expression.

Age-dependent patterns of expression of a subset of genes within the neocortex

have been experimentally implicated in guiding both the development of distinct

cortical areas and the characteristic patterns of INCs in these areas (Huffman et

al., 2004; Dye et al., 2011a; 2011b). Expression of two particular genes within

this subset, *RZRβ* and *Id2*, have been consistently shown to be altered in the

neocortex of newborn mice due to PrEE (El Shawa et al., 2013; Abbott et al.,

2018). In order to assess choline's ability to ameliorate PrEE-induced abnormal

gene expression of *RZRβ* and *Id2*, we employed *in situ* hybridization in coronal

hemisphere sections at P0 in all 4 groups (Fig. 2.7).

As demarcated by the arrow in Fig. 2.7A1, P0 control brains displayed a

distinct boundary of *RZRβ* expression in layer IV of rostral parietal cortex, which

distinguishes the gradient of low expression in medial cortex and gradual high

expression in lateral cortex, which was also present in the CW group (arrow, Fig.

2.7B1). In comparison, EtOH mice displayed a dramatic medial shift in this

boundary (arrow, Fig. 2.7C1), and, thus, *RZRβ* expression extended into the

most medial regions of cortex, confirming the results of our previous reports (El

Shawa et al., 2013; Abbott et al., 2018). However, in CE mice, this abnormal

medial shift in *RZRβ* expression was not present (arrow, Fig. 2.7D1) and

expression patterns were qualitatively indistinguishable from either control

groups, suggesting choline can prevent altered cortical gene expression due to

PrEE at P0.

Id2 expression patterns in early postnatal control mice contain laminar

specific expression gradients that vary depending on the area of the neocortex

(Rubenstein et al., 1999). At the level of the rostral parietal cortex of controls in

our study, Id2 was expressed in the subplate, deep layers V and VI, as well as in

superficial layers I and II/III, where a boundary denoted a gradient of high medial

expression and lower lateral expression (arrow, Fig. 2.7A2), which was also

present in CW mice (arrow, Fig. 2.7B2). However, in EtOH mice this boundary

was shifted medially (arrow, Fig. 2.7C2), and thus low expression of *Id2* was

similarly shifted medially. In contrast, CE mice did not display this aberrant shift in *Id2* expression (arrow, Fig. 2.72), further suggesting that choline can mitigate gene expression deficits induced by PrEE in the neocortex at P0.

Semiquantitative analyses of these gene expression patterns were conducted using binary-converted raw images and transcript density counts (Fig. 2.8). Transcript densities were measured in static ROIs indicated on the illustrations in Fig. 2.8A1 (*RZRβ*) and Fig. 2.8B1 (*Id2*) and were reported as area fractions (%) of black pixel containment within the ROIs. Significant main effects of ethanol [$F_{1, 18}$ = 44.32, *p* < 0.0001] and choline [$F_{1, 18}$ = 50.69, *p* < 0.0001], as well as an ethanol X choline interaction [$F_{1, 18}$ = 30.63, *p* < 0.0001], were present for *RZRβ* transcript density (Fig. 2.8A2). Post hoc analyses revealed a significant increase of *RZRβ* transcript density in the ROI of EtOH mice compared to control (****p* < 0.0001), CW (****p* < 0.0001), and CE groups (****p* < 0.0001). Additionally, 2-way ANOVA revealed significant main effects of ethanol [$F_{1, 13}$ = 14.72, *p* = 0.016] and choline [$F_{1, 13}$ = 28.65, *p* = 0.002], as well as an ethanol X choline interaction [$F_{1, 13}$ = 24.15, *p* = 0.004], on *Id2* transcript density (Fig. 2.8B2). Post hoc analyses reveal a significant decrease in *Id2* area fractions within the ROI of EtOH compared to control (***p* = 0.002), CW (***p* = 0.002), and CE mice (***p* = 0.001). Together, these results confirm the qualitative analyses and suggest choline supplementation can prevent PrEE-induced abnormal expression patterns of two genes known to participate in the guidance of development of INCs at P0.

Global DNA methylation.

In order to investigate choline's function in DNA methylation and whether its supplementation can prevent PrEE-induced epigenetic dysregulation, we examined global DNA 5-methylcytosine (5mC) levels in rostral and caudal cortex at P0 in all 4 groups (Fig. 2.9). Previously, our laboratory has shown significant hypomethylation in both rostral and caudal cortical samples in PrEE mice compared to controls at P0 (Abbott et al., 2018). Using the same ELISA-like colorimetric assay, a two-way ANOVA revealed significant main effects due to ethanol [$F_{1, 13}$ = 8.696, *p* = 0.011] and choline [$F_{1, 13}$ = 14.90, *p* = 0.002] on global DNA %5mC in rostral cortex. For the caudal cortex, significant main effects due to ethanol [$F_{1, 13}$ = 21.08, *p* = 0.001] and choline [$F_{1, 13}$ = 6.099, *p* = 0.028] were also present. No ethanol X choline interactions were present for either region. Post hoc analyses detected a significant DNA hypomethylation in EtOH mice in both rostral and caudal cortex compared to controls (rostral: **p* = 0.049; caudal: **p* = 0.030). In contrast, CE 5mC DNA levels were not statistically significant from control animals in either rostral (*p* = 0.924) or caudal cortex (*p* = 0.498) and were significantly increased when compared to EtOH mice in rostral cortex (**p* = 0.050), suggesting that choline supplementation can prevent PrEE-induced hypomethylation in newborn cortex. Choline supplemented control animals (CW) seemed to display a trend in increased DNA methylation, which was supported by the post hoc comparisons which revealed a stronger difference when

compared to EtOH (rostral: **p = 0.001; caudal: ***p = 0.001) than what was seen in control vs. EtOH comparisons (rostral: *p = 0.049; caudal: *p = 0.030). However, CW 5mC DNA levels were not statistically different from the control group in rostral (p = 0.105) or caudal cortex (p = 0.180), suggesting that our choline dose alone does not significantly impact DNA methylation in the cortex of normally developing mice at P0. Overall, these results suggest that choline supplementation, when administered at the time of PrEE insult, can prevent PrEE-associated hypomethylation in the cortex at P0.

Behavioral analyses.

At P20, two separate behavioral assays were used to test the hypothesis that concurrent prenatal choline supplementation can prevent the adverse behavioral outcomes associated with PrEE (Fig. 2.10). Previously, our laboratory has shown motor deficits (which may be rooted in sensorimotor integration) and increased incidence of behaviors that may be indicative of anxiety-like states in PrEE mice at P20 (El Shawa et al., 2013; Abbott et al., 2018) using these same behavioral assays.

Potential anxiety-like behavioral measures scored included latency-to-leave center of the bar (Fig. 2.10A), directed exploration events (Fig. 2.10B), and rearing/grooming events (Fig. 2.10C). A significant effect of treatment was found on all anxiety-like measures: [Latency to leave center: H = 8.196, p = 0.042; Directed exploration: H = 16.61, p = 0.001; Rearing/grooming: H = 15.33, p=

70

0.002]. Post hoc analyses revealed a significant increase in latency to leave

center in EtOH animals (Fig. 2.10A) compared to control (*p = 0.043) mice. Post

hoc analyses also revealed a significant decrease in directed exploration events

in EtOH mice (Fig. 2.10B) compared to control (*p = 0.026), CW (**p = 0.002),

and CE (**p = 0.001) mice. Lastly, both EtOH and CE mice displayed decreased

rearing and grooming events (Fig. 2.10C) compared to controls (EtOH: *p =

0.010; CE: *p = 0.021) at P20. Overall, these results suggest that prenatal

choline has the ability to partially ameliorate potential anxiety-like behaviors

induced by PrEE at P20.

Sensorimotor integration and motor function were also assessed by

missteps and falls within the Suok test, as well as by the overall score of the

Ledge test. Significant main effects of ethanol [$F_{1,61}$ = 23.79, p < 0.0001], choline

[$F_{1, 61}$ = 10.31, p = 0.0010] and an ethanol X choline interaction [$F_{1, 61}$ = 13.33, p

= 0.0002] were found on missteps. A significant effect of treatment was also

found on falls [H= 23.54, p < 0.0001] in the Suok test. Post hoc test revealed that

EtOH mice showed significantly increased missteps (Fig. 2.10D) compared to

control (****p < 0.0001), CW (****p < 0.0001), and CE (****p < 0.0001) groups.

Additionally, EtOH mice displayed significantly increased falls (Fig. 2.10E)

compared to control (****p < 0.0001), CW (**p = 0.004), and CE (*p = 0.036)

groups. Finally, we report a significant effect of treatment on Ledge test score [H

= 9.864, p = 0.020], and post hoc analyses revealed a decrease in the EtOH

groups scores (Fig. 2.10F) compared to control (**p = 0.033). In contrast, CE

mice did not display scores that were statistically significant from either control group. Overall, these data suggest that choline supplementation, when given at the time of PrEE insult, can partially prevent potential anxiety-like behaviors and fully prevent deficits that may be rooted in motor function or sensorimotor integration in offspring at P20.

Sex-specific behavioral analyses.

Both EtOH and choline supplementation have been reported to perturb and prevent PrEE-induced behavioral deficits, respectively, in a sex-specific manner (Thomas et al., 2007; Bearer et al., 2015; Schneider and Thomas, 2016). Thus, we also analyzed behavioral data separated by sex, as detailed below, to determine if any sex-specific effects are present within our model.

Behavioral analyses- Females.

For the Suok test, no differences were present in latency to leave center in females [H = 4.553; p = 0.208], however main effects of treatment were found on both directed exploration [H = 13.35; p = 0.004], and rearing/grooming [H = 13.16; p = 0.004]. Post hoc tests revealed female EtOH mice displayed significantly decreased directed exploration events compared to control (*p = 0.011), CW (*p = 0.026), and CE (*p = 0.046) females (Fig. 2.11B). Both female EtOH and CE mice display decreased rearing/grooming events compared to controls (EtOH: *p = 0.030; CE: **p = 0.006) (Fig. 2.11C).

Significant main effects of both ethanol [$F_{1,27}$ = 5.043, p =0.033] and choline [$F_{1,27}$ = 7.588, p = 0.010] were found for missteps in females. Post hoc tests showed EtOH females had increased missteps compared to control (*p = 0.036), CW (*p = 0.011), and CE (*p = 0.028) females (Fig. 2.11D). Additionally, a significant effect of treatment was found on falls [H = 12.24, p = 0.007], as EtOH females had increased falls compared to control females (**p = 0.006) (Fig. 2.11E). Lastly, no effect of treatment was found on female Ledge test scores.

Behavioral analysis- Males.

For the Suok test, no effects of treatment were present in latency to leave center in males [H = 1.990; p = 0.575], directed exploration [H = 5.654; p = 0.130], or rearing/grooming [H = 3.314; p = 0.346].

A significant main effect of ethanol [$F_{1,27}$ = 6.298, p =0.014] was found on missteps for males. Post hoc tests showed EtOH males have increased missteps compared to control (*p = 0.018), CW (*p = 0.033) males (Fig. 2.12D). Additionally, a significant effect of treatment was found on falls [H = 12.15, p = 0.007], as EtOH males increased falls compared to control (**p = 0.007) and CW males (*p = 0.036) (Fig. 2.12E). Lastly, no effect of treatment was found on male Ledge test scores.

DISCUSSION

We report that prenatal choline supplementation can attenuate some physical and behavioral dysfunction associated with PrEE. Specifically, gestational choline supplementation was able to rescue gross developmental deficits, as well as dysregulated intraneocortical connectivity and gene expression gradients. Choline also mitigated performance deficits in most behavioral tasks which may model anxiety-like behavior and sensory-motor integration in PrEE mice. Choline, a primary methyl group donor, also prevented global DNA hypomethylation that results from PrEE, providing a window of insight into a possible epigenetic mechanism of ethanol's detrimental developmental effects. Together, these results broaden our understanding of choline's potential as a prophylactic agent for FASD and provide key, novel insight on how it affects patterns of neuronal connectivity and cortical development. As behavioral testing was conducted 20 days following cessation of choline supplementation, it is likely the beneficial effects of choline were not related to acute action, but rather to its inhibition of long-lasting organizational changes in brain development normally generated by PrEE.

Choline prevents PrEE-induced developmental alterations in brain.
PrEE causes gross developmental abnormalities in rodent offspring, including decreased perinatal body weight (Datta et al., 2008) and total brain weight (Komada et al., 2017). In the present study, we report significant reductions in

body weight, brain weight, and cortical length in newborn EtOH-exposed pups. In contrast, concurrent choline supplementation prevented these effects in CE pups. These results support those observed in rats who received concurrent choline supplementation over the course of a timed gestational day (GD) 5-20 EtOH exposure (Thomas et al., 2009; Thomas et al., 2010). Despite promising results when co-administered with EtOH at early developmental timepoints, choline is unable to prevent body weight reductions when administered after EtOH exposure in a rodent model of third-trimester PrEE (Ryan et al., 2008; Thomas and Tran, 2012), likely due to its absence at the time of PrEE insult. Together, these results suggest that choline can mitigate EtOH-induced gross developmental abnormalities within certain critical periods.

Development of a functional neocortex results from a series of highly-regulated processes, which are consistently disrupted following PrEE (Ikonomidou, et al., 2000; Cuzon et al., 2008; Pascual et al., 2017). These effects can manifest as reductions in cortical length, volume and area in PrEE offspring (El Shawa et al., 2013; Smiley et al., 2015). Despite the ability of preventative treatments such as choline supplementation to ameliorate these effects, there remains a paucity of research examining the mode, and extent of impact on PrEE-impaired cortical development. In the present report, we characterize genetic and epigenetic aspects of early mammalian CNS development, and associate these changes with juvenile behavior.

Choline's prophylactic action is likely achieved through the positive regulation of multiple developmental pathways, including direct influence of cortical neurogenesis and migration (Wang et al., 2016; Trujillo-Gonzales, et al., 2019), as well as the prevention of underlying aberrant gene expression. Indeed, by mapping INC patterns of putative V1 we found that CE pups, while still displaying an altered areal boundary compared to control mice, exhibit a marked reduction in visual cortex projection zones compared to EtOH animals. This recovery may also be related to the observed ability of choline supplementation to prevent altered patterns of *RZRβ* and *Id2* expression in newborn neocortex due to PrEE. These findings expand on previous work which showed that choline can mitigate PrEE-induced alterations to gene expression in hypothalamus (Bekdash et al., 2013) and miRNA expression in hippocampus (Balaraman et al., 2017), suggesting that choline may be sufficient for prevention of widespread gene expression changes induced by PrEE.

The two genes analyzed within the current study*, RZRβ* and *Id2,* play key roles in cortical development. *Id2,* a transcription factor, and *RZRβ* (also known as *RORβ*) are known to influence several key factors of neurodevelopment including neurogenesis (Toma et al., 2000), apoptosis (Gleichmann et al., 2002) and layer formation (Oishi et al., 2016). However, in late embryonic and early postnatal ages in mice, both genes are instrumental in proper patterning of postmitotic neurons into functionally distinct areas, a phenomenon known as arealization (Rubenstein et al., 1999). More specifically, *Id2* affects

axonal/neurite outgrowth (Lasorella et al., 2006; Ko et al., 2016; Huang et al., 2019) and *RZRβ* is involved in clustering of neurons to generate proper connectivity patterns (Jabaudon et al., 2012). Thus, by preventing ectopic cortical expression of *RZRβ* and *Id2,* which is hypothesized to underlie aberrant INC patterning in both genetically manipulated (Huffman et al., 2004) and PrEE cortex (Abbott et al., 2018), choline provides a potential novel mechanistic framework for the partial prevention of altered INC patterns and areal size perturbations in CE neocortex. Furthermore, abnormal areal boundaries within the neocortex have been shown to directly impact mouse behavior (Leingärtner et al., 2007; Scearce-Levie et al., 2008), a facet of development heavily affected by PrEE.

One attractive, alternative hypothesis to purely aberrant expression of genes and INC patterns is that PrEE produces a developmental delay, an idea based largely on behavioral observations in humans with FASD (Davies et al., 2011). A review of previous work done in our laboratory in wild-type CD1 mice demonstrates the life-long natural progression of developmental changes in cortical gene expression and connections (Dye et al., 2011a; 2011b). From these data, we can conclude that neither the observed ectopic expression of *RZRβ* and *Id2* or the aberrant INC patterns reported here exist at any time within the normally developing mouse cortex, suggesting a developmental delay likely does not describe and/or underlie the phenotypes reported within the current study.

It is important to note that P0 endpoints, where neocortical aspects of neurodevelopment were analyzed, were not examined in a sex-specific manner.

Although the late embryonic period is considered a critical time for the effects of hormones on sexual dimorphic development (McCarthy, 2016), a recent study has found that anatomical changes in dimorphic brain structures typically emerge in later postnatal life (e.g. around P10) (Qiu et al., 2018). Thus, we do not expect sexually dimorphic features to be present in the infant mouse brain. However, future studies must take into account the potential sex differences within brain at all ages due to the differential effect of both EtOH and choline on offspring behavior reported here and elsewhere (Thomas et al., 2007; Schneider and Thomas et al., 2016).

Choline prevents PrEE-induced developmental alterations in behavior.
Several previous studies have examined choline's ability to mitigate PrEE-induced abnormal behavior, with a majority focusing on learning and memory behaviors (Thomas et al., 2007; Ryan et al., 2008; Schneider and Thomas, 2016). Here, we demonstrate that concurrent choline supplementation fully or partially prevents the development of motor deficits and increased potential anxiety-like behaviors present in peripubescent EtOH-exposed mice. Notably, the interpreted, specific behavioral alterations that choline prevented within the current study are among the myriad of dysfunctions consistently observed in rodent models (Thomas et al., 1996; Akers et al., 2011; Baculis et al., 2015), and humans with FASD (Barr et al., 2006; Connor et al., 2006; Carr et al., 2010). This is in contrast to previous studies which have reported that concurrent choline

supplementation during a P4-9 EtOH exposure does not prevent motor deficits (Thomas et al., 2004a). However, EtOH-induced motor developmental delays in offspring were also prevented by concurrent choline during a GD 5-20 exposure (Thomas et al., 2009). Taken together with our findings, this suggests that choline may have a critical period for mitigating sensorimotor deficits, likely restricted to specific prenatal ages.

The behavioral parameters assessed via the Suok test and Ledge tests have largely been interpreted as anxiety-like behaviors and derivatives of sensorimotor function. The anxiety-like interpretations are rooted in the classical approach-avoidance theory (Montgomery, 1955; Montgomery and Monkman, 1955) and are supported by the observed results of mice in the Suok test who have undertaken pharmacological anxiogenics or anxiolytics or have undergone predator stress (Kalueff et al., 2007; 2008). The interpretations of sensorimotor function modalities assayed in the test are, more simply, based on the parameters of the test that seemingly require both proper sensory processing of the apparatus environment and the ultimate motor function required to traverse this challenging apparatus.

However, it should be noted that like most behavioral assays, alternate interpretations of the parameters scored are also apparent. For example, missteps or falls may reflect pure motor or balance deficits rather than integration of sensorimotor information, supported by the likely cerebellar dysfunction reported that results due to PrEE (Maier et al., 1999; Thomas et al., 2010) which

was not directly examined within the current study. Additionally, the anxiety-like measures reported here (i.e. latency to leave center, directed exploration) may also reflect motor deficits due to the necessity of proper motor function to execute these phenomena. Similarly, rearing/grooming behaviors have also been interpreted as either increased or decreased in anxiety-like behavior. However, it is believed that low-stress grooming (indicative of low anxiety-like behavior) typically takes place in a highly-stereotyped cephalocaudal order, whereas stress-evoked grooming does not (Smolinksy et al., 2009). Within the current study, only stereotyped-cephalocaudal grooming was quantified in the Suok test and thus was interpreted as decreased anxiety-like behavior. Taken together, more in-depth testing is required in the future to fully parse out the behavioral modalities both disrupted by PrEE and potentially prevented by choline.

Lastly, we have included additional sex-separated behavioral analysis to determine the presence of sex-dependent variable effects of both PrEE and the ameliorative ability of choline. Largely, the behavioral trends observed in the sex-specific analyses closely mirror those seen in the combined dataset. However, it does appear that female mice may be both more sensitive to the potential increased anxiety-like behavior induced by PrEE, as well as to the ability of choline to prevent these behavioral abnormalities. This notion is supported by the finding that females display a significant decrease in directed exploration events and that choline supplementation prevents this phenomenon, which is not seen in the male-separated dataset, suggesting the observed effect in the combined

pool may be largely driven by females. Interestingly, these female-driven

observations support previous findings in preclinical choline FASD models

examining other behavioral modalities (Thomas et al., 2007; Schneider and

Thomas et al., 2016). However, others have found a greater ameliorative effect

of choline on EtOH-disrupted motor function and balance in males (Bearer et al.,

2015), suggesting that the sex-specific effects of PrEE and choline may be a

highly complex process that relies on many different factors, including timing and

dose of both choline supplementation and EtOH insult, as well as sex of

offspring. Further studies need to address this concept in depth in order to

develop a more effective intervention or treatment for the harmful consequences

of PrEE. In summary, our findings extend the established ability of choline to

mitigate PrEE-induced behavioral deficits to novel modalities that are relevant to

clinical FASD.

Potential mechanisms.

Choline influences neurodevelopment in a multitude of ways including

acting as a methyl-group donor in one-carbon metabolism (OCM), the cellular

pathway that generates methyl groups used for epigenetic modifications to DNA

and histones (reviewed in Zeisel, 2006). Here, we report global DNA

hypomethylation in rostral and caudal cortices of newborn EtOH mice, similar to

previous reports (Özturk et al., 2017). However, this effect was mitigated by

choline supplementation, suggesting choline supplementation may prevent

epigenetic dysregulation due to PrEE as previously reported (Otero et al., 2012; Bekdash et al., 2013). Since choline availability has been shown to directly influence DNA and histone methylation levels and, thus, gene expression within the developing brain (Mellot et al., 2007; Mehedint et al., 2010), the observed amelioration in cortical DNA methylation could potentially underlie the prevention of gene expression changes in PrEE neocortex observed here, however no direct testing of this hypothesis took place in the current study. Together, prevention of global epigenetic and subsequent genetic perturbations in PrEE neocortex by choline constitutes an appealing hypothesis for how choline may prevent brain and behavioral abnormalities associated with PrEE.

Despite the strong influence of choline availability on epigenetic regulation, choline also functions as a precursor to both membrane lipids and the neurotransmitter acetylcholine. Indeed, previous reports have shown supplementation can prevent PrEE-induced dysregulation in both of these systems (Monk et al., 2012; Tang et al., 2014), suggesting choline may exert its beneficial effects against PrEE insult via multiple mechanistic pathways. Additionally, it must be made clear that choline supplementation in the current report and in other studies (Thomas et al., 2004a; Hunt et al., 2014) does not reverse all adverse PrEE effects to control levels. Furthermore, although prenatal choline availability by itself has been reported to affect DNA methylation (Kovacheva et al., 2007) and gene expression (Mehedint et al., 2010) within the brain, we do not report similar differences here. Even though our significant

levels for DNA methylation and gene expression results are robust with low measured variability, we recognize that small samples size can limit the strength of conclusions drawn from the data. Thus, further work must be done to determine the precise mechanisms by which choline has its effects to develop the most effective preventative and/or therapeutic treatment for FASD.

Conclusions.

In summary, prenatal choline supplementation, when administered at the time of prenatal ethanol exposure, ameliorates abnormal brain and behavioral development. Specifically, the benefits of co-administration of choline during ethanol exposure are recovery of abnormal brain and body size and partial prevention of aberrant INC connectivity at birth, as well as the rescue of atypical *RZRβ* and *Id2* gene expression patterns and deficits in sensorimotor and anxiety-like behaviors at P20. The prevention of PrEE-induced global cortical DNA hypomethylation, suggests choline may be acting through canonical epigenetic pathways to achieve these protective effects. These findings suggest that choline supplementation offers significant protection from PrEE associated fetal growth abnormalities, and that optimal management of methyl group donors during pregnancy may be an effective way to reduce the extent of PrEE-based toxicity in high-risk individuals.

ACKNOWLEDGEMENTS

REFERENCES

Abbott CW, Kozanian OO, Kanaan J, Wendel KM, Huffman KJ (2016) The Impact of Prenatal Ethanol Exposure on Neuroanatomical and Behavioral Development in Mice. Alcohol Clin Exp Res 40:122–133.

Abbott CW, Rohac DJ, Bottom RT, Patadia S, Huffman KJ (2018) Prenatal Ethanol Exposure and Neocortical Development: A Transgenerational Model of FASD. Cereb Cortex 28:2908–2921.

Akers KG, Kushner SA, Leslie AT, Clarke L, van der Kooy D, Lerch JP, Frankland PW (2011) Fetal alcohol exposure leads to abnormal olfactory bulb development and impaired odor discrimination in adult mice. Mol Brain 4:29.

Baculis BC, Diaz MR, Fernando Valenzuela C (2015) Third trimester-equivalent ethanol exposure increases anxiety-like behavior and glutamatergic transmission in the basolateral amygdala. Pharmacol Biochem Behav 137:78–85.

Balaraman S, Idrus NM, Miranda RC, Thomas JD (2017) Postnatal choline supplementation selectively attenuates hippocampal microRNA alterations associated with developmental alcohol exposure. Alcohol 60:159–167.

Barak AJ, Beckenhauer HC, Tuma DJ, Badakhsh S (1987) Effects of prolonged ethanol feeding on methionine metabolism in rat liver. Biochem Cell Biol 65:230–3.

Bekdash RA, Zhang C, Sarkar DK (2013) Gestational choline supplementation normalized fetal alcohol-induced alterations in histone modifications, DNA methylation, and proopiomelanocortin (POMC) gene expression in ??-endorphin-producing POMC neurons of the hypothalamus. Alcohol Clin Exp Res 37:1133–1142.

Biller A, Bartsch AJ, Homola G, Solymosi L, Bendszus M (2009) The Effect of Ethanol on Human Brain Metabolites Longitudinally Characterized by Proton MR Spectroscopy. J Cereb Blood Flow Metab 29:891–902.

Carr JL, Agnihotri S, Keightley M (2010) Sensory Processing and Adaptive Behavior Deficits of Children Across the Fetal Alcohol Spectrum Disorder Continuum. Alcohol Clin Exp Res 34:1022–1032.

Chasnoff IJ, Wells AM, King L (2015) Misdiagnosis and Missed Diagnoses in Foster and Adopted Children With Prenatal Alcohol Exposure. Pediatrics 135:264–270.

Connor PD, Sampson PD, Streissguth AP, Bookstein FL, Barr HM (2006) Effects of prenatal alcohol exposure on fine motor coordination and balance: A study of two adult samples. Neuropsychologia 44:744–751.

Cuzon VC, Yeh PWL, Yanagawa Y, Obata K, Yeh HH (2008) Ethanol Consumption during Early Pregnancy Alters the Disposition of Tangentially Migrating GABAergic Interneurons in the Fetal Cortex. J Neurosci 28:1854–1864.

Datta S, Turner D, Singh R, Ruest LB, Pierce WM, Knudsen TB (2008) Fetal alcohol syndrome (FAS) in C57BL/6 mice detected through proteomics screening of the amniotic fluid. Birth Defects Res Part A Clin Mol Teratol 82:177–186.

Davies L, Dunn M, Chersich M, Urban M, Chetty C, Olivier L, Viljoen D (2011) Developmental delay of infants and young children with and without fetal alcohol spectrum disorder in the Northern Cape Province, South Africa. African J Psychiatry (South Africa) 14:298–305.

Deeney S, Powers KN, Crombleholme TM (2016) A comparison of sexing methods in fetal mice. Lab Anim (NY) 45:380–384.

Denny CH, Acero CS, Naimi TS, Kim SY (2019) Consumption of Alcohol Beverages and Binge Drinking Among Pregnant Women Aged 18–44 Years — United States, 2015–2017. MMWR Morb Mortal Wkly Rep 68:365–368.

Dye CA, Abbott CW, Huffman KJ (2012) Bilateral enucleation alters gene expression and intraneocortical connections in the mouse. Neural Dev 7:5.

Dye CA, El Shawa H, Huffman KJ (2011) A lifespan analysis of intraneocortical connections and gene expression in the mouse II. Cereb Cortex 21:1331–1350.

Dye CA, El Shawa H, Huffman KJ (2011) A lifespan analysis of intraneocortical connections and gene expression in the mouse II. Cereb Cortex 21:1331–1350.

El Shawa H, Abbott CW, Huffman KJ (2013) Prenatal Ethanol Exposure Disrupts Intraneocortical Circuitry, Cortical Gene Expression, and Behavior in a Mouse Model of FASD. J Neurosci 33:18893–18905.

Fowler A-K, Hewetson A, Agrawal RG, Dagda M, Dagda R, Moaddel R, Balbo S, Sanghvi M, Chen Y, Hogue RJ, Bergeson SE, Henderson GI, Kruman II (2012) Alcohol-induced one-carbon metabolism impairment promotes dysfunction of DNA base excision repair in adult brain. J Biol Chem 287:43533–42.

Greenmyer JR, Klug MG, Kambeitz C, Popova S, Burd L (2018) A Multicountry Updated Assessment of the Economic Impact of Fetal Alcohol Spectrum Disorder: Costs for Children and Adults. J Addict Med 12:466–473.

Guyenet SJ, Furrer SA, Damian VM, Baughan TD, la Spada AR, Garden GA (2010) A simple composite phenotype scoring system for evaluating mouse models of cerebellar ataxia. J Vis Exp.

Hashimoto-Torii K, Kawasawa YI, Kuhn A, Rakic P (2011) Combined transcriptome analysis of fetal human and mouse cerebral cortex exposed to alcohol. Proc Natl Acad Sci U S A 108:4212–7.

Huffman KJ, Garel S, Rubenstein JLR (2004) Fgf8 Regulates the Development of Intra-Neocortical Projections. J Neurosci 24:8917–8923.

Hunt PS, Jacobson SE, Kim S (2014) Supplemental choline does not attenuate the effects of neonatal ethanol administration on habituation of the heart rate orienting response in rats. Neurotoxicol Teratol 44:121–125.

Ikonomidou C, Bittigau P, Ishimaru MJ, Wozniak F, Koch C, Genz K, Price MT, Stefovska V, Tenkova T, Dikranian K, Olney JW (2000) Ethanol-Induced Ethanol-Induced Apoptotic Apoptotic Neurodegeneration Neurodegeneration and and Fetal Fetal Alcohol Alcohol Syndrome Syndrome. Science (80-) 287:1056–1060.

Infante MA, Moore EM, Bischoff-Grethe A, Migliorini R, Mattson SN, Riley EP (2015) Atypical cortical gyrification in adolescents with histories of heavy prenatal alcohol exposure. Brain Res 1624:446–454.

Institute of Medicine (US) (1998) Dietary Reference Intakes for Thiamin, Riboflavin, Niacin, Vitamin B6, Folate, Vitamin B12, Pantothenic Acid, Biotin, and Choline, Dietary Reference Intakes for Thiamin, Riboflavin, Niacin, Vitamin B6, Folate, Vitamin B12, Pantothenic Acid, Biotin, and Choline. Washington, D.C., National Academies Press.

Jacobson SW, Carter RC, Molteno CD, Stanton ME, Herbert JS, Lindinger NM, Lewis CE, Dodge NC, Hoyme HE, Zeisel SH, Meintjes EM, Duggan CP, Jacobson JL (2018) Efficacy of Maternal Choline Supplementation During Pregnancy in Mitigating Adverse Effects of Prenatal Alcohol Exposure on Growth and Cognitive Function: A Randomized, Double-Blind, Placebo-Controlled Clinical Trial. Alcohol Clin Exp Res 42:1327–1341.

Kaas JH (1995) The Segregation of Function in the Nervous System: Why Do Sensory Systems Have So Many Subdivisions? Contrib Sens Physiol 7:201–240.

Kalueff A V., Keisala T, Minasyan A, Tuohimaa P (2007) Pharmacological modulation of anxiety-related behaviors in the murine Suok test. Brain Res Bull 74:45–50.

Kalueff A V, Keisala T, Minasyan A, Kumar SR, LaPorte JL, Murphy DL, Tuohimaa P (2008) The regular and light–dark Suok tests of anxiety and sensorimotor integration: utility for behavioral characterization in laboratory rodents. Nat Protoc 3:129–136.

Kodali VN, Jacobson JL, Lindinger NM, Dodge NC, Molteno CD, Meintjes EM, Jacobson SW (2017) Differential Recruitment of Brain Regions During Response Inhibition in Children Prenatally Exposed to Alcohol. Alcohol Clin Exp Res 41:334–344.

Komada M, Hara N, Kawachi S, Kawachi K, Kagawa N, Nagao T, Ikeda Y (2017) Mechanisms underlying neuro-inflammation and neurodevelopmental toxicity in the mouse neocortex following prenatal exposure to ethanol. Sci Rep 7:4934.

Leingärtner A, Thuret S, Kroll TT, Chou S-J, Leasure JL, Gage FH, O'Leary DDM (2007) Cortical area size dictates performance at modality-specific behaviors. Proc Natl Acad Sci U S A 104:4153–8.

Maier SE, Miller JA, Blackwell JM, West JR (1999) Fetal Alcohol Exposure and Temporal Vulnerability: Regional Differences in Cell Loss as a Function of the Timing of Binge-Like Alcohol Exposure During Brain Development. Alcohol Clin Exp Res 23:726–734.

May PA, Chambers CD, Kalberg WO, Zellner J, Feldman H, Buckley D, Kopald D, Hasken JM, Xu R, Honerkamp-Smith G, Taras H, Manning MA, Robinson LK, Adam MP, Abdul-Rahman O, Vaux K, Jewett T, Elliott AJ, Kable JA, Akshoomoff N, Daniel F, Arroyo JA, Hereld D, Riley EP, Charness ME, Coles CD, Warren KR, Jones KL, Hoyme HE (2018) Prevalence of fetal

alcohol spectrum disorders in 4 US communities. JAMA - J Am Med Assoc 319:474–482.

McCann JC, Hudes M, Ames BN (2006) An overview of evidence for a causal relationship between dietary availability of choline during development and cognitive function in offspring. Neurosci Biobehav Rev 30:696–712.

McCarthy MM (2016) Sex differences in the developing brain as a source of inherent risk. Dialogues Clin Neurosci 18:361–372.

Meck WH, Williams CL (1999) Choline supplementation during prenatal development reduces proactive interference in spatial memory. Dev Brain Res 118:51–59.

Mehedint MG, Niculescu MD, Craciunescu CN, Zeisel SH (2010) Choline deficiency alters global histone methylation and epigenetic marking at the Re1 site of the calbindin 1 gene. FASEB J 24:184–95.

Mellott TJ, Follettie MT, Diesl V, Hill AA, Lopez-Coviella I, Blusztajn JK (2007) Prenatal choline availability modulates hippocampal and cerebral cortical gene expression. FASEB J 21:1311–1323.

Monk BR, Leslie FM, Thomas JD (2012) The effects of perinatal choline supplementation on hippocampal cholinergic development in rats exposed to alcohol during the brain growth spurt. Hippocampus 22:1750–1757.

Montgomery KC (1955) The relation between fear induced by novel stimulation and exploratory drive. J Comp Physiol Psychol 48:254–260.

Montgomery KC, Monkman JA (1955) The relation between fear and exploratory behavior. J Comp Physiol Psychol 48:132–136.

Oishi K, Aramaki M, Nakajima K (2016) Mutually repressive interaction between Brn1/2 and Rorb contributes to the establishment of neocortical layer 2/3 and layer 4. Proc Natl Acad Sci U S A 113:3371–3376.

Otero NKH, Thomas JD, Saski CA, Xia X, Kelly SJ (2012) Choline Supplementation and DNA Methylation in the Hippocampus and Prefrontal Cortex of Rats Exposed to Alcohol During Development. Alcohol Clin Exp Res 36:1701–1709.

Öztürk NC, Resendiz M, Öztürk H, Zhou FC (2017) DNA Methylation program in normal and alcohol-induced thinning cortex. Alcohol 60:135–147.

Pascual M, Montesinos J, Montagud-Romero S, Forteza J, Rodríguez-Arias M, Miñarro J, Guerri C (2017) TLR4 response mediates ethanol-induced neurodevelopment alterations in a model of fetal alcohol spectrum disorders. J Neuroinflammation 14:145.

Qiu LR, Fernandes DJ, Szulc-Lerch KU, Dazai J, Nieman BJ, Turnbull DH, Foster JA, Palmert MR, Lerch JP (2018) Mouse MRI shows brain areas relatively larger in males emerge before those larger in females. Nat Commun 9.

Rubenstein JL, Anderson S, Shi L, Miyashita-Lin E, Bulfone A, Hevner R (1999) Genetic control of cortical regionalization and connectivity. Cereb Cortex 9:524–32.

Ryan SH, Williams JK, Thomas JD (2008) Choline supplementation attenuates learning deficits associated with neonatal alcohol exposure in the rat: Effects of varying the timing of choline administration. Brain Res 1237:91–100.

Scearce-Levie K, Roberson ED, Gerstein H, Cholfin JA, Mandiyan VS, Shah NM, Rubenstein JLR, Mucke L (2008) Abnormal social behaviors in mice lacking Fgf17. Genes, Brain Behav 7:344–354.

Schaefer ML, Wong ST, Wozniak DF, Muglia LM, Liauw JA, Zhuo M, Nardi A, Hartman RE, Vogt SK, Luedke CE, Storm DR, Muglia LJ (2000) Altered stress-induced anxiety in adenylyl cyclase type VIII-deficient mice. J Neurosci 20:4809–4820.

Schneider RD, Thomas JD (2016) Adolescent Choline Supplementation Attenuates Working Memory Deficits in Rats Exposed to Alcohol During the Third Trimester Equivalent. Alcohol Clin Exp Res 40:897–905.

Sebastiani G, Borrás-Novell C, Casanova MA, Pascual Tutusaus M, Ferrero Martínez S, Gómez Roig MD, García-Algar O (2018) The Effects of Alcohol and Drugs of Abuse on Maternal Nutritional Profile during Pregnancy. Nutrients 10.

Smiley JF, Saito M, Bleiwas C, Masiello K, Ardekani B, Guilfoyle DN, Gerum S, Wilson DA, Vadasz C (2015) Selective reduction of cerebral cortex GABA neurons in a late gestation model of fetal alcohol spectrum disorder. Alcohol 49:571–580.

Smolinsky AN, Bergner CL, LaPorte JL, Kalueff A V. (2009) Analysis of Grooming Behavior and Its Utility in Studying Animal Stress, Anxiety, and Depression, pp 21–36.

Tang N, Bamford P, Jones J, He M, Kane MA, Mooney SM, Bearer CF (2014) Choline Partially Prevents the Impact of Ethanol on the Lipid Raft Dependent Functions of L1 Cell Adhesion Molecule. Alcohol Clin Exp Res 38:2722.

Thomas JD, Wasserman EA, West JR, Goodlett CR (1996) Behavioral deficits induced by bingelike exposure to alcohol in neonatal rats: importance of developmental timing and number of episodes. Dev Psychobiol 29:433–52.

Thomas J, Garrison M, O'Neill TM (2004) Perinatal choline supplementation attenuates behavioral alterations associated with neonatal alcohol exposure in rats. Neurotoxicol Teratol 26:35–45.

Thomas JD, Abou EJ, Dominguez HD (2009) Prenatal choline supplementation mitigates the adverse effects of prenatal alcohol exposure on development in rats. Neurotoxicol Teratol 31:303–311.

Thomas JD, Biane JS, O'Bryan KA, O'Neill TM, Dominguez HD (2007) Choline supplementation following third-trimester-equivalent alcohol exposure attenuates behavioral alterations in rats. Behav Neurosci 121:120–130.

Thomas JD, Idrus NM, Monk BR, Dominguez HD (2010) Prenatal choline supplementation mitigates behavioral alterations associated with prenatal alcohol exposure in rats. Birth Defects Res Part A Clin Mol Teratol 88:827–837.

Thomas JD, La Fiette MH, Quinn VRE, Riley EP (2000) Neonatal choline supplementation ameliorates the effects of prenatal alcohol exposure on a discrimination learning task in rats. Neurotoxicol Teratol 22:703–711.

Thomas JD, O'Neill TM, Dominguez HD (2004) Perinatal choline supplementation does not mitigate motor coordination deficits associated with neonatal alcohol exposure in rats. Neurotoxicol Teratol 26:223–229.

Thomas JD, Tran TD (2012) Choline supplementation mitigates trace, but not delay, eyeblink conditioning deficits in rats exposed to alcohol during development. Hippocampus 22:619–630.

Trujillo-Gonzalez I, Wang Y, Friday WB, Vickers KC, Toth CL, Molina-Torres L, Surzenko N, Zeisel SH (2019) MicroRNA-129-5p is regulated by choline availability and controls EGF receptor synthesis and neurogenesis in the cerebral cortex. FASEB J 33:3601–3612.

Wang Q, Bardgett ME, Wong M, Wozniak DF, Lou J, McNeil BD, Chen C, Nardi A, Reid DC, Yamada K, Ornitz DM (2002) Ataxia and paroxysmal dyskinesia in mice lacking axonally transported FGF14. Neuron 35:25–38.

Wang Q, Bardgett ME, Wong M, Wozniak DF, Lou J, McNeil BD, Chen C, Nardi A, Reid DC, Yamada K, Ornitz DM (2002) Ataxia and Paroxysmal Dyskinesia in Mice Lacking Axonally Transported FGF14. Neuron 35:25–38.

Wang Y, Surzenko N, Friday WB, Zeisel SH (2016) Maternal dietary intake of choline in mice regulates development of the cerebral cortex in the offspring. FASEB J 30:1566–1578.

Wolterink-Donselaar IG, Meerding JM, Fernandes C (2009) A method for gender determination in newborn dark pigmented mice. Lab Anim (NY) 38:35–38.

Wozniak JR, Fuglestad AJ, Eckerle JK, Fink BA, Hoecker HL, Boys CJ, Radke JP, Kroupina MG, Miller NC, Brearley AM, Zeisel SH, Georgieff MK (2015) Choline supplementation in children with fetal alcohol spectrum disorders: a randomized, double-blind, placebo-controlled trial. Am J Clin Nutr 102:1113–1125.

Zeisel SH (2006) Choline: Critical Role During Fetal Development and Dietary Requirements in Adults. Annu Rev Nutr 26:229–250.

Zhou D, Rasmussen C, Pei J, Andrew G, Reynolds JN, Beaulieu C (2018) Preserved cortical asymmetry despite thinner cortex in children and adolescents with prenatal alcohol exposure and associated conditions. Hum Brain Mapp 39:72–88.

Chapter 3: The impact of paternal alcohol consumption on early postnatal development of the neocortex

ABSTRACT

Fetal alcohol spectrum disorders (FASD) describe the wide array of long-lasting developmental abnormalities in offspring due to prenatal alcohol (ethanol, EtOH) exposure via maternal gestational drinking. Although the teratogenic consequences of prenatal ethanol exposure, or PrEE, are apparent, the effects of preconception paternal ethanol exposure (PatEE) are still unclear. Previous research suggests that PatEE can induce molecular changes and abnormal behavior in the offspring. However, it is not known if PatEE impacts the development of the neocortex and behavior in offspring as demonstrated in maternal consumption models of FASD (El Shawa et al., 2013). In this study, we utilized a novel mouse model of PatEE where male mice self-administered 25% EtOH for an extended period prior to conception, generating indirect exposure to the offspring through the paternal germline. Following mating, we examined the effects of PatEE on offspring neocortical development at postnatal day (P) 0. PatEE resulted in significant impact on neocortical development, including abnormal patterns of gene expression within the neocortex at P0, as well as subtle alterations in patterns of intraneocortical connections. These results demonstrate that the developmental impact of preconception PatEE is more harmful than previously thought and provide additional insights into the biological

93

mechanisms that may underlie atypical behavior observed in children of alcoholic fathers.

INTRODUCTION

In humans, prenatal ethanol exposure (PrEE) can result in fetal alcohol spectrum disorders, or FASD. This designation incorporates a variety of long-lasting cognitive and behavioral deficits (Hoyme et al., 2016) and has incidence rates as high as 5% in the United States (May et al., 2018). Much less is known about the impact of preconception paternal ethanol exposure (PatEE), despite a growing body of preclinical evidence indicating that offspring sired by males exposed to ethanol (EtOH) prior to conception display altered brain and behavioral development similar to maternally-mediated prenatal EtOH exposure (Jamerson et al., 2004; Meek et al., 2007; Kim et al., 2014; Finegersh and Homanics, 2014; Rompala et al., 2016; 2017; Chang et al., 2017; 2019). Additionally, clinical research in humans has found associations among heavy paternal EtOH consumption and adverse developmental outcomes in offspring (reviewed in Finegersh et al., 2015; Zuccolo et al., 2017; Xia et al., 2018), providing further support for the deleterious impact of paternal drinking. Although research investigating the impact of PatEE is on the rise, it remains greatly understudied compared to models of FASD generated from EtOH exposure via maternal drinking.

The neocortex, the largest part of the human brain, has many emergent

properties that mediate complex, higher-order functions and behaviors. The

neocortex relies on a tightly regulated temporal and spatial orchestration of

genetic and environmental cues for proper development, a process that seems

particularly susceptible to prenatal EtOH insult. Animal studies focusing on

maternal EtOH exposure have found a plethora of atypical cortical phenotypes

present in offspring including increased apoptosis (Ikonomidou et al., 2000),

altered pyramidal cell morphology (Granato et al., 2003), modified development

of anatomical regions or structures (Abbott et al., 2016) and atypical

development of the intra-neocortical circuitry (El Shawa et al., 2013). Human

neuroimaging studies in children with FASD have also demonstrated

abnormalities in neocortical development (Zhou et al., 2011), suggesting that

irregular cortical phenotypes may underlie some PrEE-induced behavioral

alterations.

One particular aspect of neocortical development affected by prenatal

EtOH exposure is arealization, or the patterning of neurons into functionally and

spatially distinct areas (Krubitzer and Huffman, 2000). Specifically, prenatal EtOH

exposure results in aberrant intraneocortical connections (INCs), as well as

altered expression of genes critical for proper patterning of the neocortex in mice

(El Shawa et al., 2013). Recently, we have demonstrated that these phenotypes

pass to second and third filial generations after an initial prenatal EtOH exposure

(Abbott et al., 2018), suggesting EtOH may have potent transgenerational

effects. Despite a growing body of research on how PrEE impacts the neocortex, there is a paucity of data regarding how paternal ethanol exposure may alter cortical development.

Preclinical studies focusing on PatEE's effects on the neocortex are sparse but have shown that affected offspring have increased cortical thickness (Jamerson et al., 2004) as well as altered expression and epigenetic regulation of the dopamine transporter in frontal cortex (Kim et al., 2014). Importantly, to our knowledge, no study exists examining the effect of preconception paternal EtOH consumption on development of neocortical connections. Due to the ability of PatEE to disrupt normal development in the neocortex, as well as EtOH's particular ability to modify INCs in absence of direct exposure, we hypothesized that PatEE offspring could also demonstrate abnormal neocortical development.

The goal of this study was to characterize the impact of a paternal binge of EtOH prior to conception on offspring cortical development. Specifically, we analyzed cortical gene expression and development of INCs in newborn mice. Results from this study suggest that the paternal environment before conception is critical for healthy offspring development.

MATERIALS AND METHODS

Animal care.

All studies were conducted under research protocol guidelines approved by the Institutional Animal Care and Use Committee (IACUC) at UCR. CD-1 mice were

initially purchased from Charles River Laboratories (Wilmington, MA/USA). All subjects were housed in UCR animal facilities under a standard 12h/12h light/dark cycle. All efforts were made to minimize animal discomfort and the number of mice utilized.

Ethanol administration and breeding.

Male mice, aged 3-6 months, were separated into control and EtOH exposed groups. Initially, experimental EtOH-treated male mice (n = 10) were provided a 25% EtOH-in-water solution, *ad libitum,* for 15 days as well as standard mouse chow (Fig. 3.1). Control males (n = 10) were provided *ad libitum* water and standard mouse chow. After the binge period, P90 female mice were paired with control or EtOH-treated sires at the beginning of the dark cycle for breeding. The day of conception was determined by the presence of a vaginal plug, after which males were removed from the dam's cage. If no vaginal plug was observed, the male was returned to his home cage for continued treatment of EtOH or water for the remainder of the day and then placed back into the breeding cage at the start of the dark cycle. The average time to conception was 3.5 days for EtOH sires and 2.8 days for control sires. Each group had a time-to-conception of 0-8 days with total length of treatment being 15-23 days. All pregnant female mice were housed individually and provided standard mouse chow and water *ad libitum*. All female dams were EtOH-naïve and did not have access to EtOH.

Sire daily intake and blood ethanol content measurements.

Daily measurements of food and liquid intake of male mice were recorded at 1200 h to assess confounding nutritional differences between experimental and control groups. Each male was provided 100g of food and the chow was re-weighed daily at noon and replenished to 100g. Daily liquid intake (25% EtOH-in-water or water alone) for sires was measured using a graduated drinking bottle. Average daily values for food and liquid intake of experimental mice as well as weight gain were compared to control mice using *t*-test analyses. Also, body weights, in grams, were recorded for all mice at the beginning of exposure, when the ethanol solution was provided and at the end when ethanol was removed, to eliminate weight gain differences as a potential confound. Blood ethanol concentration (BEC) of a separate subset of males, resulting from treatment of 25% EtOH in water (n = 7) or water alone (n = 7), was determined using an alcohol dehydrogenase-based enzymatic assay (Pointe Scientific, Canton, MI/USA; see Supplemental Methods for details).

Tissue preparation.

On the day of birth, P0, the litter sizes were recorded. Pups born to dams bred with EtOH-treated sires were designated as PatEE pups and pups born to dams bred with water-treated sires were designated as controls. For each litter (n = 10, both groups), subsets of offspring were randomly designated for P0 analyses in an effort to reduce potential litter effects and ensure an even sampling for each

experimental endpoint. Experimental/control subsets per litter were limited to 2 ±

2 pups for P0 endpoints, dependent on total litter size. P0 pups used for dye

tracing and gene expression studies were sacrificed via hypothermia and

exsanguination, and transcardially perfused with 4% paraformaldehyde (PFA) in

0.1M phosphate buffer, pH 7.4. Due to the absence of distinguishing sexual

characteristics at P0, the relative inaccuracy of using anogenital distances at this

age (Greenham and Greenham, 1977), and the absence of pigment in albino

CD-1 mice (Wolterink-Doselaar et al., 2009), no sex differences were assessed

at P0. Next, brains were quickly removed from the skull and weighed. After post-

fixation in 4% PFA, brains were hemisected and hemispheres were designated

for either anatomy, gene expression assays, or dye tracing. Table 1 summarizes

the total animal usage within the study.

Gene expression assays.

Analysis of gene expression within P0 brain hemispheres was carried out via *in

situ* RNA hybridization (ISH). Standard protocols for free-floating non-radioactive

ISH were used to visualize neocortical *Id2* and *RZRβ* gene expression of P0

control and PatEE brains, as previously described (Dye et al., 2011a; 2011b; El

Shawa et al., 2013). Briefly, hemispheres were first embedded in gelatin-albumin,

and sectioned at 100µm via vibratome. After hybridization to probes for *Id2* and

RZRβ synthesized from cDNA (gifts from John Rubenstein, UCSF; see Abbott et

al., 2018 for details), sections were mounted in a 50% glycerol solution onto

glass slides, coverslipped, and imaged using a Zeiss Axio HRm camera attached to a dissecting microscope. Anatomically matched ISH sections from PatEE and control P0 brains are presented to highlight the effects of altered gene expression of *Id2* and *RZRβ* associated with PatEE. Additionally, analysis of gene expression was also quantified at specific, highlighted ROIs, by calculating transcript densities using ImageJ (NIH). Briefly, images at identical anatomical levels were converted to binary and a standardized threshold was defined. ROIs were then defined by static electronic grid positioning over the specific cortical areas in both control and PatEE brains. Using landmarks such as hippocampus, anterior commissure, and corpus callosum, sections were matched carefully and multiple cases were used, as published previously, to ensure reliability (El Shawa et al., 2013). Individual transcript density signals (as pixel densities) were measured and reported as area fraction of total ROI.

Anatomical tracing.

To determine patterns of ipsilateral INC development in P0 mice 1,1-Dioctadecyl-3,3,3,3-tetramethylindocarbocyanine (DiI; Invitrogen, Carlsbad, CA/USA) and 4-(4-(dihexadecylamino)styryl)-N-methylpyridinium iodide (DiA; Invitrogen) dye crystals were placed in putative somatosensory (S1) or putative visual cortex (V1), as described previously (Dye et al., 2011a; 2011b; El Shawa et al., 2013). A coordinate grid was used for reliability of dye placement locations (DPLs) across cases. Following placement of crystals, hemispheres were placed in 4% PFA in

the dark at 30°C for 4-6 weeks to allow for dye transport. Upon confirmation of retrograde thalamic nuclei labeling, brains were embedded in 5% low melting point agarose, and sectioned at 100µm via vibratome in 1X phosphate buffered saline. Sections were then counterstained with 4′, 6-diamidino-2-phenylindole dihydrochloride (DAPI; Roche, Basel/Switzerland), mounted onto glass slides, and coverslipped using FluoroMount (Sigma; St. Louis, MO/USA). A Zeiss Axio Upright Imager microscope equipped with a Zeiss Axio high resolution (HRm) camera and three filters was used to visualize and capture images of dye tracing sections via PC running Axiovision software (version 4.8). The three filters used are detailed in the following: red for DiI, green for DiA, and blue for DAPI counterstain labeling (Excitation wavelengths-red: Cyanine 3, 550 nm; green: green fluorescent protein (GFP), 470 nm; blue: DAPI, 359 nm. Emission wavelengths-red: Cyanine 3, 570 nm; green: GFP, 509 nm; blue: DAPI, 461 nm). Images from all 3 filters per section were merged for subsequent analysis. Matched sections from PatEE and control brains using DAPI counter-stained landmarks were used to compare the development and trajectory of INCs between treatment groups.

Dye placement locations (DPLs) were quantified as a percentage of total cortical length to ensure that the relative size of the injection remained consistent. Dye projection zones (DPZs) in the visual and somatosensory cortices were quantified as a percentage of total cortical length by measuring the distance from the most rostral and caudal retrogradely labeled cells using a

micrometer. Additionally, the lateral dispersion of cells stemming from V1 injections was quantified by electronically measuring the distance from the corpus callosum to the furthest laterally labeled cell in anatomically matched sections.

Statistical analysis.

All statistical analyses were completed using GraphPad Prism 6 (La Jolla, CA/USA). For all sire measurements and P0 pup brain analyses (ISH, dye-tracing, anatomy), unpaired two-tailed *t*-tests were used to compare results between control and experimental groups. For all statistical measures, a *p* value of < 0.05 was set for significance. All data are expressed as mean ± S.E.M. and these values are presented in Table 3.2.

RESULTS

Paternal measurements.

In order to assess potential differences in liquid intake among EtOH-exposed and control fathers, we measured liquid intake daily for the length of exposure (Fig. 3.2). We found no significant differences in daily liquid intake between control and EtOH-exposed sires (Fig. 3.2A, *p* = 0.560). We also found no significant differences in total weight gain during the exposure period between control and EtOH-exposed sires or in daily average food intake. To confirm EtOH exposure, as well as measure the level of EtOH intoxication, we measured blood EtOH

concentration (BECs) in 7 males exposed to 25% EtOH for 20 days, as well as 7

control males (Fig. 3.2). The 20-day exposure time point was chosen to measure

BECs due to it being near average position in the 15-23 day exposure paradigm

used. As expected, sires exposed to 20 days of 25% EtOH showed elevated

BEC levels and control (water exposed) sires did not display any detectable BEC

levels (Fig. 3.2B, **p < .01). Overall, these results suggest that no disparity in

liquid intake, food intake, or weight gain occurs due to EtOH exposure in sire

mice, and that sufficient levels of EtOH intoxication occur in male mice following

a 20-day exposure period.

Cortical gene expression analyses.

Id2 and *RZRβ* are two genes important for neocortical patterning and arealization

(Rubenstein et al., 1999). Previously, we demonstrated that cortical expression of

these two genes is altered by maternal prenatal EtOH exposure at P0 (El Shawa

et al., 2013; Abbott et al., 2018). Accordingly, we investigated expressions of *Id2*

and *RZRβ* in neocortex to determine whether this patterning is affected by PatEE

in mice at P0. Using *in situ* RNA hybridization, we examined patterns of gene

expression in P0 coronal hemisections via side-by-side analyses of anatomically

matched sections from both control and PatEE brains (Fig. 3.3). In control mice,

Id2 expression is highly complex, spanning multiple cortical layers including II/III,

V, and VI (Fig. 3.3A1-5). Additionally, a distinct boundary of the most superficial

Id2 expression occurs in control mice at P0 (arrows, Fig. 3.3A2-3), which marks

the border of absent lateral *Id2* expression. In anatomically matched sections of PatEE mice, however, this border appears to be visually shifted to further lateral cortical regions (arrows, Fig. 3.3B2-3), and, thus, *Id2* expression also extends further laterally compared to controls. *RZRβ* expression in control animals is largely limited to cortical layer IV (Fig. 3.3C1-5). However, a typical border occurs that delineates an absence of expression in the medial cortical wall (arrow, Fig. 3.3C3). In contrast, PatEE brains exhibit a medial shift in this boundary (arrow, Fig. 3.3C4), and *RZRβ* expression extends medially as a result.

In order to quantify and confirm these visually identified cortical gene expression shifts, we used binary-converted images of raw data to measure density of transcript within static ROIs in both control and PatEE anatomically matched sections (Fig. 3.4). *RZRβ* expression was quantified in the medially positioned ROI (black box) designated within the line drawing (Fig. 3.4C1). As seen in the representative ISH images (Fig. 3.4A1; B1), medial expression of *RZRβ* was increased significantly in the ROI in the rostral region of the parietal cortex in PatEE mice compared to controls at P0 (Fig. 3.4D1, $p < .01$). *Id2* expression was similarly quantified within a static ROI, however this ROI was positioned further laterally (black box, Fig. 3.4C2). *Id2* expression was increased significantly within the ROI in PatEE brains compared to controls (Fig. 3.4D2, $p < .0001$).

Importantly, these concurrent shifts in both *Id2* and *RZRβ* cortical boundaries of expression occur at the same anatomical levels i.e. both shifts

were quantified in anatomically matched sections among both groups (compare representative images and line drawings in Fig. 3.4A1, B1, C1 to Fig. 3.4A2, B2, C2). As seen in control mice, *RZRβ* and *Id2* expression boundaries approximately abut each other near the visual-sensory cortex border at P0 (compare arrow in Fig. 6A1 to arrow in Fig. 6A2). However, in PatEE mice, both of these two boundaries of expression extend in opposite directions i.e. *RZRβ* extends medially and *Id2* expression extends laterally (compare arrow in Fig. 6B1 to arrow in Fig. 6B2)*,* producing an atypical overlapping region of expression.

Dye tracing experiments.

Ipsilateral intraneocortical connections (INCs) constitute a distinct feature of mature cortical areas (Kaas, 1982) and prenatal EtOH results in disorganized INC patterns within the cortex of exposed P0 mice (El Shawa et al., 2013; Abbott et al., 2018). Here, we characterized development of ipsilateral INCs in control and PatEE brains at P0 using lipophilic dyes (Fig. 3.5). and present the patterns of INCs stemming from putative S1 (asterisks, Fig. 3.5A2, B2) and putative V1 dye placements (asterisks, Fig. 3.5A5, B5). No significant differences in dye placement locations (DPLs) in the putative S1 (Fig. 3.6A, $p = 0.78$) and putative V1 (Fig. 3.6C, $p = 0.15$) were observed, ensuring that the relative injection size was consistent across cases.

No significant differences in dye projection zones (DPZs) of the

somatosensory cortex were observed (Fig. 3.6B, *p* = 0.289), as well as in visual

cortex DPZs, although a trend towards significance was noted (Fig. 3.6D, *p* =

0.09). However, PatEE brains contained aberrant labeled cells in rostral regions

not present in controls (Fig. 3.5B3), which were present in variable amounts in

PatEE mice. Additionally, in control mice, labeled S1-derived cells extend

caudally, and are located laterally to the visual cortex forming the

somatosensory-visual boundary in controls (Fig. 3.5A4). However, a clear

boundary between these regions was not consistently observed in PatEE mice,

as some mixing between S1-derived and V1-derived cells was present (Fig.

3.5B3, B4). In order to quantify this phenomenon, we used a novel technique to

measure the lateral cortical cell dispersion at this region and found that labeled

cells stemming from V1 injections are present in further lateral cortical positions

in PatEE mice compared to controls (Fig. 3.7, *p* = 0.0410), suggesting abnormal

patterning of INCs at P0 due to PatEE. Interestingly, this areal cell mixing was

also seen at the same anatomical level of the abnormal *RZRβ* and *Id2*

overlapping region observed at P0 in PatEE mice (compare levels: Fig. 3.4A1-2,

B1-2 to Fig. 3.5A4, B4). These data suggest that PatEE results in subtle

alterations in INC patterns in newborn mice, which may be related to altered

cortical patterning gene expression.

DISCUSSION

In this study, we demonstrate that paternal ethanol exposure can induce

dramatic alterations in offspring neocortical gene expression and subtle changes

in neocortical connectivity. Overall, these results suggest that 15-23 days of

PatEE can alter brain developmental trajectories in rodent offspring.

Impact of PatEE on cortical gene expression and INC development

In previous rodent models, PatEE has been shown to disturb gene expression in

the brain (Liang et al., 2014; Finegersh and Homanics, 2014; Przybycien-

Szymanska et al., 2014; Kim et al., 2014; Rompala et al., 2017) and liver (Chang

et al., 2017; 2019) of offspring. In this study, we examined two specific genes

involved in governing arealization, and found that both *RZRβ* and *Id2* expression

were altered in the cortex of P0 offspring sired by male mice exposed to EtOH.

Functionally, *Id2* is a helix-loop-helix transcription factor important for neural stem

cell renewal and normal CNS development (Park et al., 2013), while *RZRβ,* a

nuclear receptor*,* influences proper cortical structural patterning, including

development of the barrel cortex in S1 (Jabaudon et al., 2012). Importantly, both

genes are present within murine neocortex at embryonic and early postnatal

ages and are expressed in distinct layer and area-specific patterns, suggesting

their role in arealization (Rubenstein et al., 1999; Dye et al., 2011a). In particular,

Id2 and *RZRβ* expression boundaries have been implicated in guidance of

regional development of early INCs (Huffman et al., 2004). Within our model,

transcript densities of cortical *Id2* and *RZRβ* were increased in specific ROIs in

PatEE mice. Particularly, we observed a lateral shift in Id2 expression and a

medial shift in *RZRβ* expression that co-registered at the same anatomical level.

This anatomical co-registration results in *Id2* and *RZRβ* expression in PatEE

neocortices that overlap each other in a way that is not typically seen in control

mice.

We examined the functional significance of this overlapping region using

tracing of INCs via lipophilic dyes. We found that PatEE produces subtle changes

in INC development at P0, including a distinct mixing of putative V1 and S1

projection zones that is not present in normal, developing mice. At the

somatosensory-visual border, control mice display a clear border at this region

but, in PatEE mice, the boundaries of this border show overlapping connections.

As this region also corresponds to the level of overlapping *Id2* and *RZRβ*

expression, we propose that the shift in expression may underlie the altered INC

patterns seen in newborn PatEE mice. To our knowledge, this is the first study

reporting concurrent altered cortical genetic and neuronal patterning in the

context of PatEE.

Results from the current study are also interesting in comparison to PrEE

results. In newborn PrEE mice, whose mothers consumed 25% EtOH throughout

pregnancy, we observe consistent shifts in *Id2* and *RZRβ* expression, severely

disrupted INC patterns, and altered behavior at later ages (El Shawa et al., 2013;

Abbott et al., 2018). Although PatEE may not result in the level of disruption in

INC development seen in our PrEE model, similar mechanisms may be affected.

Overall, we suggest that a 15-23 day paternal exposure directly before

conception results in subtle changes in INC connectivity that may be due to

shifted cortical gene expression patterns. As patterns of INCs remain a

characteristic component of cortical area form and function (Kaas, 1982), subtle

changes in INC development due to PatEE may underlie (or contribute to)

behavioral changes seen in rodents (reviewed in Finegersh et al., 2015), as well

as in human children of alcoholic fathers (Tarter et al., 1989; Knopik et al., 2005).

Possible mechanisms underlying PatEE's effects on offspring
Although the current study characterized the alterations in offspring brain and

behavior due to PatEE, several previous studies have examined potential

mechanisms for transmission of PatEE's harmful effects from sperm to offspring

(for more details, please see review by Rompala and Homanics, 2019). Because

EtOH is a known disruptor of epigenetic regulation in both adult (Cervera-Juanes

et al., 2017) and prenatal exposure (Garro et al., 1991) contexts, most research

has focused on the potential mechanism of PatEE germ cell alteration as one

that is epigenetically mediated. This hypothesis has also been supported by

studies that have shown EtOH exposure alters DNA methylation (Bielawski et al.,

2002), histone acetylation (Kim and Shukla, 2006), and small noncoding RNA

profiles (Rompala et al., 2018) of rodent male sperm cells and/or testis. This

hypothesis is especially compelling considering human sperm cell DNA

hypomethylation of typically hypermethylated imprinted genes is associated with EtOH consumption (Ouko et al., 2009).

PatEE rodent model studies have examined this question of mechanism and have found various results revealing EtOH's effect on spermatogenesis. For example, Liang and colleagues (2014) reported DNA methylation decreases at paternally imprinted genes in EtOH-exposed sire sperm. However, other studies have found no evidence for PatEE's effects being mediated through epigenetic regulation of imprinted genes (Chang et al., 2017; 2019), suggesting other epigenetic mechanisms may underlie observed effects on offspring brain and behavior. Because small noncoding RNAs (sncRNAs), such as microRNAs, transfer RNA-derived RNAs, and mitochondrial small RNAs, are present in male gametes (Krawetz et al., 2011), these have also been hypothesized to play a key role in PatEE. In fact, a recent study has confirmed that paternal exposure alters expression of several of these sncRNAs in male sperm (Rompala et al., 2018).

While the exact mechanisms and molecular players are still unclear, evidence points towards an epigenetically mediated alteration of EtOH-exposed sperm. Extrapolating data from the current study, we hypothesize that PatEE may cause sperm cell epigenetic dysregulation, which in turn may result in gene expression alterations within offspring brain (such as in *Id2* and *RZRβ* expression), resulting in altered cortical patterning and ectopic development of neocortical circuits (such as the mixing of S1 and V1 intraneocortical connections). Furthermore, we suggest that the altered neuronal patterning may underlie the abnormal behavior

seen within other animal models of PatEE (Kim et al., 2014; Hollander et al.,

2019) as well as in children of male alcoholics (Tarter et al., 1989; Knopik et al.,

2005)

Conclusions

We report altered gene expression and intraneocortical connectivity in newborn

mice (PatEE) sired by males that had 15-23 days of preconception exposure to

EtOH. Future directions include examining epigenetic regulation of *Id2* and *RZRβ*

within the cortex of PatEE mice to further discern potential mechanisms, as well

as extending the current study to later ages to determine if the reported

differences in offspring brain are transient or long-lasting. Also, since many

prenatal ethanol exposure phenotypes have been shown to pass

transgenerationally (Abbott et al., 2018; see review by Chastain and Sarkar,

2017), an investigation of whether the observed phenotypes and sex differences

from preconception PatEE also persist into future generations beyond the F1

generation should occur. In conclusion, our data support the notion that the

preconception paternal environment is more impactful on offspring development

than previously thought, and that paternal EtOH exposure may cause harmful

consequences in offspring.

ACKNOWLEDGEMENTS

REFERENCES

Abbott CW, Kozanian, OO, Kanaan, J, Wendel, KM, Huffman, KJ (2016) The impact of prenatal ethanol exposure on neuroanatomical and behavioral development in mice. Alcohol Clin Exp Res 40:122–133.

Abbott CW, Rohac DJ, Bottom RT, Patadia S, Huffman KJ (2018) Prenatal ethanol exposure and neocortical development: a transgenerational model of FASD. Cereb Cortex 28:2908–2921.

Bielawski DM, Zaher FM, Svinarich DM, Abel EL (2002) Paternal alcohol exposure affects sperm cytosine methyltransferase messenger RNA levels. Alcohol Clin Exp Res 26:347–351.

Cervera-Juanes R, Wilhelm LJ, Park B, Grant KA, Ferguson B (2017) Genome-wide analysis of the nucleus accumbens identifies DNA methylation signals differentiating low/binge from heavy alcohol drinking. Alcohol 60:103–113.

Chang RC, Skiles WM, Chronister SS, Wang H, Sutton GI, Bedi YS, Snyder M, Long CR, Golding MC (2017). DNA methylation-independent growth restriction and altered developmental programming in a mouse model of preconception male alcohol exposure. Epigenetics 12:841–853.

Chang RC, Wang H, Bedi Y, Golding MC (2019) Preconception paternal alcohol exposure exerts sex-specific effects on offspring growth and long-term metabolic programming. Epigenetics Chromatin 12:9.

Chastain LG, Sarkar DK (2017) Alcohol effects on the epigenome in the germline: Role of inheritance of alcohol-related pathology. Alcohol 60:53-66.

Dye CA, El Shawa H, Huffman KJ (2011a) A lifespan analysis of intraneocortical connections and gene expression in the mouse I. Cereb Cortex 21:1311–1330.

Dye CA, El Shawa H, Huffman KJ (2011b) A lifespan analysis of intraneocortical connections and gene expression in the mouse II. Cereb Cortex 21:1331–1350.

El Shawa H, Abbott CW, Huffman KJ (2013) Prenatal ethanol exposure disrupts intraneocortical circuitry, cortical gene Expression, and behavior in a mouse model of FASD. J Neurosci 33:18893–18905.

Finegersh A, Homanics GE (2014) Paternal alcohol exposure reduces alcohol drinking and increases behavioral sensitivity to alcohol selectively in male offspring. PLoS One 9:e99078.

Finegersh A, Rompala GR, Martin DIK, Homanics GE (2015) Drinking beyond a lifetime: New and emerging insights into paternal alcohol exposure on subsequent generations. Alcohol 49:461–470.

Garro AJ, McBeth DL, Lima V, Lieber CS (1991) Ethanol consumption inhibits fetal DNA methylation in mice: implications for the fetal alcohol syndrome. Alcohol Clin Exp Res 15:395–398.

Granato A, Di Rocco F, Zumbo A, Toesca A, Giannetti S (2003) Organization of cortico-cortical associative projections in rats exposed to ethanol during early postnatal life. Brain Res Bull 60:339–44.

Greenham LW, Greenham V (1977) Sexing mouse pups. Lab Anim. 11: 181-184.

Hollander J, McNivens M, Pautassi RM, Nizhnikov ME (2019) Offspring of male rats exposed to binge alcohol exhibit heightened ethanol intake at infancy and alterations in T-maze performance. Alcohol 76:65–71.

Hoyme HE, Kalberg WO, Elliott AJ, Blankenship J, Buckley D, Marais A-S, Manning MA, Robinson LK, Adam MP, Abdul-Rahman O, Jewett T, Coles CD, Chambers C, Jones KL, Adnams CM, Shah PE, Riley EP, Charness ME, Warren KR, May PA (2016) Updated clinical guidelines for diagnosing Fetal Alcohol Spectrum Disorders. Pediatrics 138:e20154256–e20154256.

Huffman KJ, Garel S, Rubenstein JLR (2004) Fgf8 regulates the development of intra-neocortical projections. J Neurosci 24:8917–8923.

Ikonomidou C, Bittigau P, Ishimaru MJ, Wozniak F, Koch C, Genz K, Price MT, Stefovska V, Tenkova T, Dikranian K, Olney JW (2000) Ethanol-induced apoptotic neurodegeneration and Fetal Alcohol Syndrome. Science 287:1056–1060.

Jabaudon DJ, Shnider SJ, Tischfield DJ, Galazo M, Macklis JD (2012) RORβ induces barrel-like neuronal clusters in the developing neocortex. Cereb Cortex 22:996–1006.

Jamerson PA, Wulser MJ, Kimler BF (2004) Neurobehavioral effects in rat pups whose sires were exposed to alcohol. Dev Brain Res 149:103–111.

Kaas JH 1982. The segregation of function in the nervous system: why do sensory systems have so many subdivisions? Contrib Sens Physiol 7:201–240.

Kim J-S, Shukla SD (2006) Acute in vivo effect of ethanol (binge drinking) on histone H3 modifications in rat tissues. Alcohol Alcohol 41:126–132.

Kim P, Choi CS, Park JH, Joo SH, Kim SY, Ko HM, Kim KC, Jeon SJ, Park SH, Han S-H, Ryu JH, Cheong JH, Han JY, Ko KN, Shin CY (2014) Chronic exposure to ethanol of male mice before mating produces attention deficit hyperactivity disorder-like phenotype along with epigenetic dysregulation of dopamine transporter expression in mouse offspring. J Neurosci Res 92:658–670.

Knopik VS, Sparrow EP, Madden PAF, Bucholz KK, Hudziak JJ, Reich W, Slutske WS, Grant JD, McLaughlin TL, Todorov A, Todd RD, Heath AC (2005) Contributions of parental alcoholism, prenatal substance exposure, and genetic transmission to child ADHD risk: a female twin study. Psychol Med 35:625–635.

Krawetz SA, Kruger A, Lalancette C, Tagett R., Anton E, Draghici S, Diamond MP (2011) A survey of small RNAs in human sperm. Hum Reprod 26:3401–3412.

Krubitzer L, Huffman KJ (2000) Arealization of the neocortex in mammals: Genetic and epigenetic contributions to the phenotype. Brain Behav Evol 55:322–335.

Liang F, Diao L, Liu J, Jiang N, Zhang J, Wang H, Zhou W, Huang G, Ma D (2014) Paternal ethanol exposure and behavioral abnormities in offspring: Associated alterations in imprinted gene methylation. Neuropharmacology 81:126–133.

May PA, Chambers CD, Kalberg WO, Zellner J, Feldman H, Buckley D, Kopald D, Hasken, JM, Xu R, Honerkamp-Smith G, Taras H, Manning MA, Robinson LK, Adam MP, Abdul-Rahman O, Vaux K, Jewett T, Elliott AJ, Kable JA, Akshoomoff N, Daniel F, Arroyo JA, Hereld D, Riley EP, Charness ME, Coles CD, Warren KR, Jones KL, Hoyme HE (2018) Prevalence of fetal alcohol spectrum disorders in 4 US communities. J Am Med Assoc 319:474–482.

Meek LR, Myren K, Sturm J, Burau D (2007) Acute paternal alcohol use affects offspring development and adult behavior. Physiol Behav 91:154–160.

Ouko LA, Shantikumar K, Knezovich J, Haycock P, Schnugh DJ, Ramsay M (2009) Effect of alcohol consumption on CpG methylation in the differentially methylated regions of H19 and IG-DMR in male gametes: implications for fetal alcohol spectrum disorders. Alcohol Clin Exp Res 33:1615–27.

Park HJ, Hong M, Bronson RT, Israel MA, Frankel WN, Yun K (2013) Elevated Id2 expression results in precocious neural stem cell depletion and abnormal brain development. Stem Cells 31:1010–1021.

Paxinos G, Halliday G, Watson C, Koutcherov Y, Wang H (2007) Atlas of the developing mouse brain. 1st edition. Academic Press/Elsevier, Burlington MA.

Przybycien-Szymanska MM, Rao YS, Prins SA, Pak TR (2014) Parental binge alcohol abuse alters F1 generation hypothalamic gene expression in the absence of direct fetal alcohol exposure. PLoS One 9:e89320.

Rompala GR, Finegersh A, Homanics GE (2016) Paternal preconception ethanol exposure blunts hypothalamic-pituitary-adrenal axis responsivity and stress-induced excessive fluid intake in male mice. Alcohol 53:19–25.

Rompala GR, Finegersh A, Slater M, Homanics GE (2017) Paternal preconception alcohol exposure imparts intergenerational alcohol-related behaviors to male offspring on a pure C57BL/6J background. Alcohol 60:169–177.

Rompala GR, Mounier A, Wolfe CM, Lin Q, Lefterov I, Homanics GE (2018) Heavy chronic intermittent ethanol exposure alters small noncoding RNAs in mouse sperm and epididymosomes. Front Genet 9:32.

Rompala GR, Homanics GE (2019) Intergenerational effects of alcohol: A review of paternal preconception ethanol exposure studies and epigenetic mechanisms in the male germline. Alcohol Clin Exp Res 43:1032-1045.

Rubenstein JLR, Anderson S, Shi L, Miyashita-Lin E, Bulfone A, Hevner R (1999) Genetic control of cortical regionalization and connectivity. Cereb Cortex 9:524–532.

Tarter RE, Jacob T, Bremer DL (1989) Specific cognitive impairment in sons of early onset alcoholics. Alcohol Clin Exp Res 13:786–789.

Wolterink-Donselaar IG, Meerding JM, Fernandes C (2009) A method for gender determination in newborn dark pigmented mice. Lab Anim (NY) 38:35-38.

Xia R, Jin L, Li D, Liang H, Yang F, Chen J, Yuan W, Miao M (2018) Association between paternal alcohol consumption before conception and anogenital distance of offspring. Alcohol Clin Exp Res 42:735–742.

Zhou D, Lebel C, Lepage C, Rasmussen C, Evans A, Wyper K, Pei J, Andrew G, Massey A, Massey D, Beaulieu C (2011) Developmental cortical thinning in fetal alcohol spectrum disorders. Neuroimage 58:16–25.

Zuccolo L, DeRoo LA, Wills AK, Smith GD, Suren P, Roth C, Stoltenberg C, Magnus P (2017) Erratum: Pre-conception and prenatal alcohol exposure from mothers and fathers drinking and head circumference: results from the Norwegian Mother-Child Study (MoBa). Sci Rep 7:45877.

General Conclusions

The current dissertation aimed to address three disparate, yet related topics

associated with ethanol exposure whose results have considerable implications

for human health. By both building directly upon previous research and

answering unique, novel questions, work contained in this thesis will contribute to

the field by enhancing information pertaining to the wide-reaching extent of

PrEE's damage, potential preventive/therapeutic approaches to mitigate the

harmful effects of PrEE, and the newly emerging contribution of PatEE on

offspring CNS development.

Using a plethora of anatomical, molecular, and behavioral tools, we

addressed several aims. First, we determined how PrEE induces

transgenerational adverse effects on multi-modality adolescent behaviors and

described several novel phenotypes in directly exposed adolescent offspring that

may contribute to PrEE-induced brain and behavioral dysfunction. Second, we

mapped the robust ability of choline supplementation to prevent and/or reduce

several novel aspects of neocortical and behavioral development and uncovered

evidence of the molecular underpinnings. Third, we described, for the first time, a

direct impact of preconception PatEE on distinct neocortical developmental

processes which may be mechanistically linked. Overall, each section of this

dissertation provides new insights into the still unclear etiology of both

preconception and prenatal EtOH exposure.

Even with the significant findings reported here, there are an abundance of future directions to pursue in order to further understanding of these topics. Regarding work in Chapter 1, a broad search of the underlying neurobiology in later life that drives the strong transgenerational behavioral disruption by PrEE should be undertaken. Despite the lack of anatomical and molecular evidence presented here, these results inform the directions to be investigated including functional, cell-type specific analyses of brain connectivity, as well as mechanisms implicated in circuit refinement and maintenance. Additionally, the ability to directly correlate PrEE-induced circuit-specific disruptions to related behavioral deficits remains a key cornerstone in understanding the etiology underlying PrEE.

Concerning the findings in Chapter 2, further work must be initiated to fully elucidate both the full extent of choline's protective abilities on the EtOH-exposed developing CNS, as well as the contributing mechanisms to these phenomena. Genome-wide screens using recently developed methodologies, such as single cell RNA sequencing, would be extremely powerful to determine if choline can prevent PrEE-induced changes on a gene-specific and global scale. Further epigenetic experiments, including whole genome bisulfite sequencing, will provide support to choline's' epigenetically-driven mechanisms. Studies investigating choline's other cellular and molecular roles including cell membrane composition, myelination, and acetylcholine-related processes should be

undertaken to examine how these secondary functions may contribute to the robust amelioration of PrEE phenotypes by choline.

Lastly, a great deal of work is left to extend the findings seen in Chapter 3. The full breadth of the adverse effects generated by PatEE are very much unclear at this point, including both CNS- and behavioral-based readouts. Mechanistically, how paternal exposure produces phenotypic variation in offspring is imprecise, and causative evidence would be incredibly forceful for supporting this burgeoning dogma of epigenetic inheritance. Further research into clinical populations of human offspring with PatEE will also be key to supporting this concept.

In conclusion, the studies contained within the 3 chapters here further inform the etiology of EtOH exposure by illuminating the extent of PrEE's transgenerational damage, providing preclinical evidence for a preventive approach tuned for an abstinence-resistant clinical population, and describing potent, novel effects of PatEE on offspring brain development. Results from these studies will no doubt have a significant impact on global human health as it relates to one of its most ancient vices.

TABLES:

Table 1.1: List of experimental replicates (*n*).

Measure	Control	F1	F2	F3
Accelerated Rotarod	9	9	9	9
Adhesive Removal	11	11	11	11
Elevated Plus Maze	8	8	8	8
Forced Swim Test	8	8	8	8
Body weight	21	17	34	29
Brain weight	7	7	7	7
Cortical length	6	6	6	6
Dye tracing	8	8	6	6
ISH- RZRβ	6	6	4	3
ISH- ID2	4	4	5	4
Spine density	14	17	12	15

Table 1.2: Summarized *P* values for all group interactions.

	Behavior								
	Accelerated Rotarod				Adhesive Removal			EPM	FST
	Trial 1	Trial 2	Trial 3	Trial 4	Trial 1	Trial 2	Trial 3	Time in Open Arms	Time immobile
Con-F1	0.0005	0.0018	0.2507	0.5913	0.0469	0.0580	0.9234	0.0179	0.0270
Con-F2	0.0689	0.0218	0.6382	0.9482	0.0488	0.0379	0.6743	0.0310	0.0135
Con-F3	0.1139	0.0850	0.9927	0.8691	0.0465	0.1108	0.6120	0.0371	0.0474
F1-F2	0.3038	0.4019	0.9442	0.9920	0.9798	0.9113	0.9613	0.9955	0.9913
F1-F3	0.2943	0.0649	0.8031	0.9957	0.9755	0.7589	0.9773	0.9893	0.9945
F2-F3	0.9992	0.8233	0.9519	0.9997	>0.999	0.9640	0.9972	0.9998	0.9489

	Pup measures			Brain measures	
	P20 Body Weight	P20 Brain Weight	P20 Cortical length	*Id2* -distance from medial wall	Spiny stellate cell-Spine density
Con-F1	0.0009	0.0084	0.0045	0.0217	0.0016
Con-F2	0.9997	0.9978	0.8733	0.4861	>0.999
Con-F3	0.1685	0.9751	0.9999	0.3322	0.6662
F1-F2	0.0003	0.0128	0.0242	0.1978	0.0032
F1-F3	<0.0001	0.0221	0.0053	0.3953	<0.0001
F2-F3	0.0742	0.9953	0.9001	0.9776	0.6605

Table 2.1: Group means and number of replicates for all statistical measures. Data presented as mean ± SEM.

Measure (units)	Control, *n*	CW, *n*	EtOH, *n*	CE, *n*
Dam food intake (g/day)	6.812 ± 0.293, *8*	7.133 ± 0.242, *8*	6.381 ± 0.198, *8*	6.469 ± 0.188, *8*
Dam liquid intake (mL/day)	12.24 ± 0.776, *8*	12.64 ± 0.594, *8*	12.31 ± 1.133, *8*	11.94 ± 0.583, *8*
Dam GD9 BEC (mg/dL)	0.0 ± 0.0, *7*	0.0 ± 0.0, *5*	106.5 ± 1.693, *10*	106.9 ± 1.040, *10*
Dam GD19 BEC (mg/dL)	0.0 ± 0.0, *7*	0.0 ± 0.0, *5*	136.9 ± 2.794, *10*	136.3 ± 2.894, *10*
Dam POSM (mosm/kg)	315.4 ± 2.001, *10*	311.0 ± 2.813, *10*	313.9 ± 2.614, *10*	308.0 ± 2.801, *10*
Dam weight gain (g/day)	31.65 ± 1.362, *8*	29.46 ± 1.216, *8*	26.25 ± 1.212, *8*	30.29 ± 1.134, *8*
Litter size (# of pups)	12.25 ± 0.773, *8*	11.63 ± 0.778, *8*	8.750 ± 0.750, *8*	11.88 ± 0.854, *8*
P0 body weight (g)	1.615 ± 0.023, 26	1.628 ± 0.031, 25	1.454 ± 0.024, 24	1.543 ± 0.023, 23
P0 brain weight (g)	0.09877 ± 0.002, 17	0.09838 ± 0.002, 13	0.0894 ± 0.001, 15	0.09834 ± 0.001, 10
P0 brain/body weight ratio	0.05868 ± 0.001, 17	0.05730 ± 0.001, 13	0.06090 ± 0.002, 15	0.05925 ± 0.002, 10
P0 cortical length (mm)	4.623 ± 0.020, *10*	4.612 ± 0.017, *10*	4.464 ± 0.037, 10	4.573 ± 0.034, *10*
DPL spread (% total cortical length)	13.33 ± 0.960, *5*	12.82 ± 0.811, *5*	13.25 ± 0.428, *6*	13.33 ± 0.983, *6*
Dye projection zone (% total cortical length)	49.18 ± 1.461, *5*	49.61 ± 1.572, *5*	79.06 ± 1.920, *6*	68.23 ± 2.078, *6*
Frontal cortex cell count (# of cells)	0.0 ± 0.0, *5*	0.0 ± 0.0, *5*	25.33 ± 3.43, *6*	0.0 ± 0.0, *6*
RZRβ transcript density (% area fraction)	4.345 ± 0.851, *6*	2.629 ± 0.315, *4*	17.54 ± 1.548, *6*	3.844 ± 0.768, *6*
Id2 transcript density (% area fraction)	23.67 ± 3.634, *4*	24.59 ± 3.556, *4*	5.322 ± 1.628, *5*	26.85 ± 2.810, *4*
Global DNA methylation- rostral cortex (% 5-mC DNA)	0.761 ± 0.007, *5*	0.951 ± 0.094, *4*	0.570 ± 0.051, *5*	0.812 ± 0.033, *3*

Table 2.1, continued:

Global DNA methylation- caudal cortex (% 5-mC DNA)	0.734 ± 0.016, *5*	0.891 ± 0.073, *4*	0.515 ± 0.049, *5*	0.621 ± 0.074, *3*
Latency to leave center (s)	3.750 ± 0.732, *18*	4.899 ± 0.610, *14*	7.824 ± 1.366, *17*	4.103 ± 0.702, *16*
Directed exploration (# of events)	70.00 ± 4.567, *18*	80.14 ± 6.874, *14*	51.94 ± 2.895, *17*	72.56 ± 3.824, *16*
Rearing/grooming (# of events)	1.944 ± 0.189, *18*	1.929 ± 0.245, *14*	0.9412 ± 0.201, *17*	1.125 ± 0.221, *16*
Missteps (# of events)	9.176 ± 1.075, *18*	9.857 ± 1.586, *14*	22.35 ± 1.819, *17*	11.75 ± 1.135, *16*
Falls (# of events)	1.000 ± 0.352, *18*	1.533 ± 0.376, *14*	4.706 ± 0.803, *17*	1.875 ± 0.301, *16*
Ledge test score (s)	60.00 ± 0.000, *18*	60.00 ± 0.000, *14*	49.18 ± 4.829, *17*	54.99 ± 3.556, *16*

Table 3.1: List of experimental replicates (*n*).

	Control	PatEE
Litters	10	10
BEC	7	7
RZRβ ISH	7	6
ID2 ISH	7	7
INC tracing	6	5

Table 3.2: Group means for all statistical measures. Data presented as mean ± SEM.

Measure (units)	Control	PatEE
Sire food intake (g/day)	7.38 ± 0.97	5.49 ± 0.64, *9*
Sire liquid intake (mL/day)	9.775 ± 0.470	9.928 ± 0.888
Sire BEC (mg/dL)	0.0 ± 0.0	125.6 ± 10.50
Sire weight gain (g)	0.67 ± 0.9	0.20 ± 0.8
RZRβ transcript density (% area fraction)	6.475 ± 0.678	17.21 ± 4.55
Id2 transcript density (% area fraction)	6.849 ± 3.422	48.503 ± 6.151
Putative S1 DPL spread (% total cortical length)	14.94 ± 0.93	15.35 ± 1.072
Putative V1 DPL spread (% total cortical length)	13.86 ± 0.57	12.65 ± 0.46
SCx Dye projection zone (% total cortical length)	45.17 ± 2.842	49.96 ± 3.183
VCx Dye projection zone (% total cortical length)	38.78 ± 2.16	48.12 ± 3.83
V1 Lateral cortical cell dispersion (µm)	1081 ± 158.5	1524 ± 96.28

FIGURES:

Figure 1.1: Transgenerational FASD model breeding paradigm. Initially, ethanol (EtOH) naïve P90 CD-1 mice were paired for breeding. Upon confirmation of copulation via vaginal plug, dams were given 25% EtOH in water throughout gestation (EtOH treated; gradient) to generate the prenatal EtOH exposed F1 experimental group (PrEE F1; black). P90 F1 males were then paired with EtOH naïve females to generate the PrEE F2 experimental group (dark gray). Lastly, P90 F2 males were then paired with EtOH naïve females to generate the PrEE F3 experimental group (light gray).
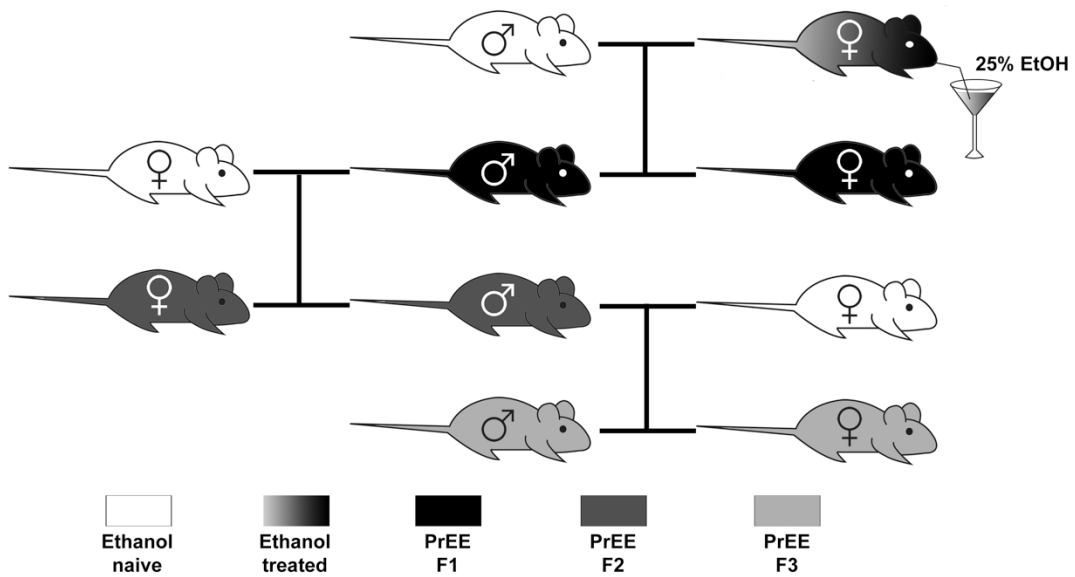
Figure 1.2: Multi-modality behavioral analysis. Results from behavioral testing in P20 control, F1, F2, and F3 mice in Accelerated Rotarod (A), Adhesive Removal test (B), Elevated Plus Maze (C), and Forced Swim Test (D). F1 mice display significantly decreased scores on trials 1 and 2 of the Rotarod compared to controls (**$P < 0.01$, ***$P < 0.001$), and F2 mice only show significantly decreased scores on Trial 2 compared to controls (+$P < 0.05$). All 3 experimental generations display significant increased score in Trial 1 of the adhesive Removal test compared to controls (F1: *$P < 0.05$; F2: +$P < 0.05$; F1: &$P < 0.05$), and this difference persists to Trial 2 in F1 mice alone (F1: **$P < 0.01$). All 3 PrEE generations display increased time spent on the open arms of the Elevated Plus Maze, as well as increased time spent immobile in the Forced Swim Test (*$P < 0.05$).
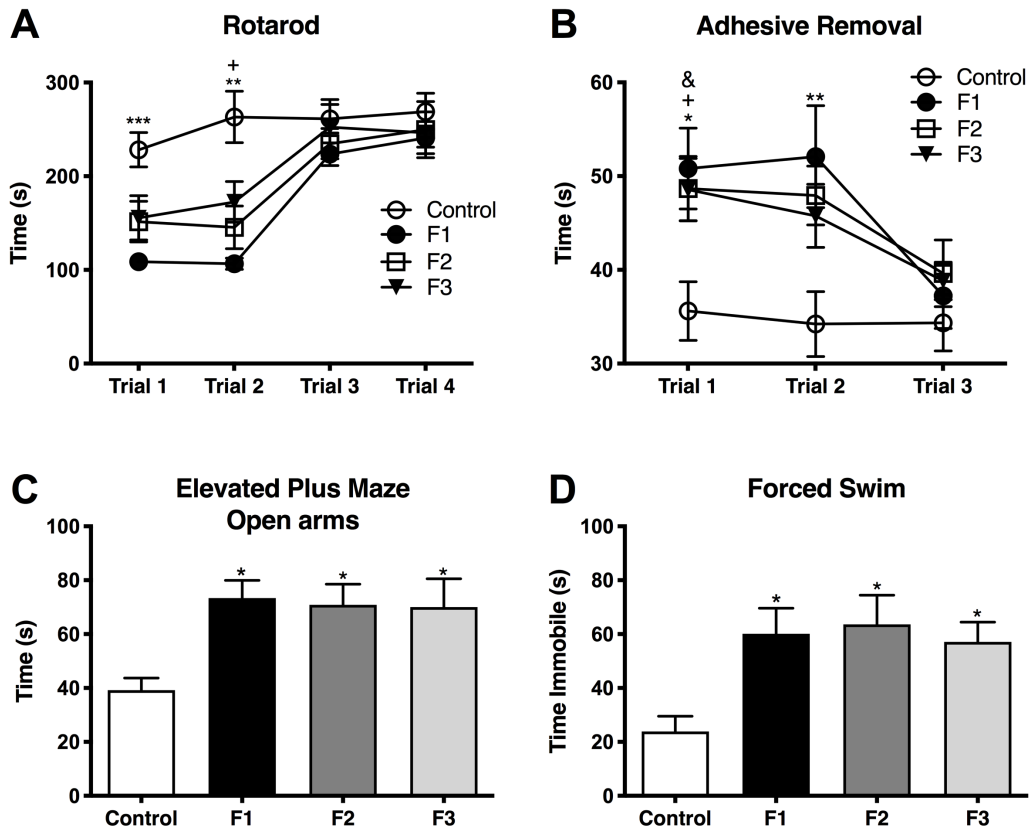
Figure 1.3: Gross body and brain measurements in P20 mice. (A) F1 mice weigh significantly less than controls at P20 (***$P < 0.001$). P20 F1 mice also have significantly decreased brain weights (B) and cortical lengths (C) compared to controls (**$P < 0.01$).

A   **P20 Body Weight**

B   **P20 Brain Weight**

C   **Cortical Length**
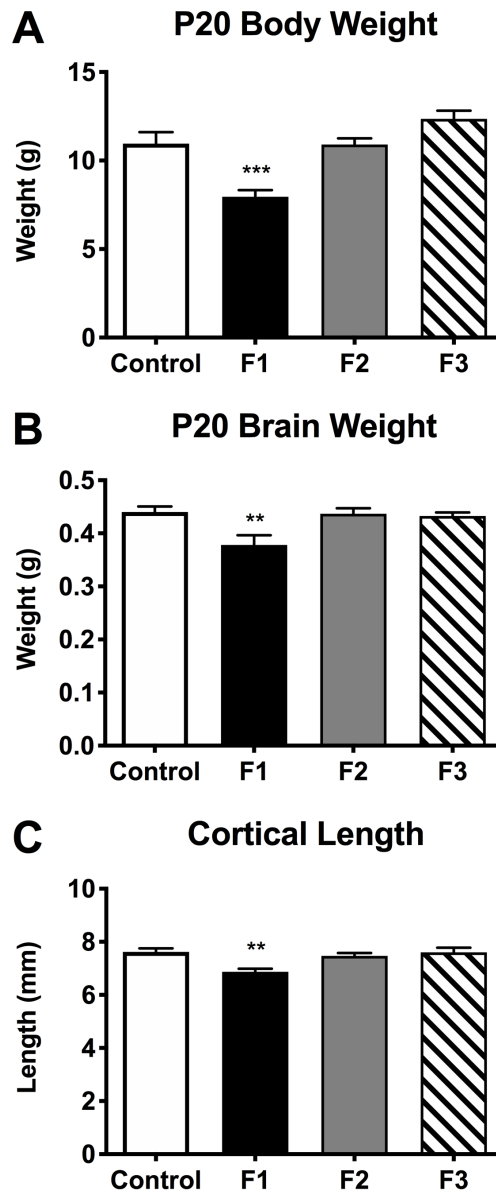
Figure 1.4: Analysis of primary somatosensory (S1) and primary visual (V1) cortex INC patterns at P20. Rostral-to-caudal series of hemisected coronal sections in Control (A1-4) and F1 (B1-4), F2 (C1-4) and F3 (D1-4) P20 mice brains following DiA (green) placement in S1 (*S, A2-D2) and DiI (red) placement in V1 (*V, A4-D4). No significant phenotypic differences in S1or V1 projection zones were found between experimental generation and control brains. All 100-μm sections counterstained with DAPI (blue). Images oriented dorsal (D) up and medial (M) left. Scale bar, 500 μm.
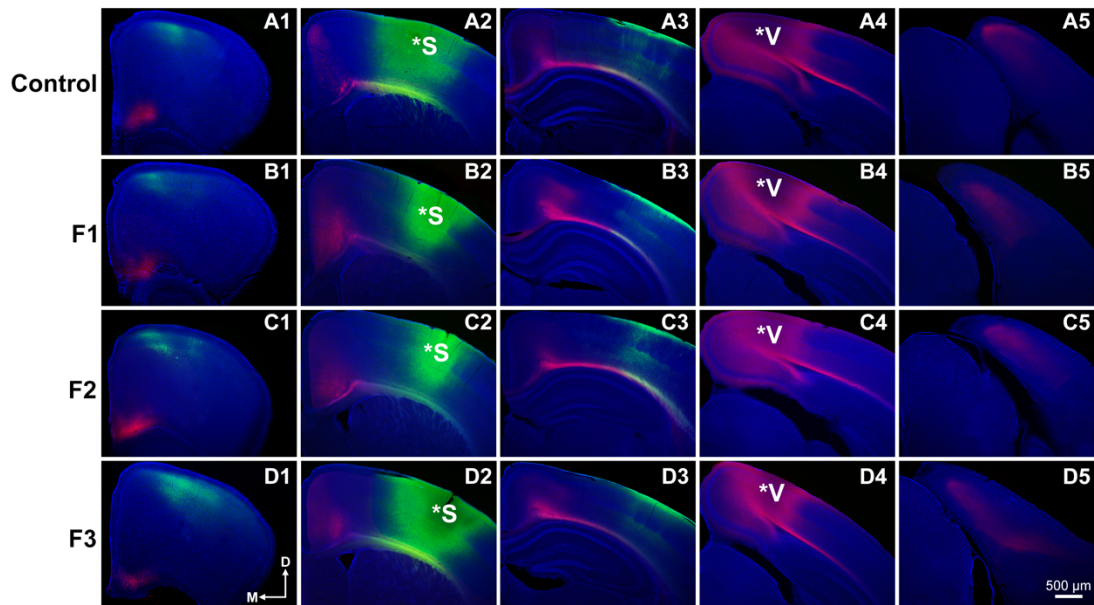
Figure 1.5: Cortical *RZRβ* expression at P20. Rostral-to-caudal series of coronal sections following in situ hybridization with probes for *RZRβ* in control (A1-4), F1 (B1-4), F2 (C1-4), and F3 (D1-4) mice. No significant phenotypic differences were found between any groups. Images oriented dorsal (D) up, lateral (L) right. Scale bar, 1 mm.
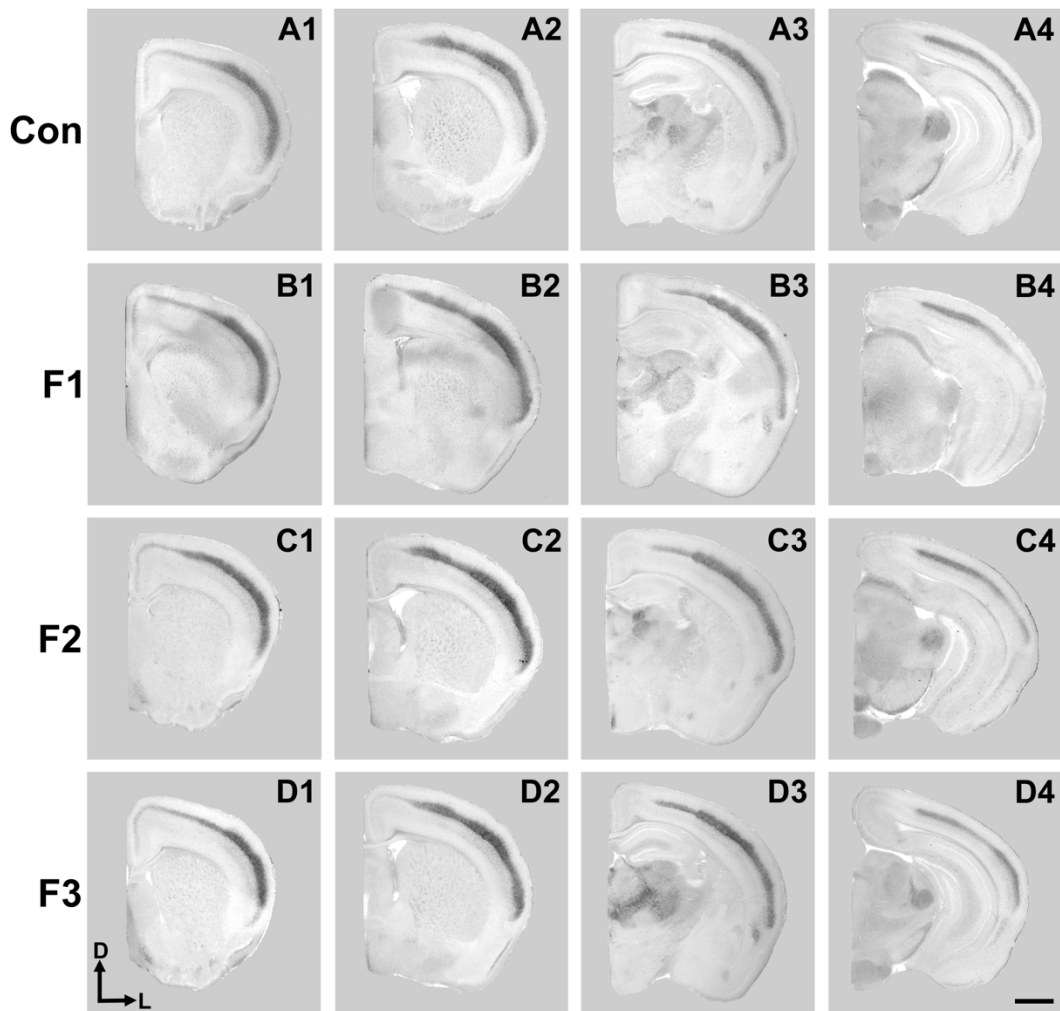
Figure 1.6: Cortical *Id2* expression at P20. Rostral-to-caudal series of coronal sections following in situ hybridization with probes for *Id2* in control (A1-4), F1 (B1-4), F2 (C1-4), and F3 (D1-4) mice. F1 mice display a pronounced shift in the lateral limit of the superficial *Id2* band compared to controls (A4 vs. B4, arrows). Images oriented dorsal (D) up, lateral (L) right. Scale bar, 1 mm.
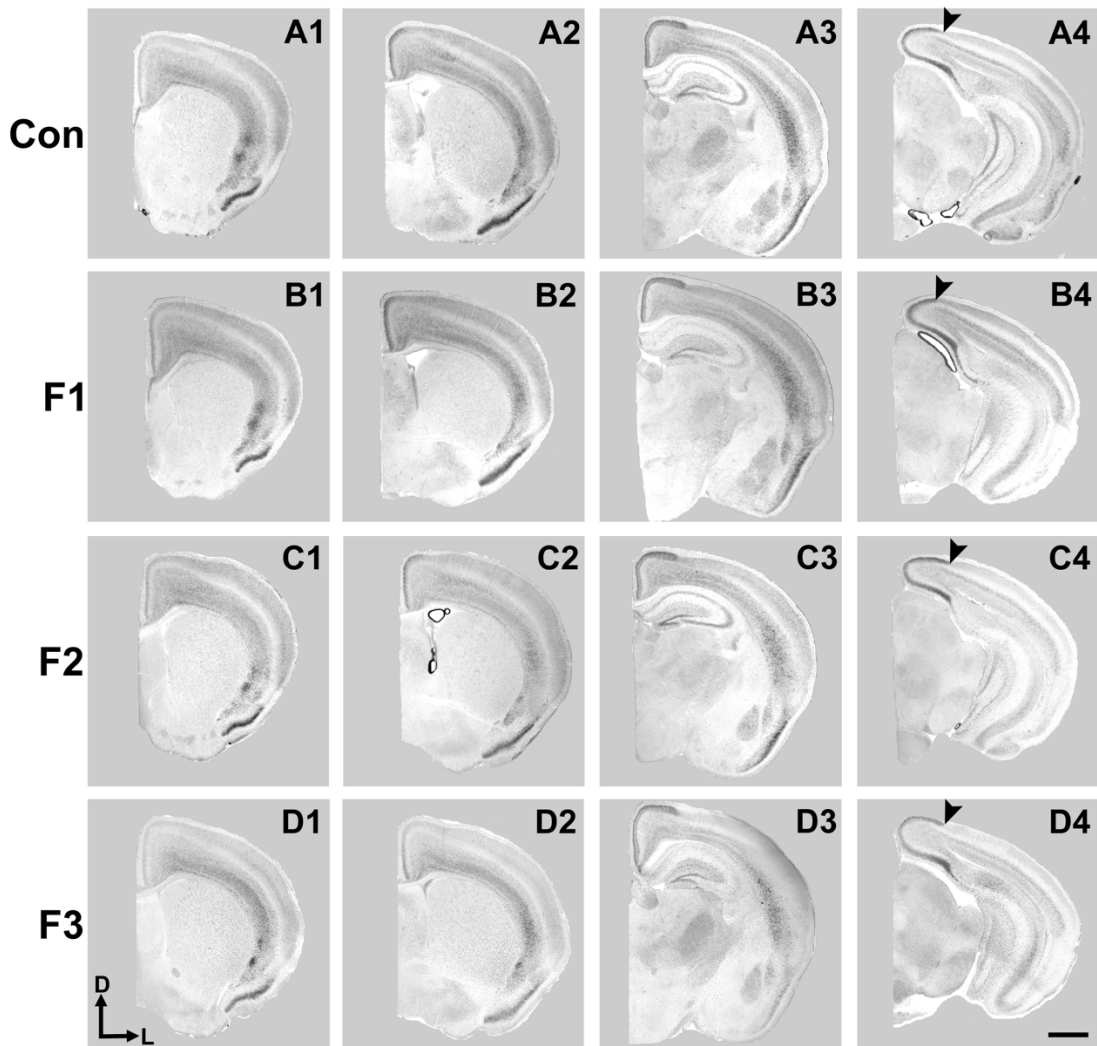
Figure 1.7: Quantification of cortical *Id2* phenotype in F1 mice. Distance from the midline to the limit of the robust superficial band of *Id2* expression was calculated for all cases at anatomically-matched sections in Control (A), F1 (B), F2 (C), and F3 (D) mice at P20. (E) F1 mice display significantly decreased distances from the midline compared to controls (*P < 0.05). Coronal images of *in situ* hybridization sections oriented dorsal (D) up, lateral (L) right. Scale bar, 1 mm.
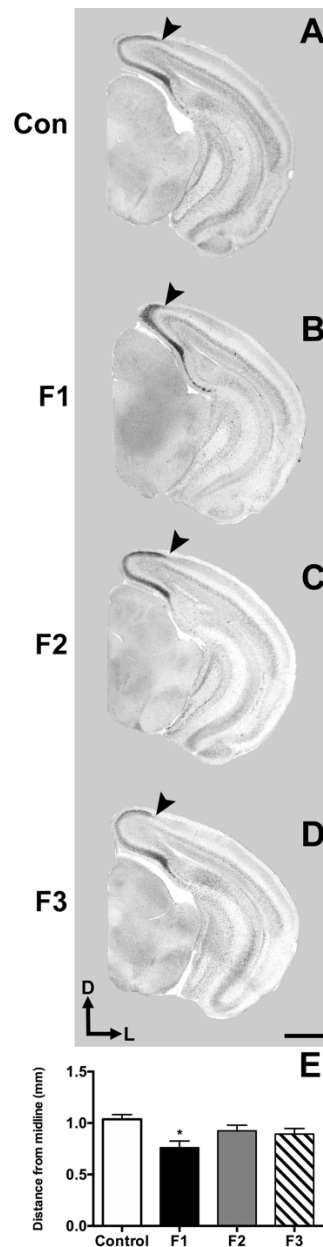
Figure 1.8: Dendritic spine density analysis in layers IV of spiny stellate neurons in S1 at P20. Two example dendrites are shown for each experimental group originating from separate animals. Spine density (spines/µm) is significantly decreased in S1 spiny stellate cells of F1 mice compared to cells of control mice (**$P < 0.01$). Neurons of F2 and F3 mice display no significant differences in dendritic spine density compared to controls. Scale bar, 20 µm.
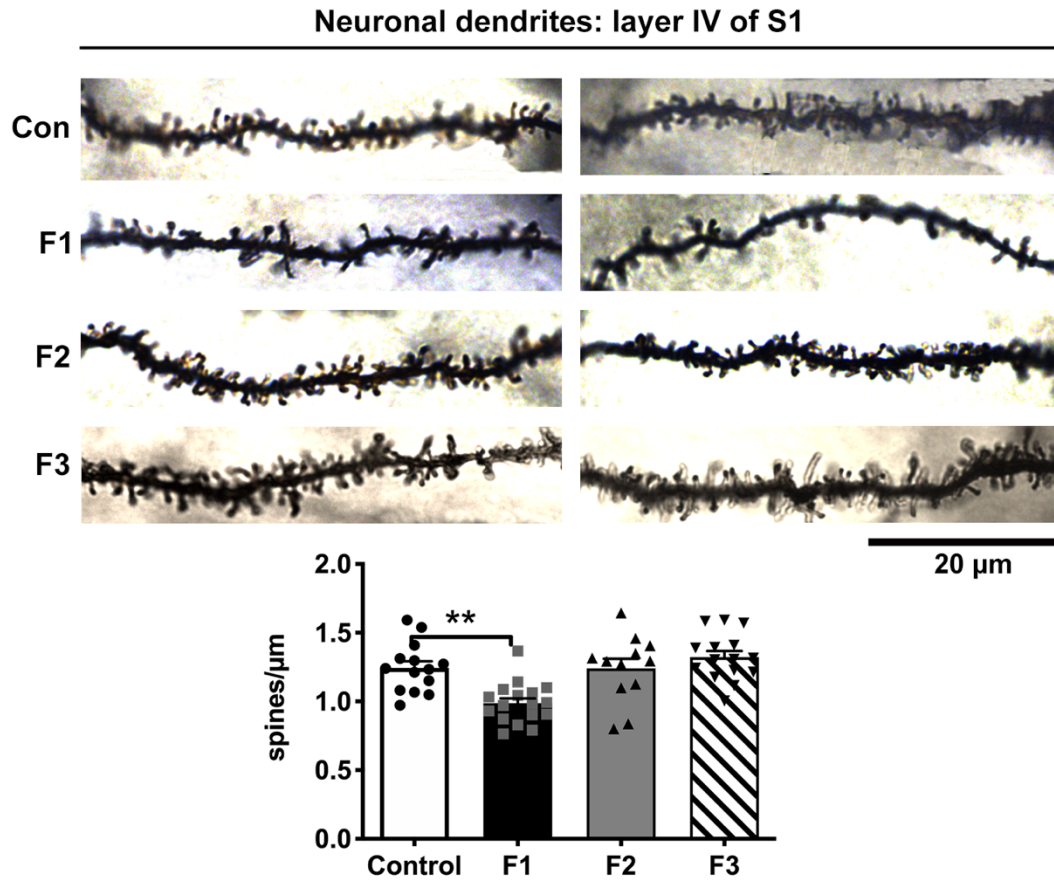
Figure 2.1: Experimental timeline.
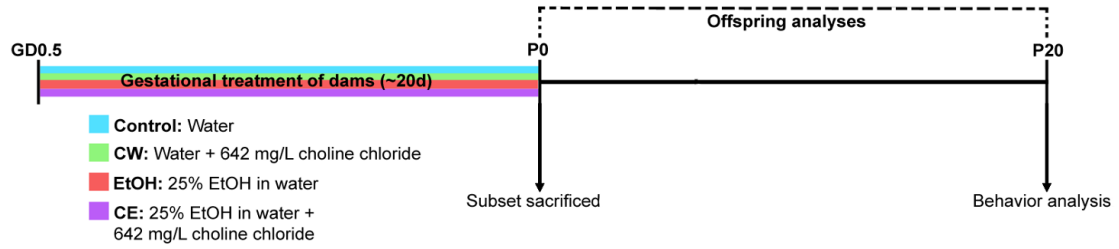
Figure 2.2: Dam measures. No differences in food (**A**) or liquid (**B**) intake are present among groups (n = 8, all groups). **C,** EtOH (n = 10) and CE dams (n = 10) show elevated blood ethanol content (BEC; mg/dL) at gestational day (GD) 9 and 19 compared to CW (n = 7) and Controls (n = 7) (****p < 0.0001). **D,** No differences are present among groups in plasma osmolality (mosm/kg) (n = 10, all groups). **E, F,** Dam weight gain and litter size are significantly decreased in EtOH dams compared to Controls (*p < 0.05, n = 8, all groups), and EtOH litter size is significantly different from CE dam's average litter size (*p < 0.05).
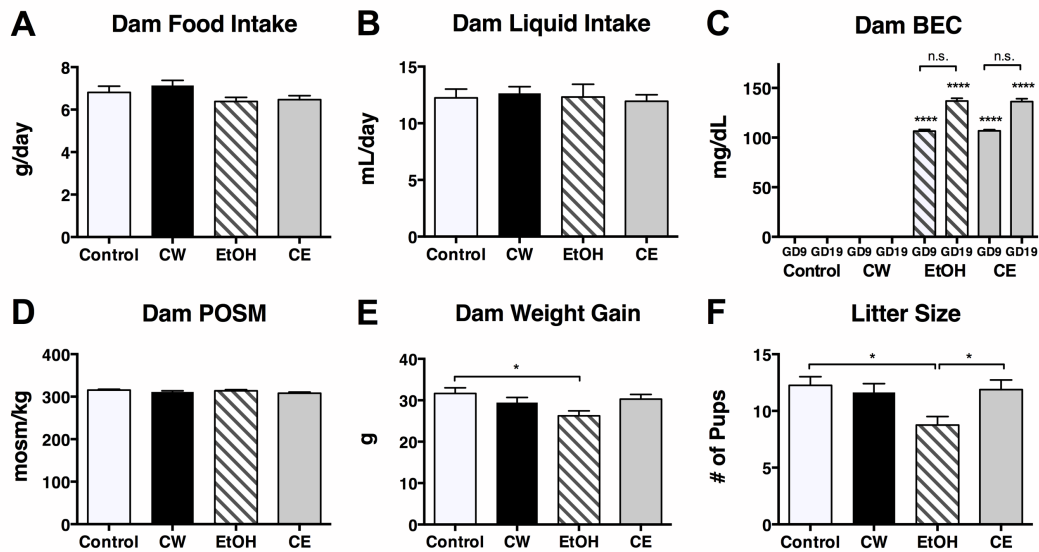
Figure 2.3: Pup measures at P0. **A,** EtOH pups also display decreased body weights at P0 (n = 24) compared to controls (n = 26; **p < 0.01), CW (n = 25; **p < 0.01), and CE pups (n = 23; **p < 0.01). **B,** EtOH pups display decreased brain weights at P0 (n = 15) compared to controls (n = 17; **p < 0.01), CW (n = 13; **p<0.01), and CE pups (n = 10; **p<0.01). **C,** No differences are present in brain/body weight ratios among any groups.
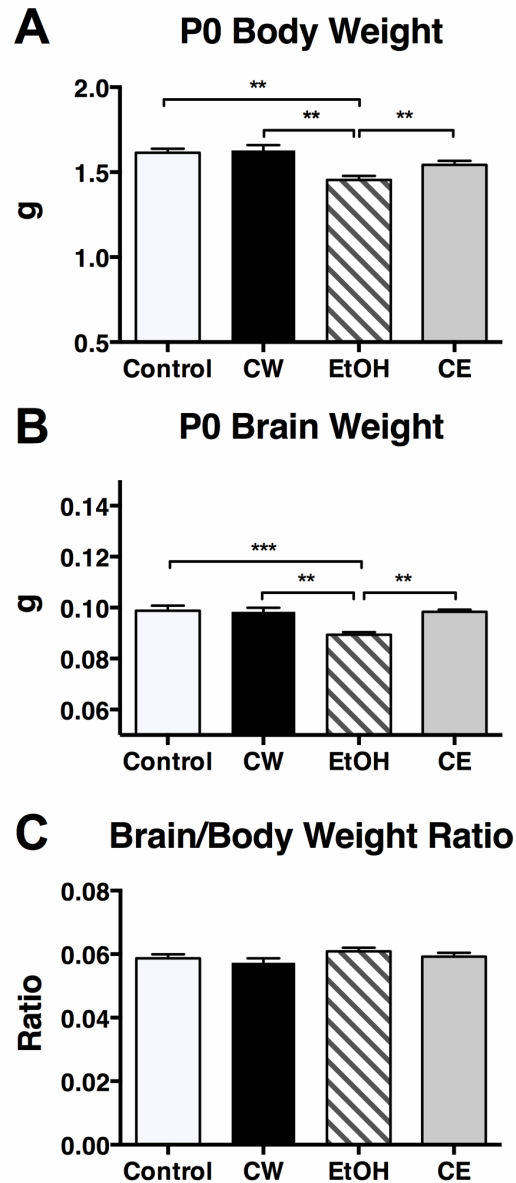
Figure 2.4: Cortical lengths at P0. A-D, Representative dorsal views of whole brains of control (**A**), CW (**B**), EtOH (**C**), and CE (**D**) pups at P0. **E,** EtOH pups display decreased cortical lengths at P0 (n= 10) compared to controls (n = 10; **$p<0.01$), CW (n = 10; **$p<0.01$), and CE pups (n = 10; *$p<0.05$). Scale bar, 2 mm.
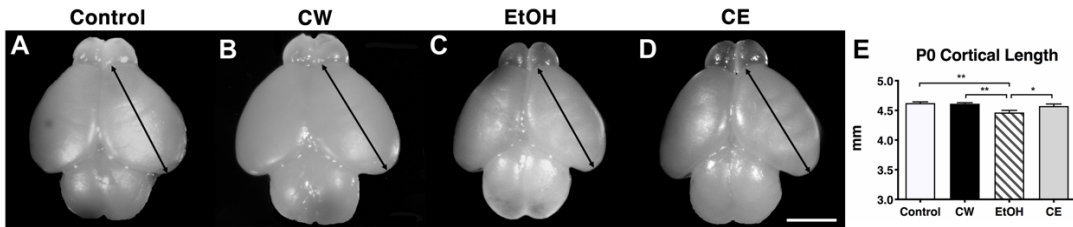
Figure 2.5: Analysis of intraneocortical connections (INCs) at P0. Rostral to caudal series of P0 100m coronal sections of control (**A1-E1**), CW (**A2-E2**), EtOH (**A3-E3**), and CE (**A4-E4**) brains that have been injected with DiI in putative primary visual cortex (VCx, *V in **D1-4**). EtOH brains display altered patterns of connections stemming from VCx injections, specifically red-labeled cells are present in far rostral sections (**A3, B3**, arrows) not present in control or CW brains. CE brains show labeled cells not present in control or CW brains (**B4**, arrow), but do not in far rostral sections as occurs in EtOH brains (**A4** vs. **A3**). Altered connectivity in EtOH and CE brains is present in absence of altered thalamocortical connectivity i.e. appropriate dorsal lateral geniculate nucleus labeling is present in all groups (**D1-D4**, arrows). These overall patterns are clearly visualized in 2D flattened reconstructions of the neocortex in F1-4, where CE brains (**F4**) display altered INC connectivity compared to control and CW brains, but do not show the magnitude of cortical disorganization seen in EtOH brains (**F3**). Coronal hemispheres: Scale bar: 500µm (white). Images oriented dorsal (D) up and lateral (L) right. Reconstructions: red dots: labeled cells, red fills: injection locations; scale bar: 1mm (black). Images oriented dorsal (D) up and caudal (C) right.
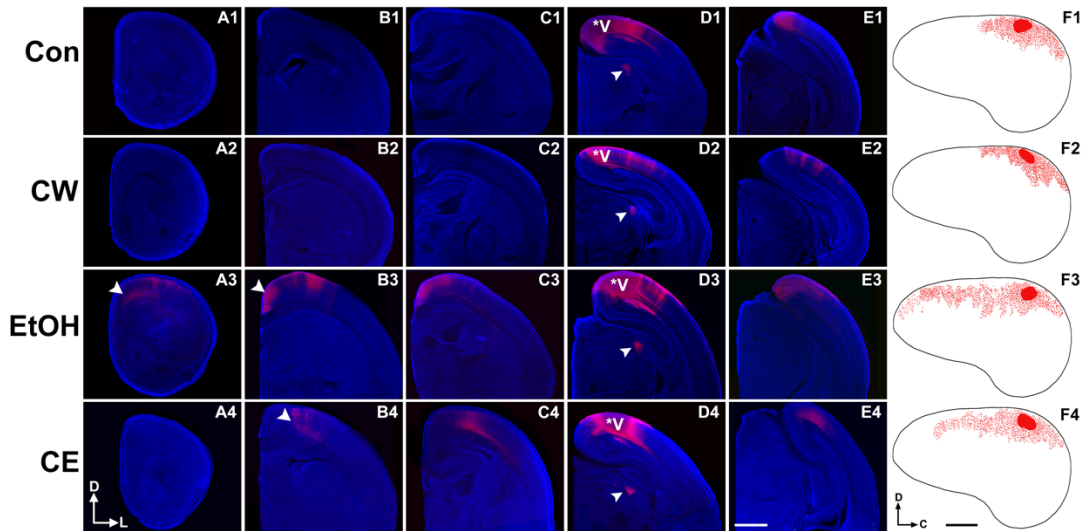
Figure 2.6: Quantitative analysis of visual INC development at P0*. A,* Putative visual cortex (VCx) dye placement location (DPL) spread as a function of total cortical length. No differences are present among groups. **B,** VCx projection zones as a function of total cortical length. EtOH brains display increased projection zones (*n* = 6) compared to Control (*n* = 5, *****p* < 0.0001) and CW (*n* = 5, *****p* < 0.0001). CE brains also display altered projection zones (*n* = 6) compared to Control and CW brains, but are significantly reduced when compared to the EtOH group (***p* < 0.01). **C,** Representative section of anatomical level of cell count in graph **D.** Region of interest (ROI), box denotes where cells were counted amongst sections/groups. Dorsal (D) up, lateral (L) left; Scale bar 500m. **D,** EtOH brains (*n* = 6) contain 25.33± 3.43 labeled cells from VCx injections in the ROI. No other groups contain labeled cells in any region at this level (***p* < 0.01; Con, *n* = 5; CW, *n* = 5; CE, *n* = 6).
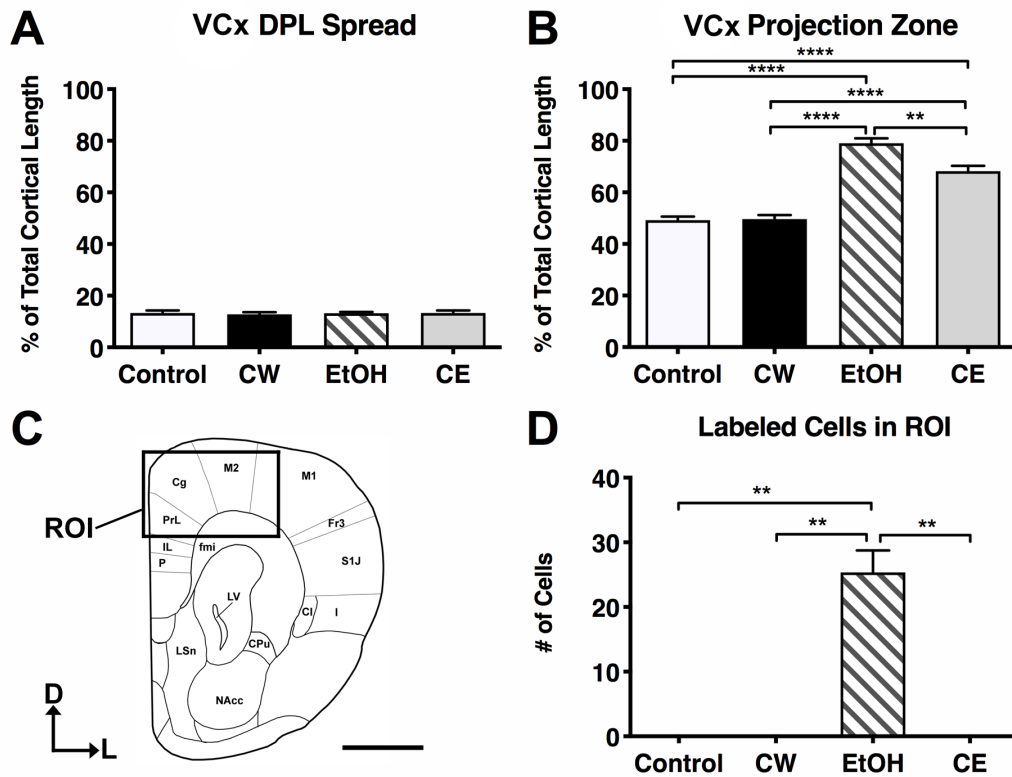
Figure 2.7: Cortical expression of RZR and Id2 at P0. *In situ* hybridizations in P0 100m coronal sections of hemispheres at the level of rostral parietal cortex. **A1-D1,** EtOH brains display an abnormal medial shift in expression in *RZR* (**C1**, arrow), compared to Control (**A1**), CW (**B1**), and CE (**D1**) brains. **A2-D2,** EtOH brains show a medial shift of expression (**C2**, arrow) in the most superficial layer of *Id2* expression, which normally extend laterally in Controls, CW, and CE brains (**A2, B2, D2**, arrows). In both genes analyzed, Choline supplementation (CE) ameliorates altered expression to levels indistinguishable from controls. Images oriented dorsal (D) up, medial (M) left. Scale bar, 500 µm.
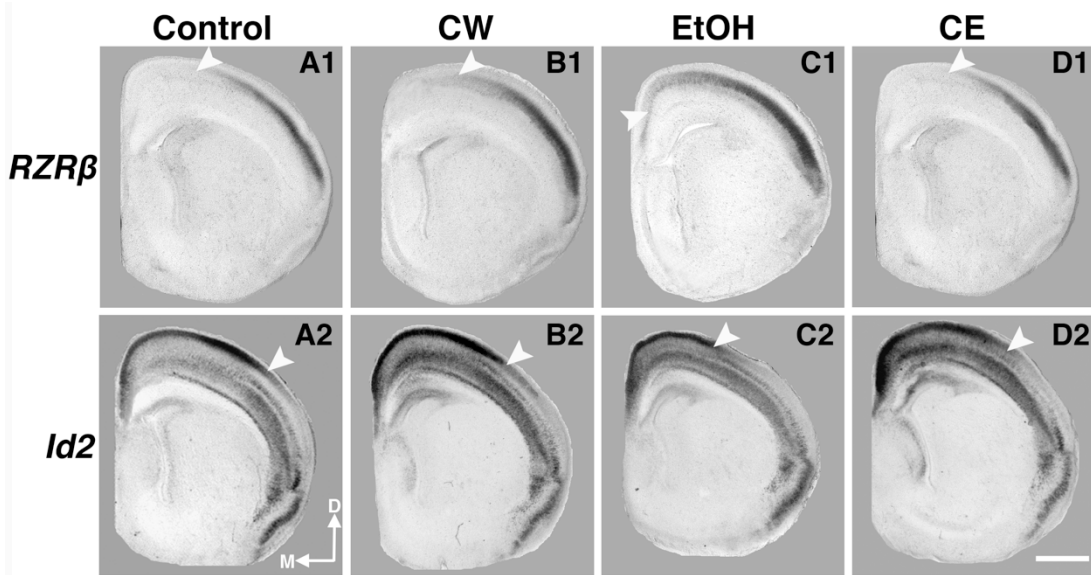
Figure 2.8: Transcript density analysis of RZRβ and Id2 at P0. A1, B1, Line drawings of the anatomical level in which static electronically-drawn regions of interest (ROIs) were placed on sections of binary-converted ISH experiments to quantify levels of mRNA expression. **A2,** EtOH brains display an increase in *RZRβ* transcript densities (*n* = 6) compared to Control (*n* = 6; ****$p<0.0001$), CW (*n* = 4; ****$p<0.0001$), and CE (*n* = 6; ****$p<0.0001$) in the ROI defined in A1. **B2,** EtOH brains display a significant decrease in *Id2* transcript densities (*n* = 5) compared to Control (*n* = 4; **$p<0.01$), CW (*n* = 4; **$p<0.01$), and CE (*n* = 4; ***$p<0.005$) in the ROI defined in B1. Scale bar, 500 μm.
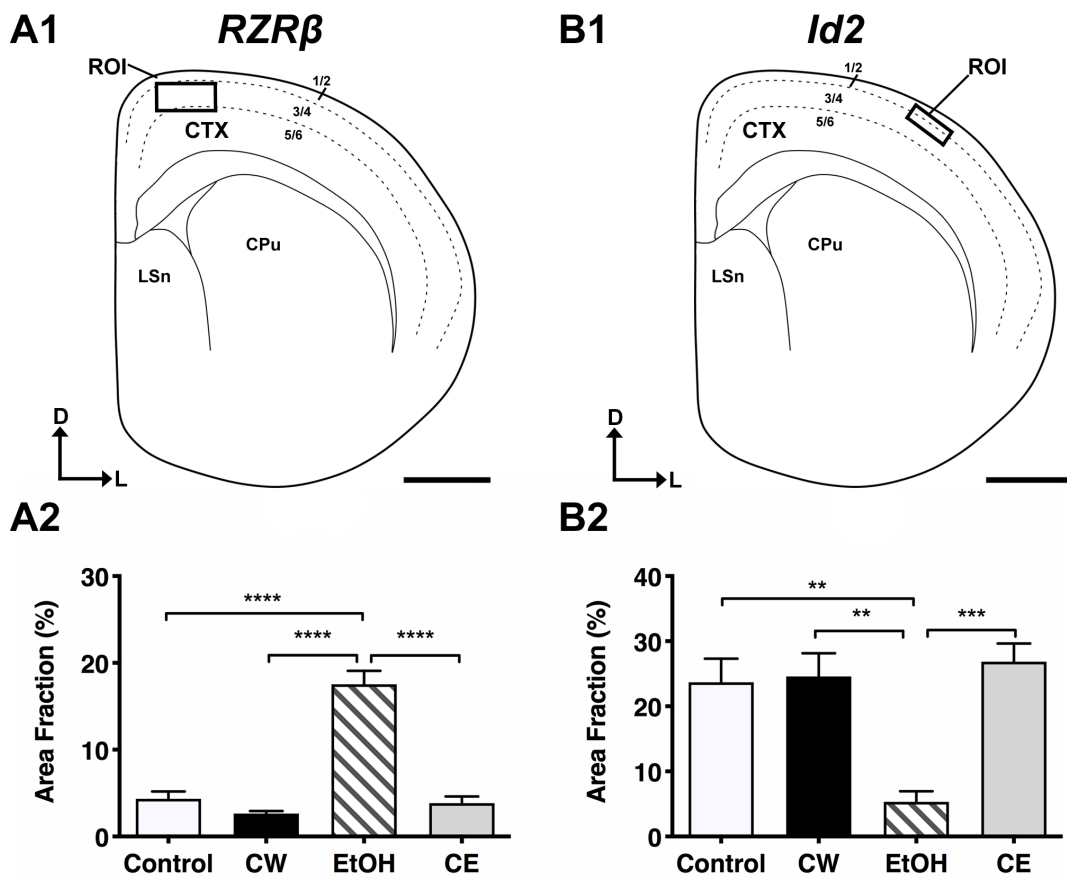
Figure 2.9: Global DNA methylation in rostral and caudal cortex at P0. EtOH brains at P0 display significantly reduced %5-mC DNA ($n = 5$) compared to controls ($n = 5$; *p<0.05), and CW mice ($n = 4$; **$p < 0.01$, ***$p < 0.005$) in both rostral and caudal cortex. CE brains show significantly increased %5-mC DNA ($n = 3$) compared to EtOH (*$p < 0.05$, rostral cortex), and are not different from controls in rostral or caudal cortex.
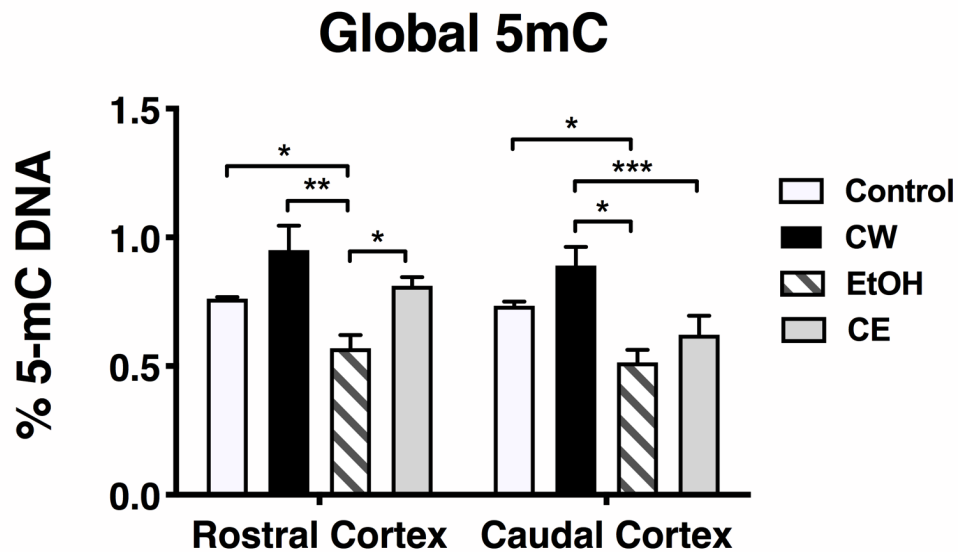
Figure 2.10: Behavioral measures at P20 in the Suok (A-E) and Ledge (F) tests. EtOH animals (*n* = 15) display increased anxiety-like behavior as measured by latency to leave center (**A**), number of directed exploration events (**B**), and rearing/grooming events (**C**) compared to control mice (*n* = 18; *p < 0.05). CE mice (*n* = 16) show decreased number of rearing/grooming events compared to controls but show significantly different directed exploration events compared to EtOH mice (**p < 0.01) indicating partial amelioration of PrEE-induced anxiety-like behaviors. EtOH mice also display sensorimotor deficits as indicated by increased missteps (**D**) and falls (**E**) on the Suok test, and decreased time on the Ledge test (**F**) compared to controls (**p < 0.01, ****p < 0.0001), CW (*n* = 14; **p < 0.01, ****p < 0.0001) and CE (*p < 0.05, ****p < 0.0001) mice. In contrast, CE mice do not show any significant sensorimotor or motor deficits in any aforementioned measure compared to control or CW mice at P20.
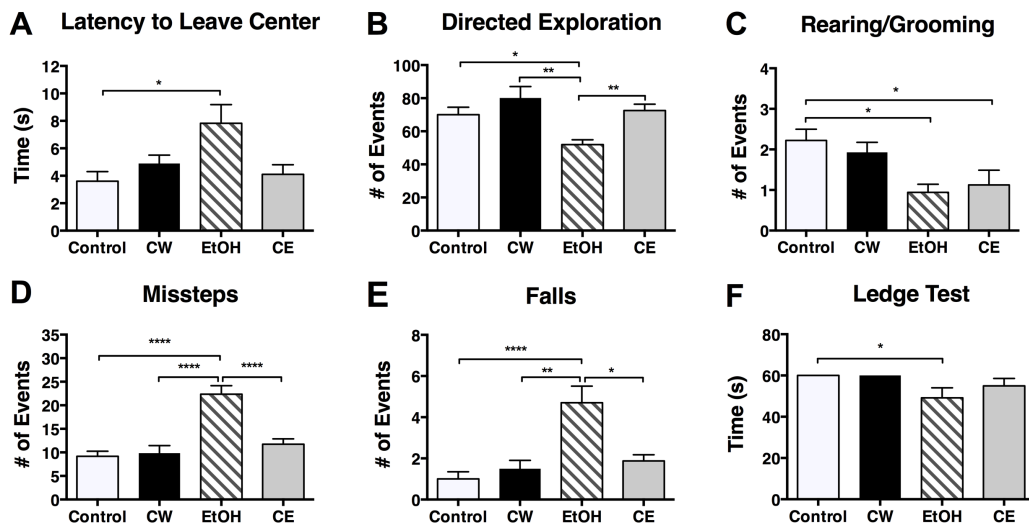
Figure 2.11: Behavioral measures at P20- Females. No significant differences present between groups in latency to leave center (**A**). EtOH female mice (n = 10) display significantly decreased directed exploration events (**B**) compared to control (n = 10; *$p < 0.05$) CW (n = 7; *$p < 0.05$) and CE (n = 7; *$p < 0.05$) female mice. Rearing and grooming events are significantly decreased in both EtOH and CE females (**C**). EtOH females also display increased missteps (**D**) and falls (**E**) compared to control (*$p < 0.05$, **$p < 0.01$). No differences are present on the Ledge test (**F**) for females only. CE females do not display any differences compared to controls in any 3 motor tests.
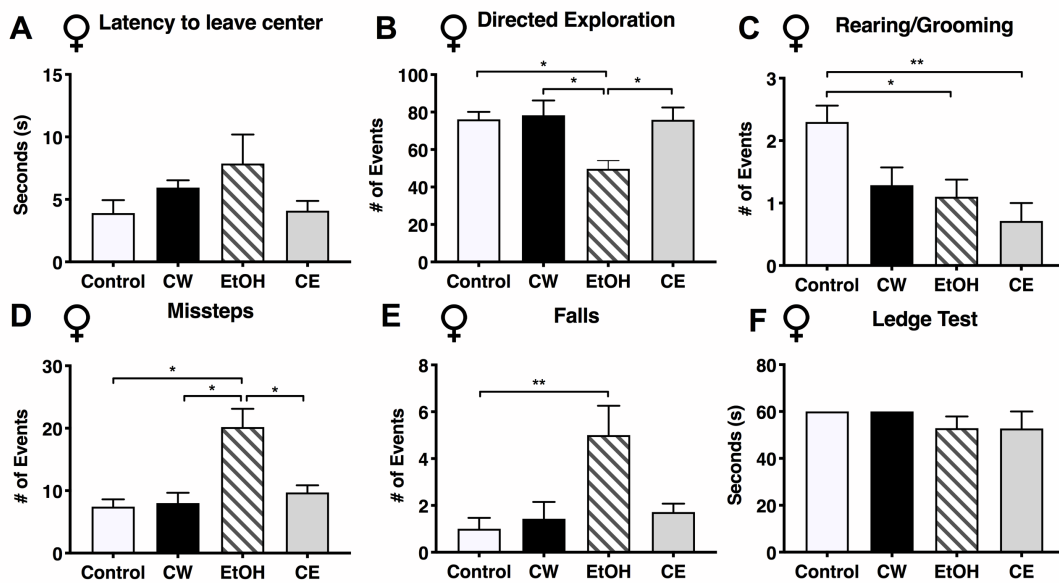
Figure 2.12: Behavioral measures at P20- Males. No significant differences are present in latency to leave center (**A**), directed exploration (**B**) or rearing/grooming events (**C**) among any group of males. EtOH males (n = 7) display increased missteps (**D**) and falls (**E**) compared to control (n = 8;*p < 0.05, **p < 0.01) and CW males (n = 7;*p < 0.05). No differences are present among any groups in Ledge test (**F**). CE males (n = 9) do not display any difference compared to controls in any measure tested.
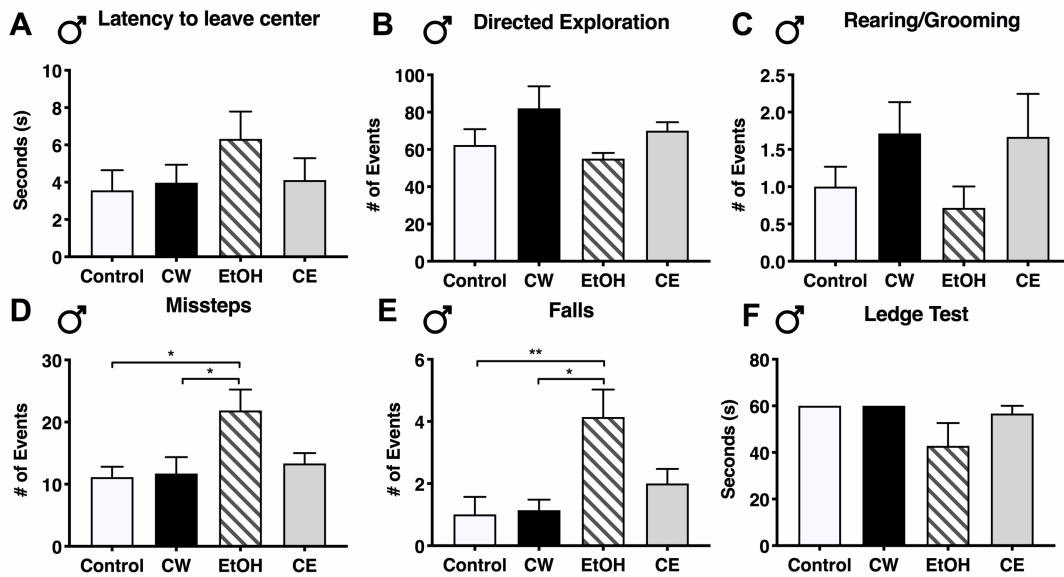
Figure 3.1: Experimental timeline.
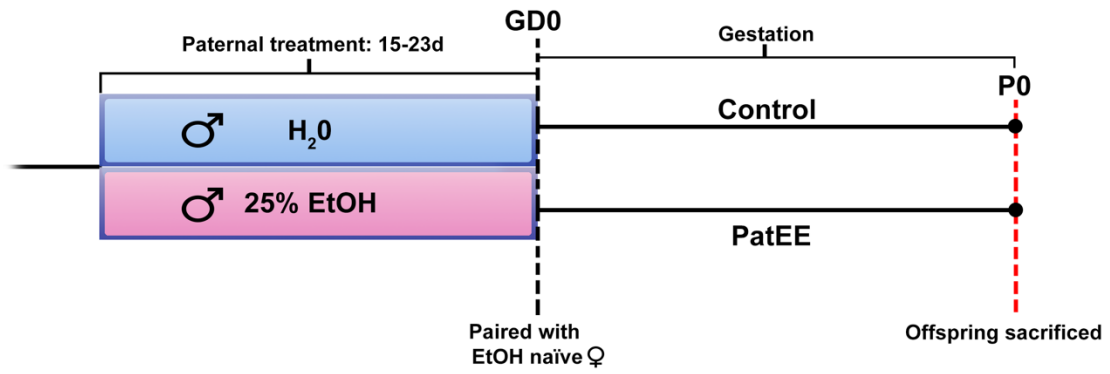
Figure 3.2: Measurements of EtOH-exposed and control sires. A, Average daily liquid intake of sires (mL/day). No differences present between control (n = 10) and EtOH-exposed (n = 10) males. **B**, BEC measurements in male sires after a 20-day exposure to 25% EtOH or water (control). Sires exposed to 25% EtOH (n = 7) had an average BEC of 125.6 mg/dL compared to controls (n = 7) which had a BEC of 0 mg/dL (****p < .0001).
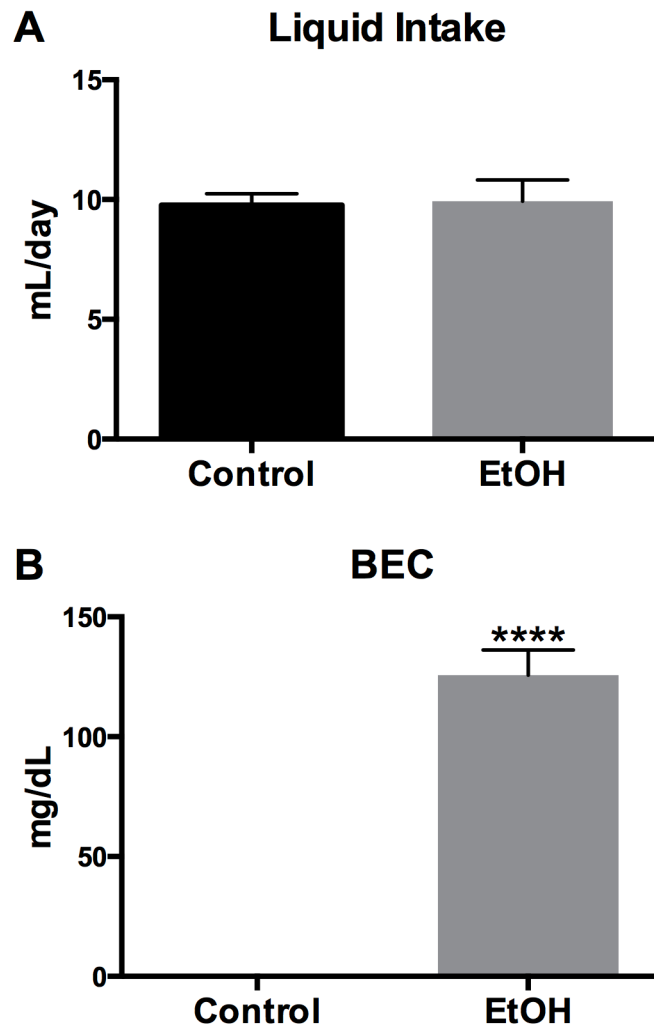
Figure 3.3: Neocortical gene expression of P0 mice: Id2 and RZRβ expression in the neocortex. High magnification of 100 μm coronal sections following free-floating *in situ* RNA hybridization with *Id2* (control: **A1-A5**, PatEE: **B1-B5**) and *RZRβ* (control: **C1-C5**, PatEE: **D1-D5**) probes. **A2**, **A3,** section through the parietal cortex where arrows denote the lateral boundary of the most superficial layer of *Id2* expression in a control brain. **B2**, **B3**, *Id2* expression extends further laterally in PatEE brains compared to controls as seen by comparing arrow locations. Arrow in **C3**, medial boundary of *RZRβ* expression in control parietal cortex. In PatEE brains this medial boundary for *RZRβ* has shifted medially (arrow in **D3**). Sections oriented dorsal (D) up and lateral (L) to the right. Scale bar, 1000 μm.
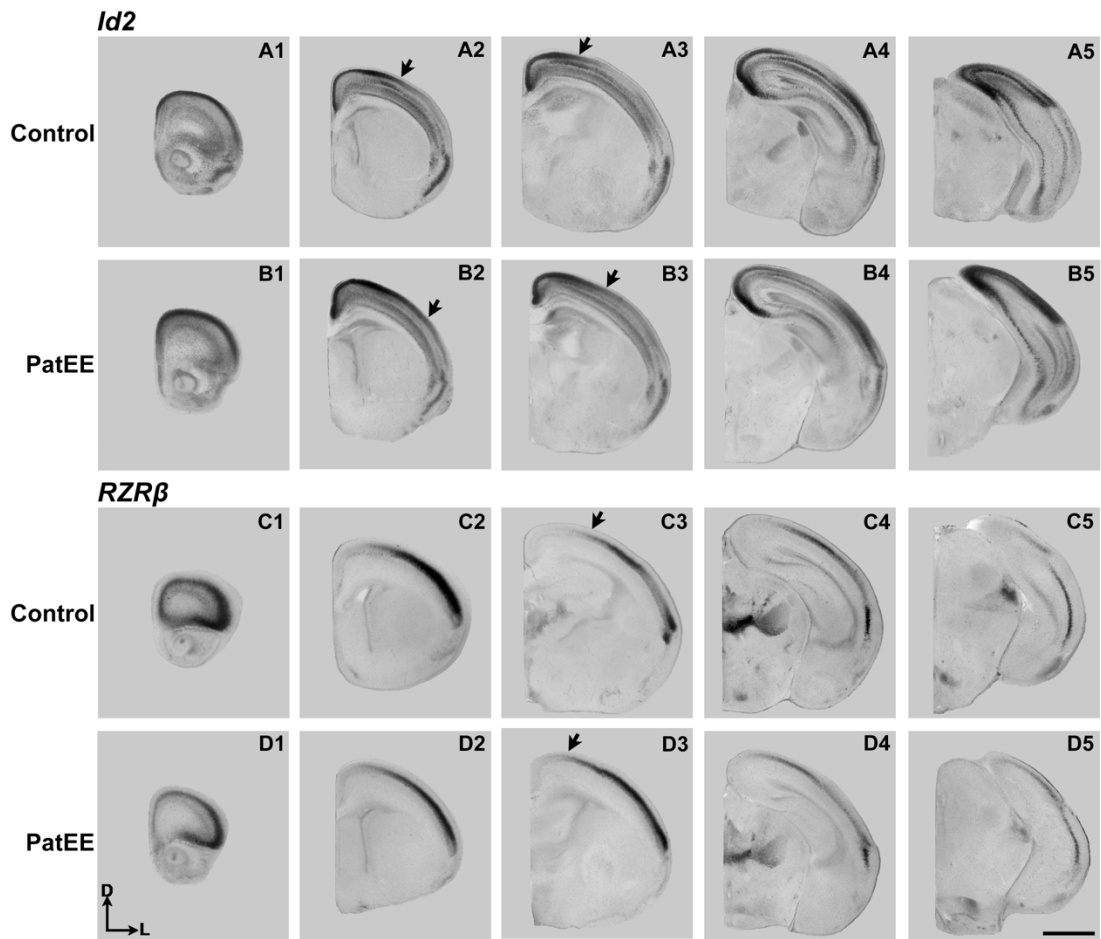
Figure 3.4: Analysis of gene expression. High magnification coronal sections of *in situ* hybridization using *RZRβ* (control: *n = 7;* PatEE: *n = 6*) (**A1-D1**) and *Id2* (control: *n = 7;* PatEE: *n = 7*) (**A2-D2**) probes in P0 cortex of control (**A1**, **A2**) and PatEE (**B1**, **B2**) mice. **C1**, **C2**, Line drawings at the cortical level where gene expression was quantified. Black boxes within the line drawings (**C1**, **C2**) indicate the ROI in which transcript densities were quantified in *RZRβ* (**D1**) and *Id2* (**D2**) sections. PatEE brains exhibited increased transcript densities in the designated ROIs for both genes compared to controls, indicating altered borders of gene expression due to PatEE. Quantified sections for both genes are at matching levels, indicating an abnormal expression phenotype that co-registered anatomically. Sections oriented dorsal (D) up and lateral (L) to the right. Scale bar, 500 μm. (*******p* < 0.01, ******** *p* < 0.0001).
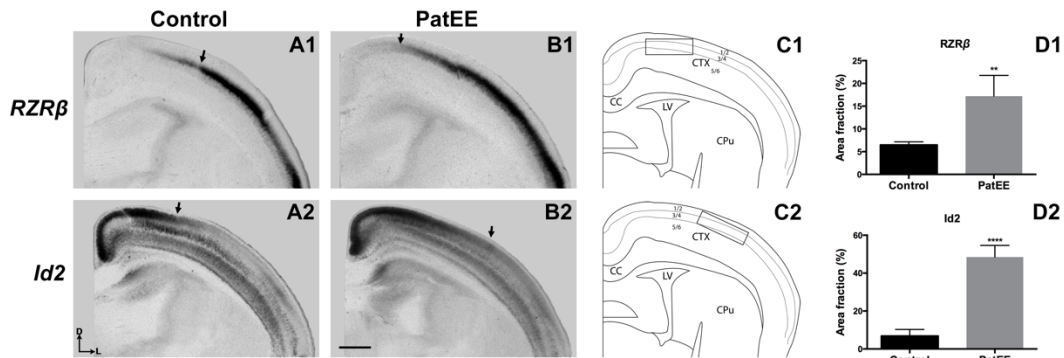
Figure 3.5: Dye tracing of intraneocortical connections. Putative somatosensory and visual INC development in control (**A1-6**) and PatEE (**B1-6**) P0 brains. Rostral to caudal series of 100 μm coronal hemisections following dye placements of DiI (red) in putative somatosensory cortex (**A2**, **B2**, **asterisks**) and DiA (green) in putative visual cortex (**A5**, **B5**, **asterisks**) and dye transport. DAPI (blue) was used as counterstain. Mixed labeling of INCs is present at the somatosensory-visual boundary in PatEE (**B3-4, white arrow**) but not in controls (**A3-4**). Images oriented dorsal (D) up and lateral (L) to the right, scale bar, 1000 μm.
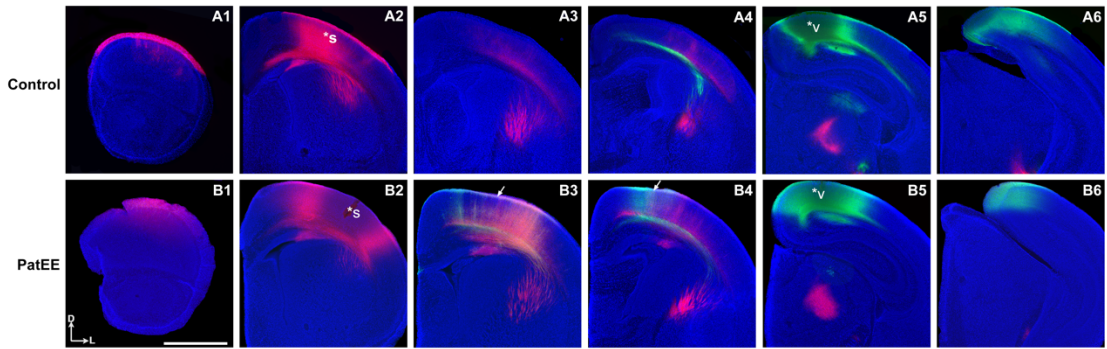
Figure 3.6: Dye tracing quantification. Average visual cortex DPL spread and projection zones for P0 control (*n* = 6) and PatEE (*n* = 5) brains. **A**, Average spread of putative somatosensory cortex (S1) DPLs. PatEE brains showed no significant difference in DPL spread when compared to controls indicating consistency across cases. **B**, Average projection zone of retrogradely labeled cells from the putative S1 DPLs. There was no significant difference in S1 DPZs of PatEE mice compared with controls. **C**, Average spread of putative visual cortex (V1) DPL. PatEE brains showed no significant difference in DPL spread when compared to controls indicating dye injection size was consistent throughout cases. **D**, Average projection zone of retrogradely labeled cells from the putative V1 DPLs. All DPL spread and projection zones are recorded as a percentage of total cortical length.
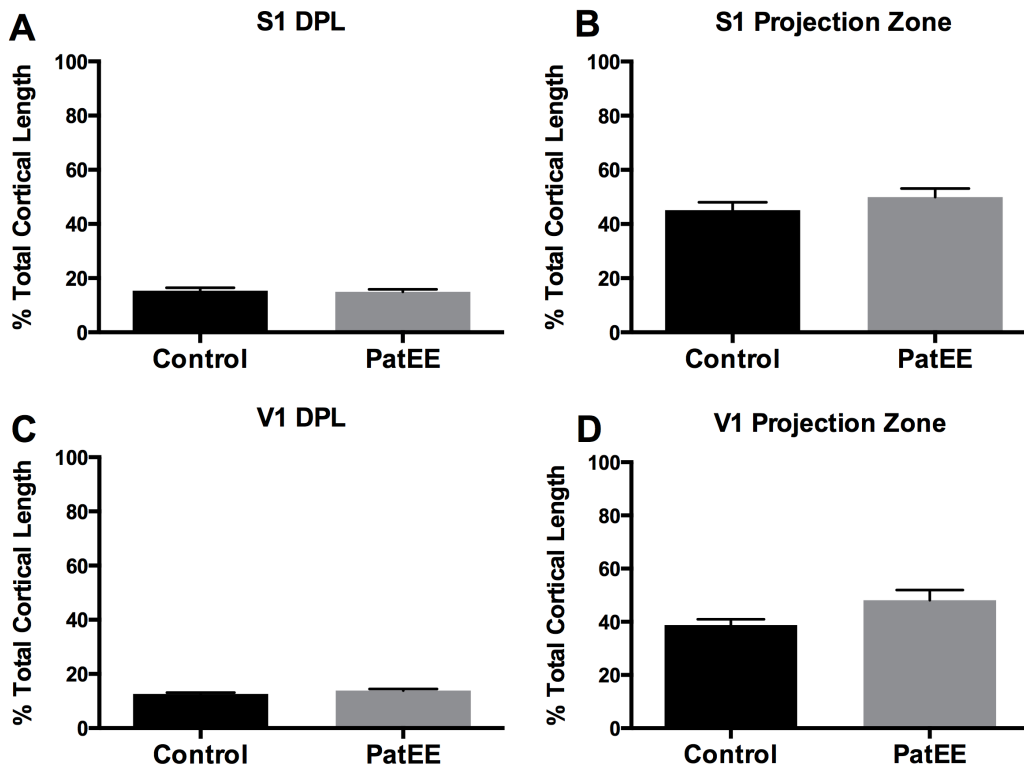
Figure 3.7: Lateral cell dispersion quantification. Putative somatosensory and visual INC development in control (**A**) and PatEE (**B**) P0 brains at the region where mixed cell labeling and gene expression changes co-registered anatomically. **C**, Line drawing at the cortical level where cell labeling was quantified. Arrows indicate where measurements of furthest lateral labeled cells were made. **D**, Average distance from the corpus callosum of furthest laterally labeled cell from putative V1 injection. PatEE mice display increased distance of cells from the corpus callosum compared to controls. Images oriented dorsal (D) up and lateral (L) to the right, scale bar, 500 μm.